Implant-Delivered Alendronate Enhances Net Bone Formation Around Porous Titanium Implants

Jenny Ann Pura
Department of Experimental Surgery
McGill University, Montréal
July 2014

A thesis submitted to McGill University
in partial fulfillment of the requirements of the degree of
Master of Science

© Copyright by Jenny Ann Pura, 2014

ABSTRACT

Bisphosphonates partially inhibit osteoclasts, thereby suppressing the resorptive phase of bone remodelling. As a result, they are commonly used to prevent bone loss in patients with osteoporosis. Their ability to prevent bone resorption has also been found to enhance bone ingrowth around porous coated cementless joint implants. Local, rather than systemic exposure of the peri-implant bone is preferable in order to avoid the systemic side effects. A study was conducted to determine the outcome of using a porous coated implant as a carrier to locally deliver the bisphosphonate, alendronate (AA), and to determine the optimum dose of locally delivered AA to maximize net bone formation around porous structured titanium implants. Porous coated cylindrical implants were coated with 0.02 mg/cm^2, 0.06 mg/cm^2, or 0.18 mg/cm^2 of AA prior to bilateral surgical implantation into the femoral intramedullary canals of 15 experimental dogs. Eight weeks later, a similar procedure was carried out on the proximal humeri. In all cases, the AA-dosed implants were placed on one side and a non-dosed, or control, implant was placed in the contralateral bone. Two controls were used: a bare-metal porous control implant (BM) and an identical control implant with a coating of hydroxyapatite (HA). Twelve weeks after the initial surgery, the femora and humeri were harvested and processed for undecalcified thin section histology to quantify peri-implant bone, bone apposition, and bone ingrowth using backscattered scanning electron microscopy. Compared with paired controls, peri-implant bone was increased by 46%, 92%, and 114% in the femora with the 0.02 mg/cm^2, 0.06 mg/cm^2, or 0.18 mg/cm^2 AA bare metal control implants, respectively. In the humeri, there was a 60% and 135% net increase in peri-implant bone with the 0.02 mg/cm^2, and 0.06 mg/cm^2 AA implants, respectively, compared to bare metal controls. Bone apposition and bone ingrowth was enhanced the most in the 0.06 mg/cm^2 AA femoral implants (82% & 37%)

and the 0.02 mg/cm^2 AA humeral implants (42% & 34%), as compared to bare metal controls. The relative differences of HA-coated control implants in the femora versus all three AA-dosed implants on the contralateral side revealed that there was little to no effect of AA on bone ingrowth. Bone apposition in the femora at 12-weeks was greatest in the 0.06 mg/cm^2 AA dose (85% apposition) compared to the 0.02 mg/cm^2 AA (45% apposition) and the 0.18 mg/cm^2 AA (5% cohorts) HA cohorts. The 0.06 mg/cm^2 AA cohort was found to have significantly greater peri-implant bone than that around the 0.02 mg/cm^2 AA and 0.18 mg/cm^2 AA dosed implants (108%, 4%, and 6% respectively, p=0.0009). Overall, the 0.06 mg/cm^2 of AA appeared to have the best effect on peri-implant bone formation, bone apposition and bone ingrowth. This study provides valuable insight into the differences of dose response to locally delivered AA for enhancing the fixation of orthopaedic implants and demonstrates its ability to increase bone that forms within the immediate space surrounding the implant. These findings can have important clinical implications in arthroplasty surgery.

RÉSUMÉ

Les bisphosphonates inhibent partiellement les ostéoclastes, supprimant ainsi la phase de résorption de la reconstruction osseuse. Par conséquent, ceci sont fréquemment utilisés dans la prévention de perte osseuse chez les patients atteint d'ostéoporose. Leur aptitude à empêcher la résorption osseuse a aussi montrer une amélioration de la croissance osseuse autour des prothèses articulaires à revêtement poreux sans ciment. Une exposition locale de l'os péri-implantaire est préférable à une exposition systémique de celui-ci afin d'éviter les effets secondaires systémiques. Une étude a été menée afin de déterminer les conséquences de l'utilisation de prothèses à revêtement poreux comme transporteurs dans l'administration locale de bisphosphonates, alendronate (AA), et pour déterminer le dosage optimal de AA à administrer localement afin de maximiser la formation nette de nouvel os autour des prothèses en titane à structure poreuse. Les prothèses cylindriques à revêtement poreux ont été revêtues de 0.02mg/cm^2, 0.06 mg/cm^2, ou 0.18 mg/cm^2 de AA pour l'implantation chirurgicale bilatérale dans les canaux centromédullaires fémoraux de 15 chiens de laboratoire. Huit semaines plus tard, une procédure similaire a été effectuée sur les extrémités supérieures de l'humérus. Dans tous les cas, les prothèses comportant un dosage de AA ont été placées sur un côté et une prothèse non-dosée, ou témoin, a été placée sur l'os contralatéral. Deux témoins ont été utilisés: une prothèse poreuse métallique nu témoin et une prothèse témoin identique revêtue d'hydroxyapatite (HA). Douze semaines après l'opération chirurgicale initiale, les fémurs et humérus ont été récoltés et préparés pour une histologie à lames minces non décalcifiées pour quantifier la formation d'os péri-implantaire, l'apposition osseuse, et la croissance osseuse en utilisant une microscopie à balayage électronique rétrodiffusé. Comparé à la paire de témoins, la quantité d'os péri-implantaire a augmenté de 46%, 92%, et 144% dans les fémurs pour des prothèses à dosages

respectifs de 0.02 mg/cm^2, 0.06 mg/cm^2, et 0.18 mg/cm^2 de AA. Dans les humérus, il a été noté une augmentation nette de 60% et 135% d'os périimplantaire pour les prothèses aux dosages respectifs de 0.02 mg/cm^2, et 0.06 mg/cm^2 de AA, comparé aux témoins. L'apposition osseuse et la croissance osseuse ont augmentées le plus pour les prothèses fémorales dosées de 0.06 mg/cm^2 (82% & 37%) et pour les prothèses humérales dosées de 0.02 mg/cm^2 (42% & 34%), comparé aux témoins. Les différences relatives pour les prothèses témoins revêtues de HA dans les fémurs par rapport aux prothèses dosées de AA dans les côtés contralatéraux ont révélées que les AA ont eu peu ou pas d'effets sur la croissance osseuse. L'apposition osseuse dans les fémurs après 12 semaines a révélé être la plus grande pour les dosages de 0.06 mg/cm^2 de AA (85% d'apposition) comparé aux cohortes de dosages de 0.02 mg/cm^2 de AA (45% d'apposition) et à celles de 0.18 mg/cm^2 de AA (5% d'apposition). La cohorte de 0.06 mg/cm^2 de AA a montré une augmentation significative d'os périimplantaire par rapport à celles de 0.02 mg/cm^2 et 0.18 mg/cm^2 de AA (respectivement 108%, 4% et 6%, p=0.0009). Dans l'ensemble, le dosage de 0.06 mg/cm^2 de AA semble avoir les meilleurs effets sur les trois paramètres osseux: formation d'os périimplantaire, apposition osseuse et croissance osseuse. Cette étude fournit de précieuses informations sur les différentes réponses aux dosages de AA administrés localement afin d'améliorer la fixation de prothèses orthopédiques en augmentant la quantité d'os formé dans l'espace entourant immédiatement la prothèse. Ces découvertes peuvent avoir des implications cliniques importantes dans le domaine de la chirurgie arthroplastique.

ACKNOWLEDGEMENTS

☺ Dr. Michael Tanzer, your patience, direction, and dedication to all that you have accomplished and continue to pursue amazes me everyday. Thank you for allowing me to learn all that I can about your craft in orthopaedics and to assist in all the surgeries that you performed for this study. You showed me how to manage the art of juggling multiple appointments at the same time, Dr. T., a thousand times "thank you"! Dr. J. Dennis Bobyn for his constant encouragement and wisdom from afar. Dr. B., you gave me the initial opportunity to get a taste of what research entails at the Jo Miller Orthopaedic Research Laboratory (JMORL) and for that I will forever be grateful.

If anything were to go wrong with the McGill's scanning electron microscope (SEM), it did. From premature filament burnouts to campus floods, Line Mongeon was there to the rescue. Thanks for rushing to my aid. Cheers to Kristian Bobyn, the SEM genius. You eased my work load by scanning my samples and teaching me how to use the machine! Thank you for returning my samples in one piece with additional personal pieces you accidentally left in the bag. Thank you to Dr. Adam Hacking for creating the ImageJ macro used in the analysis.

Thanks to Pipeline Biomedical for providing all the porous titanium implants in this study. To Dale Swarts and Roberto Delgado, you answered the questions that were necessary to include in this thesis. I would also like to acknowledge my funding source, CIHR. To the animal technicians, Marie-eve Robitaille, Julie Browning, and Carolyne Mayorga James for being wonderful at their jobs and helping everything go smoothly in the animal facility. Thanks to my thesis committee: Dr. Lisbet Hagland, Dr. Michael Weber, and Dr. Peter Roughley for providing valuable advice and suggestions.

Merci beaucoup à mon ami, Jérémy Capblancq-Bégué, the French translator – my *résumé* may have described a different study if Chantal Yan and I attempted to translate it ourselves.

I'd like to squeeze in a quick but important thank you to Miekella Okyere (DDS student). Without your reference, my research experience would have ceased to exist at the JMORL. You gave me the confidence to take all I had and move to a place where I knew no one. Your will and sass inspire me! I also give many thanks to Dr. Letitia Lim, for teaching me how to be more meticulous in the lab. I value all the input you have to offer. I appreciate the time that you took to help me learn the techniques that I needed. Not only are you my lab mate but a very significant person whom I am glad to call my great friend. You and Mélissa Caron did not just help me feel welcome in Montreal but made it easier for me to quickly call it my home.

Last but not least, my pillars of support: Lilibeth Pura, Jessica Pura, Bryan Fiebelkorn, and Visitacion Pura: being blessed does not begin to encompass all that I feel and the appreciation I have for you in my life. Thank you for the things you sacrificed in order for me to follow the path I am on now: *Maraming salamat. Mahal kita lahat*! My family and friends, thank you for giving me the foundation and tools to allow me to grow. Aside from my mom, to the one who always encourages me to be the best in all I do, my one and only GPS: Greg Shew, *dòjeh*.

I dedicate this thesis to my mom, Lilibeth Pura.

TABLE OF CONTENTS

ABSTRACT ..... **II**
RÉSUMÉ ..... **IV**
ACKNOWLEDGEMENTS ..... **VI**
TABLE OF CONTENTS ..... **VII**
LIST OF FIGURES ..... **IX**
LIST OF TABLES ..... **XIV**
CHAPTER 1. INTRODUCTION **1**
CHAPTER 2. LITERATURE REVIEW **2**
2.1 Arthroplasty 2
2.1.1 Orthopaedic Joint Replacement Implants 2
2.2 Bone and Bone Remodelling 3
2.3 Cementless Implants 5
2.3.1 Ingrowth Criteria 6
2.3.2 Fixation and Strength 7
2.3.3 Fixation Challenges 8
2.4 Alternative Fixation Methods 9
2.5 Bisphosphonates 10
2.6 Systemic Studies 11
2.6.1 Animal Systemic Studies 11
2.6.2 Clinical Systemic Studies 11
2.7 Side Effects 14
2.7.1 Systemic versus Local Delivery Animal Studies 15
2.8 Local Delivery 16
2.8.1 Animal Local Delivery Studies 16
2.8.2 Clinical Local Delivery Studies 17
2.9 Implant Delivery Method 18
2.9.1 Biphasic Elution Profile 19
2.9.2 Skeletal Distribution 19

2.10 Dose Range 20
2.11 Alendronate 21
CHAPTER 3. PURPOSE 22
CHAPTER 4. MATERIALS AND METHODS 23
4.1 Implant Structure 23
4.2 Surgical Procedure 27
4.3 Undecalcified Thin Section Histology Procedure 33
4.4 Transverse Radiography Procedure 35
4.5 Backscattered Scanning Electron Microscopy Procedure 35
4.6 ImageJ Procedure 38
4.7 Statistical Analysis 40
CHAPTER 5. RESULTS 41
5.1 Post-Operative Follow-Up 41
5.2 Post-Operative Radiography 41
5.3 Undecalcified Thin Section Histology 45
5.4 Backscattered Scanning Electron Microscopy 51
5.5 ImageJ Quantification 55
5.6 Statistical Analysis 58
5.6.1 Humeri with Bare Metal Controls 59
5.6.2 Femora with Bare Metal Controls 63
5.6.3 Femora with Hydroxyapatite Coated Controls 67
CHAPTER 6. DISCUSSION 71
CHAPTER 7. CONCLUSION 76
CHAPTER 8. REFERENCES 77
APPENDIX A. LIST OF ABBREVIATIONS 85

LIST OF FIGURES

CHAPTER 2. LITERATURE REVIEW

Figure 2.1 Illustration of THA components and their placement after a THA 3

Figure 2.2 An illustration of the chemical composition (left) and half an arrangement of HA (right) 4

Figure 2.3 An illustration of a proximal femur identifying the different structures of bone. Cancellous bone is the woven network that is also called trabecular bone. The exterior compact bone is also called cortical bone 5

Figure 2.4 Illustrations of different surface modifications on orthopaedic implants for enhancing biologic fixation; A. Plasma-spray porous coating, B. Porous fiber metal, C. Sintered beads 6

Figure 2.5 An illustration shows the chemical components of a bisphosphonate 11

Figure 2.6 An illustration showing the relative potencies of various nitrogen-containing bisphosphonates relative to pamidronate. The variety of R_2 side chains with increasing complexity indicates its level of potency 11

Figure 2.7 An illustration of the localized delivery method with the arrows indicating the elution of bisphosphonate 18

Figure 2.8 An illustration of alendronate with the specific R_2 side chain 21

CHAPTER 4. MATERIALS AND METHODS

Figure 4.1 Photograph of the EOSINT M280 chamber during a deposition of the powder-based metal for DMLS 24

Figure 4.2 Left: Photograph of a HA-coated random porous titanium femoral implants (9 mm x 90 mm); Right: Photograph of the implant in cross-section 24

Figure 4.3 Scanning electron microscope magnified (25X) to show the surface morphology of the random porous titanium structure 24

Figure 4.4 Scanning electron micrograph of the Pipeline porous structure without (left) and with (right) HA coating 26

Figure 4.5 A photograph of the spindle-jig apparatus that was used to rotate the implant during the application of the AA aliquot solution so as to cover the entire surface of the implant 26

Figure 4.6 An Illustration showing the femoral implant placement of a 90 mm long AA-dosed implant on one side and the proximal BM and distal HA-coated 45 mm long control implants on the contralateral side *28*

Figure 4.7 Intraoperative photographs illustrating the operative procedure. This is a right hip with the dog lying on his left side. Left: Skin incision located on the right proximal femur and extending proximally; Middle-left: A reamer inserted into the proximal femur to ream the intramedullary canal; Middle-right: A 9 mm diameter has been reamed into the proximal femur; Right: The femoral implant is being positioned in the prepared canal opening for impaction into the intramedullary canal *30*

Figure 4.8 Intraoperative photographs illustrating the operative procedure. This is a right hip with the dog lying on his left side. Left: A punch is used to impact the 9 mm cylindrical rod implant into a canine's right proximal femoral intramedullary canal. Care is taken not to touch the implant or have soft tissue come in contact with the implant will being inserted; Right: Closing of incision site with Vicryl sutures *30*

Figure 4.9 Contact radiograph of bilateral femora after sacrifice, demonstrating the placement of the femoral implants. The 90 mm long AA implant is on the left and the two stacked 45 mm control implants are on the right - there is no gap between the BM and HA control implants..... *32*

Figure 4.10 Contact radiograph of bilateral humeri after sacrifice, demonstrating the placement of the implants within the proximal metaphysis..... *32*

Figure 4.11 Photograph of a canine femur in an aluminum bone boat with dimensions made according to size of the individual bone sample *34*

Figure 4.12 Photograph illustrating vacuum infiltration of a pair of femora contained in handmade aluminum boats filled with 5% PMMA..... *34*

Figure 4.13 Left: Photograph of the fully polymerized PMMA acrylic bone block with aluminum casing being removed; Right: Photograph of the PMMA acrylic block being cut transversely by a diamond blade precision saw into 2-3 mm thick sections *34*

Figure 4.14 A contact radiograph of anatomically paired humeral histological transverse sections. The AA dosed implants are in the right humerus and the BM control is in the left *36*

Figure 4.15 A Contact radiograph with labelled locations of the 6 pairs of femoral sections and 3 pairs of humeral sections selected for BSEM. The horizontal lines on the contact radiograph illustrate the regions selected for analysis *36*

Figure 4.16 Photograph illustrating the preparation for BSEM by polishing selected sections on a silicon carbide abrasive disc *37*

Figure 4.17 Photograph of the Hitachi S-3000 VP-SEM used for BSEM.....37

Figure 4.18 ImageJ images representing the analysis using (left) the total bone within the intramedullary space in red, (middle) the peri-implant are with the bone in red, (right) and the bone, in red, within the porous coating of the implant.....37

Figure 4.19 BSEM grayscale image with the implant seen as white, bone as gray, and void space as black. Bone apposition is defined as the percentage of the entire implant perimeter that was in direct contact with bone (seen in red).....39

Figure 4.20 BSEM grayscale image with the implant seen as white, bone as gray, and void space as black. The bone ingrowth parameter, seen in red, is quantified by the percentage of bone found within the void space of the random porous coating.....39

Figure 4.21 BSEM grayscale image with the implant seen as white, bone as gray, and void space as black. The peri-implant space of 2.5 mm, encircled in yellow, designates the area to be quantified.....39

CHAPTER 5. RESULTS

Figure 5.1 High-resolution contact anteroposterior radiograph of the femora (left) and humeri (right) in a 0.02 mg/cm^2 AA dose dog. The two femoral controls stacked upon each other are apparent. Note the absence of any reaction around the AA and control implants.....42

Figure 5.2 High-resolution contact anteroposterior radiograph of the femora (left) and humeri (right) in a 0.06 mg/cm^2 AA dose dog. The two femoral controls stacked upon each other are apparent. Note the absence of any reaction around the AA and control implants.....43

Figure 5.3 High-resolution contact anteroposterior (left pair) and lateromedial (right pair) radiograph in a 0.18 mg/cm^2 AA dose dog. The two femoral controls stacked upon each other are apparent. Note the absence of any reaction around the AA and control implants.....44

Figure 5.4 High-resolution contact anatomically paired transverse radiograph of the humeri in the 0.02 mg/cm^2 AA dose cohort. The sections are arranged from proximal to distal. Note the bone directly apposed to the implant. There is increased condensation of peri-implant bone in the AA implants. There is no evidence radiographic loosening.....46

Figure 5.5 High-resolution contact anatomically paired transverse radiograph of the femora in the 0.02 mg/cm^2 AA dose cohort. The sections are arranged from proximal to distal. Note the bone directly apposed to the implant. There is increased condensation of peri-implant bone in the AA implants. There is no evidence radiographic loosening.....47

Figure 5.6 High-resolution contact anatomically paired transverse radiograph of the humeri in the 0.06 mg/cm^2 AA dose cohort. The sections are arranged from proximal to distal. Note the bone directly apposed to the implant. There is increased condensation of peri-implant bone in the AA implants. There is no evidence radiographic loosening 48

Figure 5.7 High-resolution contact anatomically paired transverse radiograph of the femora in the 0.06 mg/cm^2 AA dose cohort. The sections are arranged from proximal to distal. Note the bone directly apposed to the implant. There is increased condensation of peri-implant bone in the AA implants. There is no evidence radiographic loosening 49

Figure 5.8 High-resolution contact anatomically paired transverse radiograph of the femora in the 0.18 mg/cm^2 AA dose cohort. The sections are arranged from proximal to distal. Note the bone directly apposed to the implant. There is increased condensation of peri-implant bone in the AA implants. Emphasized by the arrows are the areas of radiolucencies 50

Figure 5.9 BSEM paired 4-week humeral images the 0.02 mg/cm^2 AA (top pair), and 0.06 mg/cm^2 AA (bottom pair) dose cohort. The sections are through the proximal metaphyseal region. Note the marked, localized, condensation and new bone formation adjacent to the AA implants 51

Figure 5.10 BSEM paired 12-week femoral images of the 0.02 mg/cm^2 AA dose cohort with both BM and HA controls. Note the increased peri-implant bone formation around the AA dosed implants as compared to the contralateral controls. The bone response is increased with increasing dose of AA 52

Figure 5.11 BSEM paired 12-week femoral images of the 0.06 mg/cm^2 AA dose cohort with both BM and HA controls. Note the increased peri-implant bone formation around the AA dosed implants as compared to the contralateral controls. The bone response is increased with increasing dose of AA 53

Figure 5.12 BSEM paired 12-week femoral images of the 0.18 mg/cm^2 AA dose cohort with both BM and HA controls. Note the increased peri-implant bone formation around the AA dosed implants as compared to the contralateral controls. There is an increase in peri-implant bone formation around the AA-dosed implant identified by the arrow with the presence of a gap in the proximal femur AA-dosed implant 54

Figure 5.13 Graphical representation of the statistical overview of the 4-week humeri for bone ingrowth between the 0.02 mg/cm^2 AA and 0.06 mg/cm^2 AA compared to their BM control 59

Figure 5.14 Graphical representation of the statistical overview of the 4-week humeri for bone apposition between the 0.02 mg/cm^2 AA and 0.06 mg/cm^2 AA compared to their BM control. Significance, $p<0.05$ is represented by an asterisk (*) 60

Figure 5.15 Graphical representation of the statistical overview of the 4-week humeri for peri-implant bone between the 0.02 mg/cm^2 AA and 0.06 mg/cm^2 AA compared to their BM control. Significance, $p<0.05$ is represented by an asterisk (*) 61

Figure 5.16 Summary of the 4-week humeral relative differences with the 0.02 mg/cm^2 AA, and 0.06 mg/cm^2 AA dose compared to their BM control. Asterisks (*) show a significance of $p<0.05$.....62

Figure 5.17 Graphical representation of the statistical overview of the 12-week femora for bone ingrowth between the 0.02 mg/cm^2 AA, 0.06 mg/cm^2 AA and 0.18 mg/cm^2 AA dose compared to their BM control.....63

Figure 5.18 Graphical representation of the statistical overview of the 12-week femora for bone apposition between the 0.02 mg/cm^2 AA, 0.06 mg/cm^2 AA and 0.18 mg/cm^2 AA dose compared to their BM control.....64

Figure 5.19 Graphical representation of the statistical overview of the 12-week femora for peri-implant bone between the 0.02 mg/cm^2 AA, 0.06 mg/cm^2 AA and 0.18 mg/cm^2 AA dose compared to their BM control.....65

Figure 5.20 Summary of the 12-week femoral relative differences with the 0.02 mg/cm^2 AA, 0.06 mg/cm^2 AA and 0.18 mg/cm^2 AA dose compared to their HA control. Asterisks (*) show a significance of $p<0.05$ 66

Figure 5.21 Graphical representation of the statistical overview of the 12-week femora for bone ingrowth between the 0.02 mg/cm^2 AA, 0.06 mg/cm^2 AA and 0.18 mg/cm^2 AA dose compared to their HA control 67

Figure 5.22 Graphical representation of the statistical overview of the 12-week femora for bone apposition between the 0.02 mg/cm^2 AA, 0.06 mg/cm^2 AA and 0.18 mg/cm^2 AA dose compared to their HA control 68

Figure 5.23 Graphical representation of the statistical overview of the 12-week femora for peri-implant bone between the 0.02 mg/cm^2 AA, 0.06 mg/cm^2 AA and 0.18 mg/cm^2 AA dose compared to their HA control 69

Figure 5.24 Summary of the 12-week femoral relative differences with the 0.02 mg/cm^2 AA, 0.06 mg/cm^2 AA and 0.18 mg/cm^2 AA dose compared to their HA control. Asterisks (*) show a significance of $p<0.05$ 70

LIST OF TABLES

CHAPTER 4. MATERIALS AND METHODS

Table 4.1 Experimental design summarizing the random assignment of subjects with the AA dose at the time of surgery....28

CHAPTER 5. RESULTS

Table 5.1 Mean values of bone ingrowth, bone apposition, and peri-implant bone for the 4-week humeral at 0.02 mg/cm^2 AA, and 0.06 mg/cm^2 AA with BM controls.....56

Table 5.2 Mean values of bone ingrowth, bone apposition, and peri-implant bone for the 12-week femora at 0.02 mg/cm^2 AA, 0.06 mg/cm^2, and 0.18 mg/cm^2 with BM controls.....57

Table 5.3 Mean values of bone ingrowth, bone apposition, and peri-implant bone for the 12-week femora at 0.02 mg/cm^2 AA, 0.06 mg/cm^2, and 0.18 mg/cm^2 with HA controls.....57

Table 5.4 Relative differences of bone ingrowth, bone apposition, and peri-implant bone for corresponding doses of 0.02 mg/cm^2 AA, 0.06 mg/cm^2 AA, and 0.18 mg/cm^2 AA with their controls, BM and HA 57

Table 5.5 Relative differences of bone ingrowth, bone apposition, and peri-implant bone for corresponding doses of 0.02 mg/cm^2 AA, 0.06 mg/cm^2 AA, and 0.18 mg/cm^2 AA with their controls, BM and HA 58

Table 5.6 Statistical overview of the 4-week humeri for bone ingrowth between the 0.02 mg/cm^2 AA and 0.06 mg/cm^2 AA compared to their bare metal control (BM) 59

Table 5.7 Statistical overview of the 4-week humeri for bone apposition between the 0.02 mg/cm^2 AA and 0.06 mg/cm^2 AA compared to their BM control. Significance, $p<0.05$ is represented by an asterisk (*).....60

Table 5.8 Statistical overview of the 4-week humeri for peri-implant bone between the 0.02 mg/cm^2 AA, and 0.06 mg/cm^2 AA compared to their BM control. Significance, $p<0.05$ is represented by an asterisk (*).....61

Table 5.9 Statistical overview of the 12-week femora for bone ingrowth between the 0.02 mg/cm^2 AA, 0.06 mg/cm^2 AA and 0.18 mg/cm^2 AA compared to their BM control. Significance, $p<0.05$ is represented by an asterisk (*) 63

Table 5.10 Statistical overview of the 12-week femora for bone apposition between the 0.02 mg/cm^2 AA, 0.06 mg/cm^2 AA and 0.18 mg/cm^2 AA compared to their BM control. Significance, p<0.05 is represented by an asterisk (*) 64

Table 5.11 Statistical overview of the 12-week femora for peri-implant bone between the 0.02 mg/cm^2 AA, 0.06 mg/cm^2 AA and 0.18 mg/cm^2 AA dose compared to their BM control. Significance, p<0.05 is represented by an asterisk (*).....65

Table 5.12 Statistical overview of the 12-week femora for bone ingrowth between the 0.02 mg/cm^2 AA, 0.06 mg/cm^2 AA and 0.18 mg/cm^2 AA compared to their HA control. Significance, p<0.05 is represented by an asterisk (*). 67

Table 5.13 Statistical overview of the 12-week femora for bone apposition between the 0.02 mg/cm^2 AA, 0.06 mg/cm^2 AA and 0.18 mg/cm^2 AA compared to their HA control. Significance, p<0.05 is represented by an asterisk (*) 68

Table 5.14 Statistical overview of the 12-week femora for peri-implant bone between the 0.02 mg/cm^2 AA, 0.06 mg/cm^2 AA and 0.18 mg/cm^2 AA compared to their HA control. Significance, p<0.05 is represented by an asterisk (*) 69

CHAPTER 1. INTRODUCTION

Orthopaedic joint replacement implants are designed to accurately and precisely replace bone and joints that have been damaged by disease. Early and long-lasting fixation of the implant to the surrounding bone is vital for its long-term implant survival. Fixation can be achieved by using bone cement, a grouting agent, or by direct fixation of cementless implants, known as osseointegration. Osseointegration is when the patient's surrounding host bone attaches directly to the surface of the implant. As a result, the implant becomes stabilized so that it can properly function to withstand the loading that will occur postoperatively. Osseointegration of cementless implants commonly occurs in primary total joint arthroplasty and is the fixation most commonly used for total hip arthroplasty (THA) in North America. When osseointegration occurs, the patient is often asymptomatic and is less likely to undergo another surgery for aseptic loosening. Unfortunately, osseointegration does not occur in all situations and is especially challenging when the patient's bone stock or healing potential is compromised, which will be further discussed in the literature review. Many implant design strategies have been tried in order to enhance initial stability, increase contact to living host bone through optimizing bone fit and fill, as well as to ensure osseointegration of an implant by developing new porous surfaces. The results of these implant design changes have been variable and have not completely eliminated the need for another strategy to ensure osseointegration in challenging circumstances. Another approach is to use conventional cementless implants that deliver pharmaceutical agents to the surrounding bone in order to augment and/or accelerate bone growth in and around a cementless implant. Bisphosphonates partially suppress the resorptive phase of bone remodelling, and thereby have potential for use with orthopaedic devices designed for direct attachment to bone. The local elution of the bisphosphonate eliminates the issue of systemic distribution and the associated side effects. The purpose of this study was to characterize and optimize the dose response of locally released Alendronate from a cementless implant on the peri-implant bone.

CHAPTER 2. LITERATURE REVIEW

2.1 Arthroplasty

Arthroplasty is defined as the surgical reconstruction or replacement of a joint. Joint replacement or arthroplasty surgery is indicated when a damaged joint causes significant pain and/or dysfunction that is not tolerable to the patient, and cannot be alleviated with medical treatment. The Canadian Joint Replacement Registry reported 105,231 hip and knee replacements were done in Canada from 2012-2013 [1]. Of all joint arthroplasties, total hip and total knee arthroplasty (THA, and TKA, respectively) are the most common and successful procedures done on an annual basis. This success is attributed to the improvement of minimally invasive surgical techniques and innovations in implant design, which are continually explored to maximize patient outcomes and the longevity of the prosthesis.

2.1.1 Orthopaedic Joint Replacement Implants

Orthopaedic joint replacement implants have changed significantly since 1891 when Professor T. Glück from Germany attempted a hip replacement using an ivory implant as the femoral stem [2]. He laid the groundwork for the development of hip implant fixation with the addition of plaster, as the bonding agent [2]. The materials and methods were rudimentary and success was defined as the survival of the patient.

Present orthopaedic joint replacement implants used in a THA, have two main structural components which meet basic biological compatibility requirements [3]. First, the acetabular articular surface of the pelvis is replaced with a hemispherical acetabular cup with an articulating liner that is most commonly made of ultra high molecular weight polyethylene. Second, the proximal femur and femoral neck is removed and replaced with a stem. A head is then placed on the femoral stem to articulate with the acetabular component acting as the new ball-in-socket joint (Figure 2.1).

The mechanical properties of joint replacement implants must be designed to withstand long-term clinical use. A variety of mechanical tests are performed prior to being approved for human

use in order to verify the durability of joint replacement implants. This testing ensured that the implants will be able to tolerate repetitive loading and weight bearing required for everyday function.

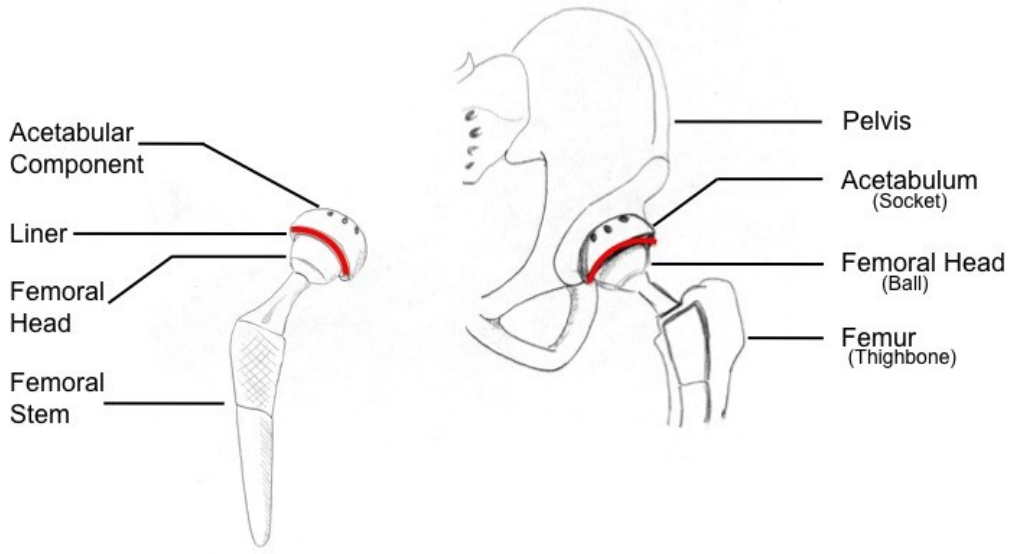

Figure 2.1 Illustration of THA components and their placement after a THA.

These implants are most commonly manufactured from cobalt chrome (Co-Cr), tantalum (Ta), and titanium alloy (Ti-6Al-4V) to ensure that they are biocompatible and that neither a local or systemic reaction occurs. In addition to being bio-inert, the implant must be non-carcinogenic. Particulate debris resulting from cyclical wear of articulating surfaces must be minimized since it creates inflammation that can lead to bone loss and/or loosening requiring revision surgery. The latter issue is clearly undesirable due to the pain that will occur and the need for additional surgery.

In addition to the mechanical properties and biocompatibility requirements, the implants itself must be able to create a stable and secure implant interface with the bone. There are 2 basic ways to fix the implant to the surrounding bone. A grouting agent, polymethylmethacrylate (PMMA) cement can be used to secure the metal implant within the surrounding bone. An alternative to the PMMA fixation method is to use a porous metal surface that the surrounding host bone can directly attach to. This biologic fixation by bone ingrowth, or osseointegration, is essential for painless and long-term function.

2.2 Bone and Bone Remodelling

The skeleton is composed of bone that has a large inorganic content and a lesser organic content. The inorganic composition is mainly the mineral hydroxyapatite (HA) (Figure 2.2). Mineral bone gives the strength and durability found in the outer, dense, thick bone that composes the skull, and the cortex of long bones [4]. Cortical bone's primary function is support because of its compact and dense composition. It also functions to protect organs and store essential elements such as calcium. The cortex encapsulates the cancellous bone. This network of cancellous, or woven trabecular bone, is less dense and has a higher surface area. This is mostly concentrated in the proximal regions of joints and is distinctly vascular. Within the trabecular network, red bone marrow, where the production of blood cells takes place and metabolic activity such as the exchange of calcium ions occur [5].

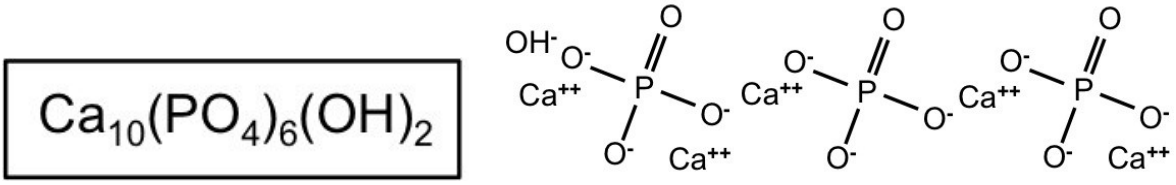

Figure 2.2 An illustration of the chemical composition (left) and half an arrangement of HA (right).

The skeleton is a dynamic structure. As such, the composition of cortical and cancellous bone changes according to its particular function (Figure 2.3). The skeleton is constantly either growing or remodelling. During childhood, early developmental stages show that bones grow in diameter, thickness, and length (as seen in long bones). As bones continue to mature, the formation and increase in bone mass is called bone modeling. In events that require a maintenance or adjustment, the bones undergo remodelling. A healthy skeleton will have a balance of two primary activities: resorption and formation [6]. The resorption, or removal of bone, is carried out by osteoclasts. Bone loss can be counter balanced by the laying down of new bone by osteoblasts. Like most systems in the human body, bone has the ability to adapt based on the changes in the environment or to the demands that it is subjected to [7]. The body's adaptive nature is described by Wolff's law as a use it or lose it requirement [8]. A known negative and positive example is seen in the lowered bone density of an astronaut or in the increased bone density of a tennis player's dominant arm, respectively [9].

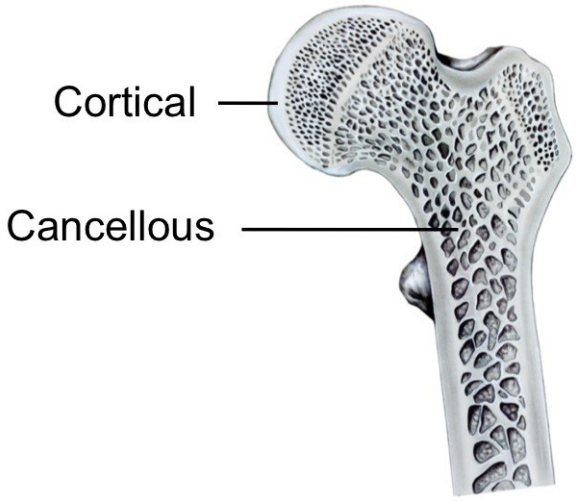

Figure 2.3 An illustration of a proximal femur identifying the different structures of bone. Cancellous bone is the woven network that is also called trabecular bone. The exterior compact bone is also called cortical bone.

An imbalance in bone homeostasis can arise when the body is incapable of managing the remodelling process. Many metabolic bone diseases can be caused by the over activation of osteoclastic or osteoblastic activity, resulting in a net increase in resorption or formation, respectively.

2.3 Cementless Implants

Cementless hip implants have been extensively used in joint replacement surgery for the past 3 decades. These implants have been designed to have a surface topography that is conducive to promoting the surrounding bone to grow into or onto the surface of the implant and thereby fixing it to the host bone. These porous surfaces can cover all or part of the implant. As well, there are various surface treatments and porous coatings that have been demonstrated to successfully attach cementless implants to the adjacent host bone (Figure 2.4). Bragdon et al. compared Co-Cr spheres and Ti fibre-mesh porous coatings used for bone ingrowth. He showed that although both topologies were able to consistently obtain bone ingrowth, the latter had a significantly higher amount of bone ingrowth, deeper penetration of bone into the porous layer, and a greater extent of bone ingrowth at the periphery of the prosthesis ($p = 0.025$, $p = 0.0005$, and $p = 0.01$, respectively) [10].

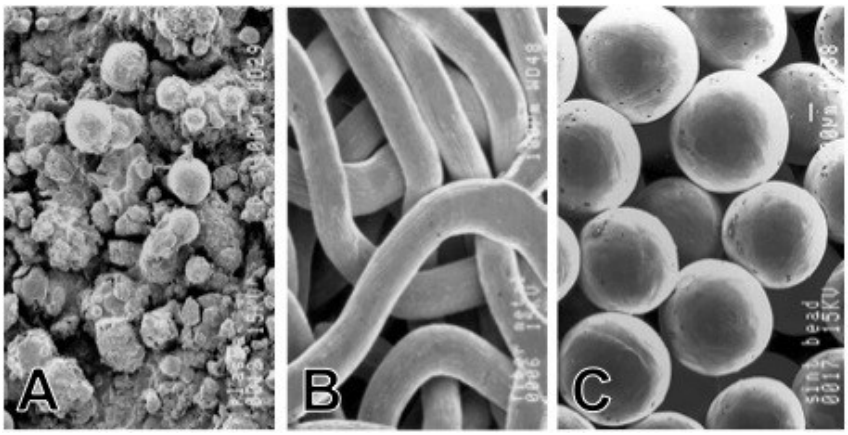

Figure 2.4 Illustrations of different surface modifications on orthopaedic implants for enhancing biologic fixation; A. Plasma-spray porous coating, B. Porous fiber metal, C. Sintered beads [11].

2.3.1 Ingrowth Criteria

The conditions that promote or increase osseointegration have been well investigated. The minimum pore size that allows osseointegration between a porous coating and the surrounding bone is known to be 100 μm [12]. In canine studies, Bragdon et al. demonstrated that there is a specific range of pore sizes that results in significant bone ingrowth [10]. They found no difference in bone ingrowth when the pore size varied between 200-450 μm. Pore sizes less than 150 μm showed significantly less bone formation ($p<0.05$). Furthermore, they confirmed that ingrowth was greater with rough surfaces than with smooth surfaces.

Historically, there has been a concern that the healing time of cementless implants would negatively impact the patient's recovery. Without the use of bone cement that stabilizes the implant immediately, the rehabilitation period of cementless implants was felt to be longer and the healing process was sensitive to a person's activity after surgery. However, more recently, clinical studies have demonstrated that it is safe to fully weight-bear on a cementless implant while it is not yet osseointegrated without affecting the long-term outcome. Ritter et al. showed THA can be performed without compromise to either hip if initial fit is achieved in both the metaphyseal and diaphyseal portions of the femur. In their follow-up months (24-77 months), 96% of the cementless THA were osseointegrated and the postoperative weight bearing did not

adversely affect the clinical outcome [13]. A study done by Rao et al. compared bilateral THA patients who began full weight bearing on both legs the day after surgery and a unilateral THA group that was only permited to put 10% of their weight on the operative limb for 6 weeks after surgery. Patients were matched for age, gender, and weight with a follow-up of up to 2 years. At 2 years, their results showed that there was no clinical difference observed between the two groups. All femoral stems radiographically appeared to be stable with no signs of loosening. [14]. Studies assessing the response of bone formation on immediate postoperative weight bearing have shown that there is little or no negative affect present on properly fitted and placed implants [13-16]. Taunt et al., reported that 99.5% of their tapered femoral stems, which gave a near-custom fit, showed reliable osseointegration with immediate weight bearing [15].

2.3.2 Fixation and Strength

The surgical technique plays a critical role in how well the host bone is capable of attaching to the implant. A gap created at surgery of less than 2 mm can still allow osseointegration. However, a gap of 2 mm or more is too large for bone to bridge [17]. Instead, the space will be filled with fibrous tissue which results in an unstable interface and a painful arthroplasty [18]. Another important criteria is the stability of the implant. Movement measuring in excess of 40 μm can impede bone growth into the implant [18, 19]. This movement is called micromotion and the possibility for this to occur is lessened by an initial tight fit at the time of surgery [20]. With a properly inserted implant, the chance of loosening decreases. Micromotion is not only dependent on the surgical technique, but also on the available healthy bone stock of the patient.

The amount of bone that is able to form in, at, and around the implant interface is a key factor in determining the fixation and strength of the implant. One particular way to measure fixation strength is to generate a force value, known as shear force, by literally pushing out the implant from its placement within the bone. The shear force generated from cortical bone ingrowth was reported by Bobyn et al. as 15-20 MPa [19]. Studies have shown that it isn't simply the bone surrounding the implant that is necessary to maintain stability but of the bone that is in direct contact, or apposed, with the implant [21]. The extent of bone ingrowth is still important, but what will essentially maintain the position of the implant is by the host bone that is apposed to the implant [22].

The consistent demonstration of osseointegration of cementless implants is encouraging [18, 23]. However, even with a properly designed and manufactured implant, surgical technique, and postoperative physiotherapy, there are high numbers of revision surgeries due to aseptic loosening [1]. The combination of HA on the surface of modified implants has shown to increase osseointegration of some implants [24]. Søballe demonstrated that the HA-coated Ti implant had a superior effect on bone ingrowth and found that there was a positive gradient that formed towards HA implant but not to implants without HA [24]. He has postulated that since bone contains an abundance of HA, coating implants with HA results in an osteoconductive effect [24].

2.3.3 Fixation Challenges

Although cementless implants are continually being improved, there are certain scenarios that are challenging for achieving a successful and stable bone-implant interface [25-28]. A controllable variable that can affect the ability to obtain the necessary host bone-implant contact needed for osseointegration is the technique used during surgery. Impaired osseointegration can occur when the bone's healing potential is compromised or when there is insufficient bone stock, such as in revision surgery. Furthermore, with metabolic bone diseases, tumour resections, or periprosthetic fractures, the ability to obtain initial stability and/or contact with normal host bone decreases To address these problematic situations, adjunct therapies to aid in the further enhancement of osseointegration and peri-implant bone formation is crucial for implant survival whether it is a primary or revision surgery.

2.4 Alternative Fixation Methods

Several means of enhancing peri-implant bone with orthopaedic implants have been investigated. In addition to obtaining the ideal porosity and pore sizes, modifications of implant surfaces such as chemical etching [29, 30] have shown to facilitate further bone formation and adhesion. Unfortunately, implant improvements through the fabrication of porous coatings lack the ability to promote the necessary bone formation in scenarios that are more challenging [31].

Environmental stimulations have such as biophysical *in vivo* loading [32, 33], electric stimulation [34], and irradiation [35] have shown bone's ability to adapt to a variety of stressors. Early positive results from the treatment of a non-invasive low intensity ultrasound were encouraging at 2-3 weeks. This method showed promise with more ingrowth, but the need for the patient have daily treatments is not ideal [36]. To date, this has not been used clinically.

The utilization of scaffolds to locally deliver therapeutic drugs has been explored to enhance osseointegration. A thorough review by Mourino et al. compared various potential materials, inorganic and organic, for use as a delivery vehicle. Many scaffolds such as calcium phosphates and bioerodible polymers are biocompatible. These materials had varying levels of osteoconductivity but require further investigation to optimize fabrication techniques and biodegradability [37].

Lind et al. evaluated the use of bone growth factors in both *in vitro* and *in vivo* settings [38, 39]. In their *in vitro* studies, several growth factors were evaluated on their effects on human osteoblasts. TGF-β 1 (transforming growth factor-beta) showed the most effects and a dose of 100 pg/mL, it had the highest chemotactic potency. The other growth factors such as (platelet-derived growth factor) PDGF-AA had a maximum effect at 10-100 mg/mL [38]. In an *in vivo* model, they used a local application of 1 and 10 μg TGF-β/day for 6 weeks with unilateral plated midtibial osteotomies. They were able to show that bone was able to be stimulated during fracture healing in rabbits [39]. However, additional clinical evaluations have not been thoroughly explored; therefore, the effectiveness of this therapy in a localized setting is not comprehensive.

Both autograft, bone from the patient, and allograft bone, obtained from a cadaveric donor, have been shown to promote the healing of bone-implant gaps [40, 41]. Hofmann et al. showed the clinical effects of autologous bone, bone derived from the same individual, on cancellous bone when placed at the interface of the host's bone and porous-coated implant's surface. They found that the bone chips that were added to the porous coated device compared to the control implant without any chips showed significantly more bone at the bone-implant interface [40]. They concluded that the use of autologous bone chips with cementless porous-coated TKA effectively enhances bone ingrowth. A study conducted in sheep by Peters et al. showed the effects of calcium sulphate ($CaSO_4$) on bone formation in bone defects. They filled metaphyseal defects with either $CaSO_4$, autograft bone, allograft bone, or nothing. was comparable to both auto and allograft This method is encouraging for patients with bone defects. They found that the use of $CaSO_4$ was biocompatible and showed that its histologic quality was comparable to both autograft and allograft bone [41]. This method showed that it was encouraging to use an alternative method to the use of autogenous bone since it is not always possible.

2.5 Bisphosphonates

The approach to use pharmaceutical agents such as bisphosphonates (BPs) to affect bone and accelerate bone growth has been used in the treatment of various bone diseases, such as osteoporosis [42]. BPs work by partially suppressing the resorptive phase of bone remodelling [43]. This affects the bone remodelling process since the normal formation of bone by osteoblasts continues, while the normal resorption of bone by osteoclasts is diminished. The chemical composition of BP not only enhances bone formation but its structure is designed to bind to bone [44-48]. In figure 2.5, the carbon, found in the center of the bisphosphonate backbone, positions all chemical entities in an ideal orientation to coordinate surrounding calcium ions [49]. The two groups of phosphonate have a high affinity to the mineralized component of bone, such as the calcium phosphate components of hydroxyapatite, while the R_1 side chain aids in the effort to bind bone. These actions work in tandem to hold bone in place.

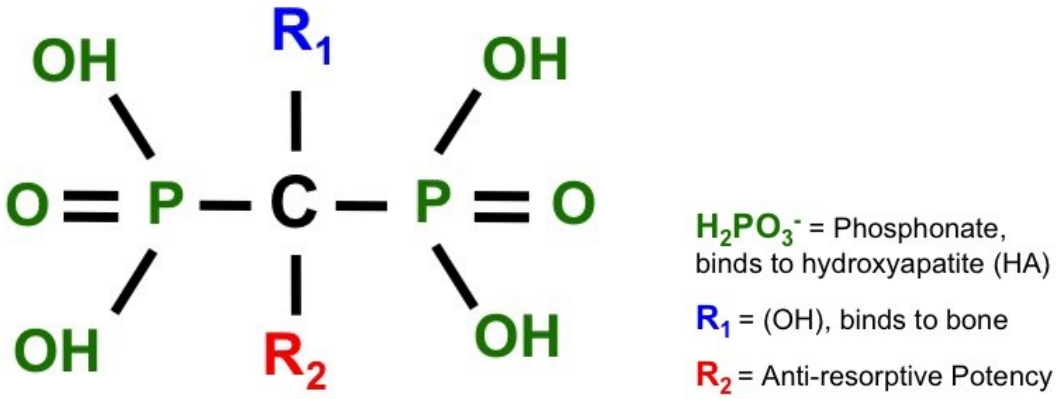

Figure 2.5 An illustration shows the chemical components of a bisphosphonate.

The remaining R_2 side chain is further divided into two BP classes: nitrogen-containing and non-nitrogen-containing bisphosphonates. This differentiation is based on the BP's efficacy on potency and mode of osteoclast inhibition [50] (Figure 2.6). Typically the BP is engulfed by the osteoclast and results in the osteoclast's cell death, or apoptosis. It has been seen *in vivo* that at certain concentrations, nitrogen-containing BPs have a heightened positive effect on osteoblasts resulting in more bone being laid down [51, 52]. The mechanism of BPs to modulate bone remodelling is useful for enhancing implant fixation [53].

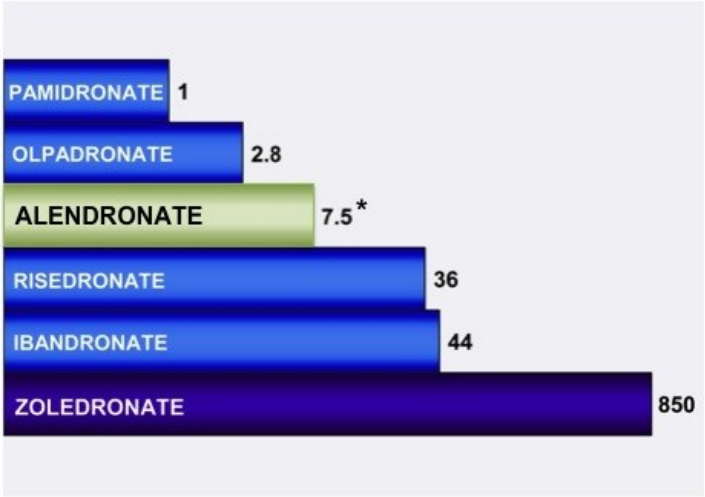

Figure 2.6 An illustration showing the relative potencies of various nitrogen-containing bisphosphonates relative to pamidronate. The variety of R_2 side chains with increasing complexity indicates its level of potency (modified from [54]).

2.6 Systemic Studies

2.6.1 Animal Systemic Studies

Many studies of systemically delivered bisphosphonates have shown to positive bone formation around implants. At a 0.1 mg/kg single dose of zoledronate (ZA) given post-operatively in canines, Bobyn et al. showed net bone formation around porous tantalum ulnar implants. There was a significant increase of bone ingrowth after 6 weeks in the ZA group compared to the controls [55].

Sugata et al. investigated the systemic effect of the BP alendronate (AA) given intravenously (IV) in a rabbit femoral model using porous hydroxyapatite/collagen composite implants. A combination of 4 groups: without AA, 3-weeks pre-treatment of AA, 3-weeks post treatment of AA, and full-term treatment of AA until sacrifice were compared. They showed that within the groups treated with the IV delivered AA, mineral densities were lower than the control group of newly formed bone and AA did suppress the resorption of the implants. Their model showed that in all three AA doses there was an apparent decrease in peri-implant bone resorption [56]. The extent of systemically delivered bisphosphonates in animals has helped researchers understand the effects in a clinical setting.

2.6.2 Clinical Systemic Studies

Applications of systemic bisphosphonates have been proven clinically effective for increasing bone mass and density around orthopaedic implants. The postoperative treatment of the bisphosphonate alendronate, has shown to reduce the loss of periprosthetic bone after a THA. In a prospective study by Arabmotlagh et al., they were interested in evaluating alendronate's long-term effects. Patients that underwent a THA, received 20 mg of oral AA and were examined after the first year and after 6 years. Patients who received the alendronate treatment had less bone loss than the group without the treatment. Furthermore, there was no significant change in bone mineral density after 6 years when compared to their observations made after the first year. They concluded that alendronate did have a long-standing effect since bone loss did not increase after the first year [57].

A prospective randomized systemic study done by Harding et al. evaluated whether treatment by one single infusion of a bisphosphonate, zoledronic acid (ZA), can enhance pin fixation. In 46 consecutive patients (35–65 years), two hydroxyapatite-coated pins were inserted in the metaphyseal bone and two non-coated pins in the diaphyseal bone of the tibia. The torque force for insertion and extraction were compared to find that the pins coated with HA had similar values as the ZA group (4.0 Nm versus 4.7 Nm). The ZA-coated pins compared to non-coated pins generated double the force upon extraction. They concluded that a single infusion of ZA was able to improve the fixation by twofold of non-coated pins in diaphyseal bone. [58]

In a review of multiple bisphosphonate studies, the association between BP use and implant survival was investigated. In a retrospective cohort study by Prieto-Alhambra et al., they examined whether there was improvement on implant survival with the use of bisphosphonates. From the United Kingdom's General Practice Research Database, they evaluated 18,726 primary TKA and 23,269 THA done from 1986-2006 in USA. Excluded patients were younger than 40 years old at the time of surgery, as well as those who had a history of hip fractures or rheumatoid arthritis before surgery. After classifying the remaining patients by their history and exposure to bisphosphonates, they were evaluated based on revision rates after 5 years. From the total 41,995 participants, the 1912 who were BP users (4.6%) had a significantly lower revision rate compared to non-users (0.93% v 1.96%) and had longer implant survival (P=0.047). They concluded with the association that BP use had an approximately twofold increase in implant survival time [59].

Although systemic deliveries of BPs have shown to reduce revision rates by enhancing fixation, and increasing the survival time of the implant, there are several concerns associated with the systemic distribution of bisphosphonates.

2.7 Side Effects

The risk of any systemically distributed therapy is not always immediately apparent. Exhaustive studies of bisphosphonate use and their adverse effects have been performed [60]. Not all BPs yields the same issues because complications arise based on the systemic delivery method: oral or intravenous (IV). The oral administration of bisphosphonates (alendronate, risedronate, and ibandronate) is associated with problems in the upper gastrointestinal tract, hypocalcaemia, musculoskeletal pain, and osteonecrosis of the jaw. Intravenous bisphosphonates like ibandronate, pamidronate, and zoledronic acid, all exhibit the above mentioned effects except the gastrointestinal problems. The latter two IV bisphosphonates have also has been found to be associated with renal toxicity.

Numerous studies have investigated the amount of time systemically delivered bisphosphonates remain in the body. Upon systemic oral delivery, the gastrointestinal tract is only able to absorb not more than 1% of the BP administered. Upon osteoclast (OC) inhibition at the surface of bone, the apoptosis of OCs release the BPs and the slow elimination process begins. From that 1%, approximately half remains unmetabolized as it is excreted through urine while the other half immediately accumulates on the skeleton due to their high affinity to hydroxyapatite [61]. The half-life of a BP is based on its, affinity to bone, and the length of time that the individual's remodelling process is exposed to it. This value ranges between 1-10 years. As described by bisphosphonate's pharmakinetics, they have very poor bioavailability. Therefore, the dose requirements often have to be higher due to the loss of the unmetabolized amounts [62].

For decades, BPs have been used to treat osteoporosis. Schneider et al. did a study to show whether there was an association with atypical femur fractures (AFF) and concurrent bisphosphonate treatment for osteoporosis. The mean year treatment for bisphosphonates of the volunteer patients was 9.5 years. Of the 94% of patients that started alendronate, 16% were diagnosed with subsequent stress fractures. From that percentage, it was found that 39.5% also endured a contralateral AFF within 4 years from their first incidence. It was found that the AFF patients had delayed healing, and continued risk of another fracture [63]. Although systemic BPs have been shown to improve bone formation, the concern is of unknown risks from prolonged use by exposing the entire skeleton. Systemic use of BPs needs to be periodically re-evaluated.

2.7.1 Systemic Versus Local Delivery Animal Studies

In two separate studies, Astrand et al. evaluated the difference in the effective dose required for systemic as compared to local delivery of the bisphosphonate, alendronate (AA). In the first study, bone chambers of cancellous bone grafts were surgically placed in the proximal tibiae of rats. They compared three systemic subcutaneous injections: saline, a high AA dose (205 μg/kg/day), and a low AA dose (4 μg/kg/day) [64]. The second study was on the local administration of a single application of AA. The local delivery showed an inhibition of bone resorption with a single exposure and only required to use 1/10 the systemic dose in order to obtain an increase in bone formation [65].

Kumar et al. compared the systemic and local effects of pamidronate (PAM) using ^{99m}Tc-labeled-PAM. Three delivery methods were used to estimate bone and soft tissue uptake of ^{99m}Tc-PAM quantitatively. Methods of administration on an exposed fractured femur were by intravenous (IV), subcutaneous injection (S.C), and direct application (D.A) [66]. Overall the IV dose revealed the highest excreted value compared to the other two methods. They suspected that the kidneys may be exposed to high concentrations of the PAM because of a surplus of 45% PAM excretion after 2 hours. However, the biological assessment of any renal damage was not done to confirm that statement. Organs were harvested to evaluate radioactivity and the kidney values were comparable between the IV and S.C methods (0.22 Å: 0.03% ID/g and 0.19 Å: 0.02% ID/g, respectively). The S.C method is not clinically practiced but the results were informative. Although 70% of the S.C. remained at the site of injection, there was a decrease to 22% after 24 hours. The results obtained from this method suggest that the BP can enter the circulatory system. In the D.A method, gamma images showed that interference of muscular activity occurred and upon further examination after sacrifice, there was an observed bone uptake. There was an increase of 8 to 26-fold over the surrounding muscle. The fractured bone had a higher uptake of ^{99m}Tc-PAM compared to the intact femur. They concluded with the suggestion that the D.A was the best method to deliver the maximum dose. For the treatment of localized conditions, “direct/local application of BPs may be a suitable approach for administration of BPs for orthopaedic purposes” [66].

2.8 Local Delivery

2.8.1 Animal Local Delivery Studies

Prior animal studies on locally delivered bisphosphonates have shown enhanced bone formation around implants. Roshan-Ghias et al. performed a study evaluating the local effect of an implant-bound bisphosphonate, zoledronate (ZA) in a compromised bone environment. Rabbits underwent bilateral femur implantation with an uncoated cancellous bone screw in one side and a ZA –loaded fibrinogen (bicoated) implant on the contralateral side. Over drilling was done to model compromised cancellous bone. At 5 different time points, (1, 5, 10 days, 6 weeks, and 11 weeks), the fixation effect on all screws was evaluated by both mechanical testing and micro-CT imaging. In the 1, 5, and 10 days time point, there was no significant difference observed between the biocoated and control groups. However, in the biocoated group at 6 weeks, there was a significantly higher bone volume fraction in the trabecular region. Furthermore, for the biocoated group at 11 weeks, both bone volume fraction and mechanical pull-out data were significantly higher than the control group. They concluded suggesting that in a compromised bone environment, local delivery of bisphosphonate enhances the stability of bone screws [67].

Niu et al. did a long-term study using hydroxyapatite-coated implants comparing two bisphosphonates: a high and low affinity BP (alendronate (AA), and risedronate (RIS), respectively) in rabbits. Implants were placed in the proximal region of the medullary canal of the left tibia. Four groups were compared (group I: HA, group II: AA-HA, and group III: RIS-HA) for the local effect of implant-bound AA. The systemic effects were compared in the right tibia and lumbar vertebrae. AA-dosed implants with their controls were evaluated on the extent of bone-implant integration, bone architecture, bone mineral density, implant stability, and serum levels of bone turnover markers. The AA-HA composite coatings demonstrated a higher peri-implant contact ratio, bone mass augmentation, bone mineral density, and implant stability. This showed a more potent effect than the RIS-HA composite coating. However, the RIS-HA had a more significant effect on the lumbar vertebrae for the systemic comparison. This indicates that bisphosphonate treatment has varying effects in distribution and efficacy [68].

Local applications of bisphosphonates have been investigated and concerns of systemic distribution have been raised. Yaffe et al. utilized a gelatinous sponge soaked in 20 mg of radio-labelled alendronate in 1ml saline. The sponge absorbed 0.2mg of AA and was topically applied on the experimental surgical side of a rat's mandible. A comparison was done between the AA-dosed side and the contralateral control mandible, and a tibia. They reported that 10% of the AA-soaked sponge was absorbed by the local bone around the surgical site whereas on the contralateral mandible, there was a 2% of AA found. Interestingly, the tibia contained 0.2% AA suggesting that the extravasated AA can enter the blood stream and circulate. This showed AA's capacity to adhere to bone in other parts of the skeleton [69]. The local positive increase and low dispersion of AA by topical application were encouraging but the systemic exposure is still a concern.

Tanzer et al. were the first to show that a bisphosphonate could be locally delivered by a porous orthopaedic implant. Using a canine ulnar model, they implanted HA coated tantalum implants doped with 0.05 mg of ZA. After twelve weeks, it was found that there was on average 2.3-fold greater peri-implant bone with the ZA-dosed implants compared with the control implants [70].

2.8.2 Clinical Local Delivery Studies

In a clinically relevant setting, the practice of using or applying an unknown dose is unreliable and inconsistent. A potential standard application would be to locally release the bisphosphonate directly from the implant to surrounding bone. Systemic issues can be largely eliminated and fixation can be enhanced by locally delivering the bisphosphonate directly from the implant to surrounding bone.

Toksvig-Larsen and Aspenberg showed a promising method of delivering a bisphosphonate where uncoated pins have high rates of loosening. In a 20 patient study, Toksvig-Larsen and Aspenberg investigated the effects of a locally delivered zoledronate using external fixation pins used in hemicallotasis. Each patient received two pairs of screws: one with coated threads of fibrinogen at a dose of 0.5 μg/mL zoledronic acid and the other coated with hydroxyapatite without ZA. One pair was placed in the shaft and the other in the metaphysis of the tibia. They concluded that a bisphosphonate coating could enhance metaphyseal fixation [71].

2.9 Implant Delivery Method

The ability of an implant to directly deliver a therapeutic agent can avoid the risk of systemic complications. Clark et al. investigated a solid prosthesis to act as the drug carrier. They had modified the surface porous coatings of an implant to contain a transforming growth factor-beta 1 (TGF-beta-1). This promoted the *in vitro* proliferation and migration of human mesenchymal stem cells towards the implant. Their positive findings suggested that it was possible to use an implant for local drug delivery [72].

The confirmation of activity when bisphosphonates are linked to hydroxyapatite was investigated in vitro. Boanini et al. found that the AA's effects were not hindered and that a positive effect on bone cell response was present around the nanocrystals. They discovered that the amount of osteoclasts measured in the alendronate HA-coated nanocrystals compared to control demonstrated enhancement of osteoblast activation. [73].

Therefore, combining these two approaches: the use of a bisphosphonate to modulate the bone healing response linked to a hydroxyapatite coating on the implant interface can potentially increase the bone formation in and around the implant (Figure 2.7).

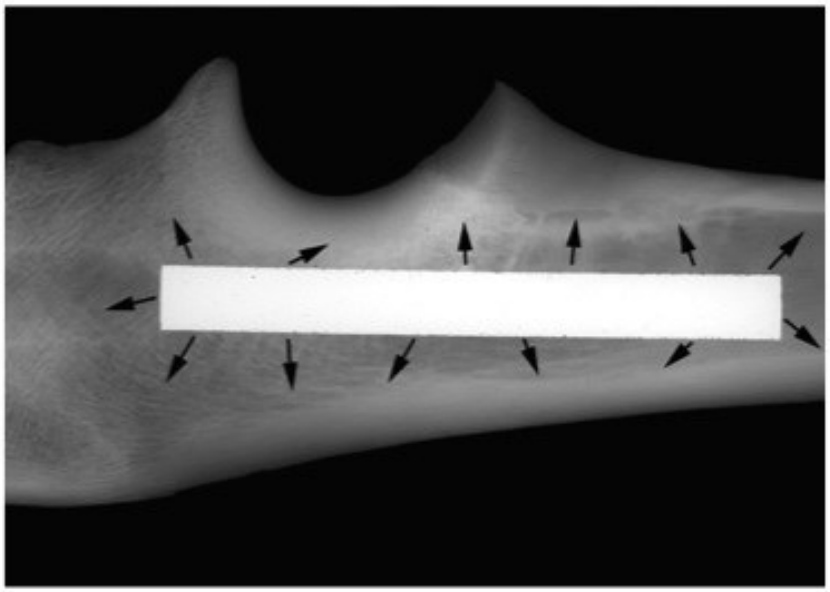

Figure 2.7 An illustration of the localized delivery method with the arrows indicating the elution of bisphosphonate [54].

2.9.1 Biphasic Elution Profile

To ensure that upon implantation, the BP's ability to be released in a controlled manner was evaluated. An elution profile was constructed to measure the release of the BP to better understand the speed and dispersion the drug elutes from the implant. This allowed the investigators to see the percentage of BP that remained bound after a given amount of time. Bobyn et al. showed that with plasma-spray coated HA implants, the bisphosphonate was bound in two ways [70, 74]. The inner struts remained uncoated (ionic bond) and the HA-coated surface had a strong association with ZA (covalent bond). This resulted in a biphasic elution profile. There was a quick and high release of the drug within the first few minutes due to the ionic binding of ZA to the inner uncoated struts. This was followed by a much slower release from the outer struts, which covalently bound the HA to the drug. This effect was sustained up to 6 weeks.

2.9.2 Skeletal Distribution

Following up with the ZA study, the systemic effect of the drug need to be investigated to ensure that as a proof of concept, the localized delivery was indeed remaining local. A long-term study was done by McKenzie et al. to show the efficacy of ZA over a year. They used a HA-coated implant that was labelled14C-l ZA to determine the distribution of the drug after implantation into a canine femur. The results showed that there was insignificant 14C-ZA in other bones in the skeleton at sub-therapeutic levels [75]. Furthermore, within the intramedullary canal of the femur where the ZA-dosed implant was inserted, the ZA remained highly localized to the implant and peri-implant space [75].

2.10 Dose Range

It is important to keep in mind that patients who currently receive bisphosphonate treatments are not only repeatedly exposed to the effects through systemic distribution but are often given higher doses to obtain any clinical effects. Dose values have been examined in various bisphosphonates and are based on different methods by systemic delivery. However, to evaluate the effect of BPs in a localized setting, the direct effect on bone cells is essential. The most potent BP is zoledronate and its toxic effect on bone cells was reported as 2.5×10^{-10} M by Li and Davis [76]. This was 250 times more potent than a more clinically relevant BP, alendronate (AA) [77]. Furthermore, Garbuz et al. reported that osteoblasts exhibited toxic effects when the concentration exceeded 10^{-4} M. Therefore, in their localized delivery, they used a concentration of 1.0×10^{-3} M of AA bound to calcium phosphate-coated tantalum implants [78]. The BP concentration was proportionately correlated to the implant size and surface area such that a smaller implant will require a less amount compared to a larger implant. In the rabbit femoral implants used by Garbuz et al. the diameter measured 0.32 cm and 0.8 cm in length. This was a surface area of 0.96 cm^2 used with 3.2 mL of AA in 10^{-4} M. They reported a total average dose of 1.37 μg AA was used resulting in a 0.0014 mg/cm^2 AA dose when related to surface area [78].

Most recently, Bobyn et al. reported that the locally delivered bisphosphonate, Alendronate, from porous structured titanium implants resulted in a net increase of bone formation in a canine model. Test implants were plasma-spray coated with HA and subsequently coated with one of two total AA doses: a 0.2 mg and 1.0 mg AA dose. The overall difference between the two AA doses was that the 1.0 mg AA had 3.2 times more peri-implant bone than 0.2 mg AA [79]. In comparison to the AA study by Garbuz et al., the surface area of the canine femoral implants used by Bobyn et al. measuring 0.9 cm in diameter and 9.0 cm in length resulted in a surface are of 26.72 cm^2 [79]. The concentration used for the 0.2 mg and 1.0 mg total AA dose were approximately 0.008 mg/cm^2 AA, and 0.04 mg/cm^2 AA, respectively. This further established that the larger the implant, more BP is needed.

2.11 Alendronate

The use of alendronate (AA) has been widely accepted and clinically effective in increasing bone mass and density (Figure 2.8). Its long clinical history and safety profile for the treatment in osteoporosis are addition reasons that alendronate is a candidate bisphosphonate to use in the adjunct therapy of a localized delivery method using orthopaedic implants [80]. The use of AA with a local delivery application has numerous benefits. AA has been shown to remain highly localized around the implant and its decreased potency compared to other BPs can possibly elimination any systemic side effects. The local dosage needed is much lower than a systemic dose due to bypassing the gut and kidneys. Furthermore, it guarantees that the drug is at the desired site of action. Local AA requires a one-time exposure to the patient as opposed to regular ongoing treatments. Therefore, from the few articles published on the effects of Alendronate's response on bone formation using porous implants, it would be beneficial to study its dose range effects.

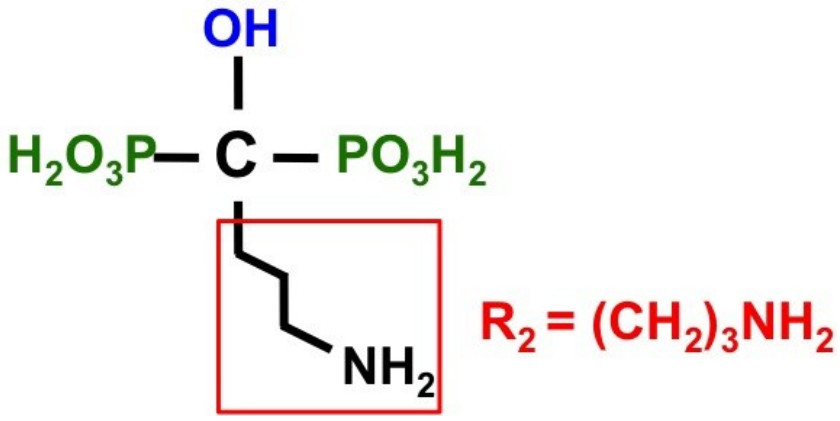

Figure 2.8 An illustration of alendronate with the specific R_2 side chain.

CHAPTER 3. PURPOSE

The purpose of this study was to determine the optimum dose of locally delivered Alendronate, in order to maximize net bone formation around porous structured titanium implants in a canine model. Local delivery was achieved via elution of 3 different doses of the drug from hydroxyapatite-coated porous implants. The local dose effect on bone apposition, bone ingrowth, and peri-implant bone, compared to contralateral controls, was assessed in 15 dogs at 4 weeks and 12 weeks, postoperatively.

CHAPTER 4. MATERIALS AND METHODS

4.1 Implant Structure

Cylindrical implants made of titanium alloy (Ti-6Al-4V) were fabricated using a direct metal laser sintering technique (DMLS) (Pipeline Biomedical, Cedar Knolls, New Jersey). This was done with the EOSINT M280 manufactured by Electro Optical Systems (Munich, Germany). The innovative laser-sintering technology is a fast 3D prototyping method. DMLS uses powder-based metals and has the ability to construct irregular and complex components layer by layer. Beginning with a thin platform of powder, a component is built from the bottom up. The computer-generated component is constructed electronically by design data with its layers connected by a laser beam. The newly laser-beamed layer with the deposition of new material is lowered and repeated until completed (Figure 4.1). Each implant had a diameter of 9 mm and was either 45 mm or 90 mm in length (Figure 4.2). The implant had a 6 mm solid core and a 1.5 mm thick outer porous structure consisting of a random network of struts with a mean pore size of 400 μm and a volume porosity of 65% (Figure 4.3). The line intercept technique was used to ascertain the mean pore size. A transparent lined paper was placed on top of a back-scattered scanning electron microscopy (BSEM) image to measure the pore diameters. Pore edges that intersected the lines were marked and measured to determine the average size.

There were two control implants used in this study. One control was left as manufactured, bare-metal (BM), without any addition to its surface (Figure 4.4 Left). The other control was plasma spray-coated with a thin, 10 - 15 μm layer of hydroxyapatite (HA) (98% purity, 99% density, 64% crystallinity, calcium:phosphate ratio of 1.67) on the outermost porous structure, leaving the innermost pores uncoated (Figure 4.4 Right). The test implants used the HA coated implants described above, which were subsequently coated with commercially pure, laboratory-grade alendronate (AA) (alendronic acid trihydrate, Reddy Laboratories, India) in 3 doses normalized to the outer implant surface area. The AA was dissolved in 2.0 ml aliquot solutions of distilled deionized water (ddH_2O) to produce doses of 0.02 mg/cm^2, 0.06 mg/cm^2, and 0.18 mg/cm^2. This resulted in a total AA dose of 0.5 mg, 1.5 mg and 4.5 mg on the 90 mm long test implants and 0.25 mg, 0.75 mg and 2.5 mg on the 45 mm long test implants.

Figure 4.1 Photograph of the EOSINT M280 chamber during a deposition of the powder-based metal for DMLS.

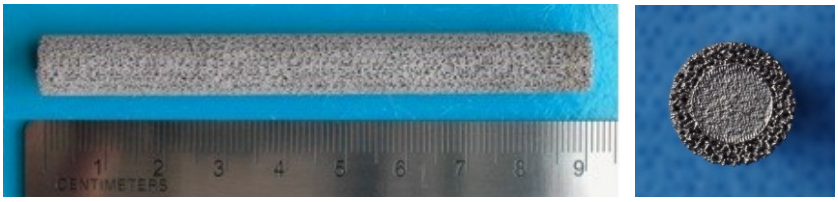

Figure 4.2 Left: Photograph of a HA-coated random porous titanium femoral implants (9 mm x 90 mm); Right: Photograph of the implant in cross-section.

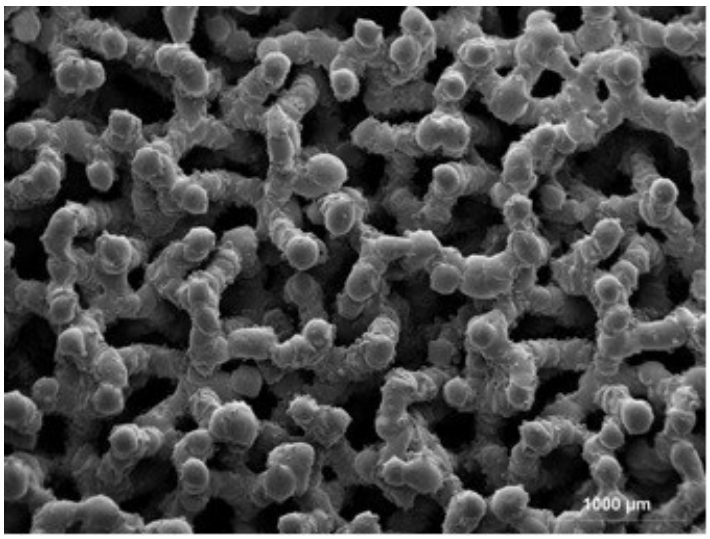

Figure 4.3 Scanning electron microscope magnified (25X) to show the surface morphology of the random porous titanium structure.

These first two doses were selected based on our previous study demonstrating the efficacy of AA around porous coated titanium implants and our desire to optimize the effect of the drug [79]. The third, uppermost dose was used to meet the Food and Drug Administration requirements to ensure safety by evaluating a dose three times higher than the optimal dose. The test implants were coated with AA by applying the alendronate aliquot in solution, with a micropipette, in a drop-wise fashion uniformly covering the entire surface of the implant (Figure 4.5). This deposition process results in homogeneous saturation of the porous structure with fluid that permeated to the inner pore depths through surface tension effects. After coating the implants, they were dried overnight in an oven at 50°C, and sterilized in surgical packaging with 2.5MRad gamma irradiation in preparation for surgery.

Unpublished elution studies performed by Pipeline Biomedical (Cedar Knolls, New Jersey) were done *in vitro* following published protocols [54, 70]. Their results confirmed an initial alendronate burst release of 40%±10% within the first hour of soaking in distilled deionized water. This is due to the disposition of AA on the surface struts which produces a strong chemical immobilization with the HA-coating and a physically weak association with the innermost, non-HA-coated struts [75]; therefore, resulting in an initial burst (diffusion of the weakly associated bisphosphonate from the innermost struts to the peri-implant space) followed by a slower and longer release of AA connected to the HA-coated struts.

A power analysis was performed to estimate the sample size required for detecting a difference in the bone formation parameters with and without alendronate coating. Increases of 60% combined with standard deviations of 40% were conservatively estimated based on prior canine studies using the same implant model [54, 70]. Setting the standard alpha error level of 0.05 and beta level error of 50%, the estimated (unpaired) sample size for each alendronate dose was 4.

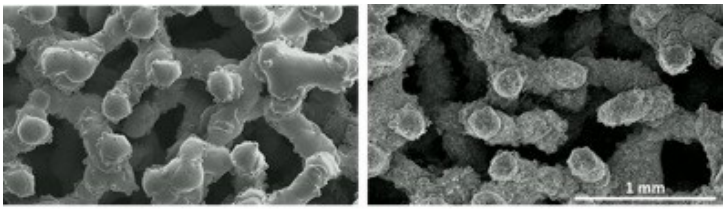

Figure 4.4 Scanning electron micrograph of the random porous structure without (left) and with (right) HA coating.

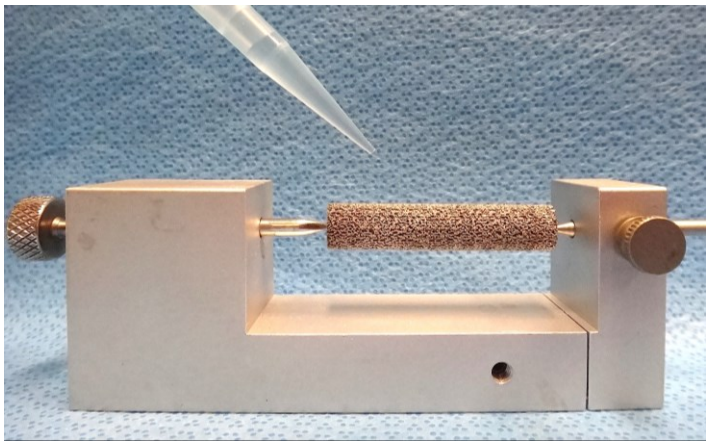

Figure 4.5 A photograph of the spindle-jig apparatus that was used to rotate the implant during the application of the AA aliquot solution so as to cover the entire surface of the implant.

4.2 Surgical Procedure

Fifteen healthy and skeletally mature mongrel dogs (age range: 3-9 years; mean: 5 years) weighing between 36 kg and 60 kg (mean: 43 kg) were used for this study. There were five dogs in each of the 3 AA dose cohorts (0.02 mg/cm^2, 0.06 mg/cm^2, and 0.18 mg/cm^2). In each dog, an open intramedullary nailing type of surgical procedure was utilized to position the implants in the proximal intramedullary canal of the femora and humeri (Table 4.1).

For each dog in the 3 dose cohorts, bilateral femoral surgery was initially performed using a 90 mm long AA-coated implant on one side and two 45 mm long control implants of BM and HA-coated, stacked directly on top of each other on the contralateral side (Figure 4.6). The most proximal of the femoral control implants had no coating of HA (BM), while the more distal implant was HA-coated. For the humeral surgery, one side received a 45 mm long AA-coated implant and the contralateral humerus received a 45 mm long BM control implant.

Approval was obtained from the Institutional Animal Care Review Committee. All dogs were prepared for surgery using an identical anaesthesia protocol. Approximately 30 minutes prior to surgery, a subcutaneous injection of 0.3 mg/ml Buprenorphine was given (McGill University, CMARC, Montreal, QC). Fifteen minutes before induction, the dog received a 10 mg/ml Butorphanol, 25 mg/ml Acepromazine, and 0.5 mg/ml Atropine (BAA) injection (CDMV, Saint-Hyacinthe, QC). A 100 μg fentanyl patch was placed on a shaved, mid-thoracic region (the effect starts within 12 hours and lasts for 72 hours) for postoperative analgesia. For induction, Sodium Pentobarbital (Somnotol) 54.7 mg/ml was given (McGill University, CMARC, Montreal, QC). The dog was then intubated and placed on a respirator. Anaesthesia was maintained with 1.5-2% isoflurane and 2L oxygen. Ventilation was set at 20 respirations per minute. Antibiotic prophylaxis was carried out with 500 mg/5ml of Cefazolin (CDMV, Saint-Hyacinthe, QC) given slowly by IV push prior to the start of surgery and repeated after skin closure.

Canine	Dose
1	0.06 mg/cm^2
2	0.18 mg/cm^2
3	0.02 mg/cm^2
4	0.06 mg/cm^2
5	0.06 mg/cm^2
6	0.18 mg/cm^2
7	0.02 mg/cm^2
8	0.02 mg/cm^2
9	0.06 mg/cm^2
10	0.18 mg/cm^2
11	0.02 mg/cm^2
12	0.18 mg/cm^2
13	0.06 mg/cm^2
14	0.02 mg/cm^2
15	0.18 mg/cm^2

Table 4.1 Experimental design summarizing the random assignment of subjects with the AA dose at the time of surgery.

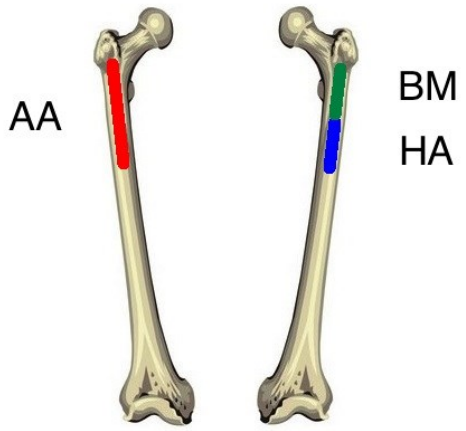

Figure 4.6 An Illustration showing the femoral implant placement of a 90 mm long AA-dosed implant on one side and the proximal BM and distal HA-coated 45 mm long control implants on the contralateral side.

For the bilateral femoral surgery, both hind legs were prepped for the insertion of the implants using standard sterile surgical techniques. A small lateral skin incision was made in the proximal end of the femur over the tip of the greater trochanter and extending proximally. After subcutaneous dissection, the posterior border of the guteus maximus muscle was identified and retracted anteriorly, exposing the greater trochanter and the piriformis fossa. A small spilt was made in the gluteus minimus muscle at the tip of the trochanter to allow direct entry of the drill into the piriformis fossa. Care was taken not to split the muscle proximally, to avoid injury to the superior gluteal nerve. A small, 5mm pilot hole was drilled through the femoral head neck region in order to broach the femoral canal. The canal was then progressively reamed up to 9 mm using femoral reamers (Figure 4.7). A porous coated AA-dosed implant, was impacted into the intramedullary canal and seated approximately 10 mm below the cortical surface of the proximal femur (Figure 4.8). The incision was closed in a standard manner using Vicryl sutures. The identical procedure was subsequently performed on the contralateral femur with control implants.

The entire operative procedure for both sides lasted approximately 1 hour. The dog was then extubated and given buprenorphine of 0.3 mg/ml as a subcutaneous injection (McGill University, CMARC, Montreal, QC). This dose of 0.01-0.02 mg/kg was given every 6-8 hours until 12-18 hours once the effects from the fentanyl patch begin. Postoperatively, another 500 mg/ml of cefazolin (CDMV, Saint-Hyacinthe, QC) was given intravenously. Then 25-50 mg/kg/day of the antibiotic cephalexin (500 mg/tab) (CDMV, Saint-Hyacinthe, QC) was given orally twice a day for 10 days, postoperatively.

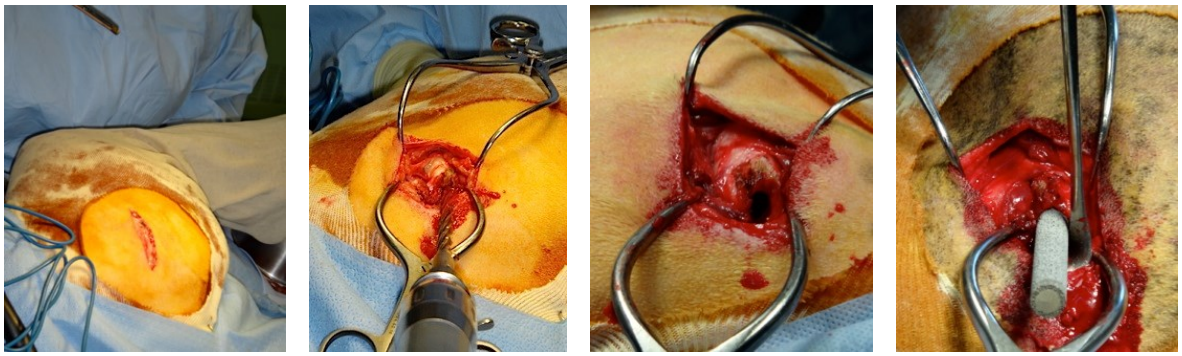

Figure 4.7 Intraoperative photographs illustrating the operative procedure. This is a right hip with the dog lying on his left side. Left: Skin incision located on the right proximal femur and extending proximally; Middle-left: A reamer inserted into the proximal femur to ream the intramedullary canal; Middle-right: The proximal femur has been reamed to create a 9 mm diameter canal in the proximal femur Right: The femoral implant is being positioned in the prepared canal opening for impaction into the intramedullary canal.

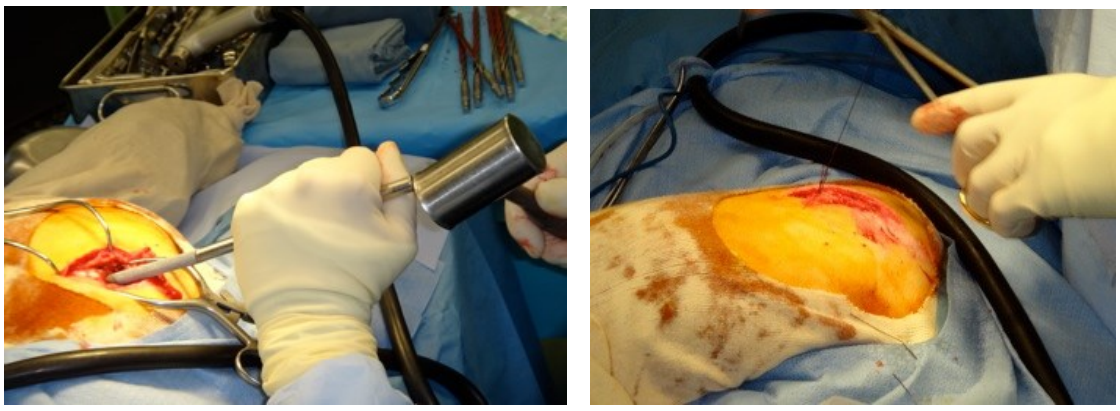

Figure 4.8 Intraoperative photographs illustrating the operative procedure. This is a right hip with the dog lying on his left side. Left: A punch is used to impact the 9 mm cylindrical implant into a canine's right proximal femoral intramedullary canal. Care is taken not to touch the implant or have soft tissue come in contact with the implant will being inserted; Right: Closing of incision site with Vicryl sutures.

Eight weeks after the bilateral femoral surgery, each dog in the 0.02 mg/cm^2 AA and 0.06 mg/cm^2 AA cohorts underwent bilateral humeral surgery. The humerus was approached surgically in a manner analogous to a humeral rodding. A small skin incision was made just distal and medial to the greater tuberosity and extended proximally. After subcutaneous dissection, the deltopectoral interval was identified and the deltoid muscle was retracted laterally, exposing the rotator cuff. A small vertical incision was made in the rotator cuff just medial and posterior to the anterior border of the proximal humerus. The humeral canal was then opened and reamed in an analogous fashion as described for the femur. Each canine received a 45 mm long AA-dosed implant on one side and the 45 mm long BM control on the contralateral humerus. The implant was inserted to be just below the subchondral bone, so that it was in the metaphysis of the proximal humerus. The surgical site was closed in layers using Vicryl sutures. Only one canine received the 0.18 mg/cm^2 AA humeral implants.

All dogs were euthanized 4 weeks after the second surgery and their femora and humeri were harvested. This yielded 4-week humeral specimens and 12-week femoral specimens. The harvested femora and humeri of each dog were manually stripped of soft tissue, radiographed (Figures 4.9 and 4.10) in the anteroposterior and lateral views with high-resolution film using a Hewlett Packard Faxitron (Oregon, USA).

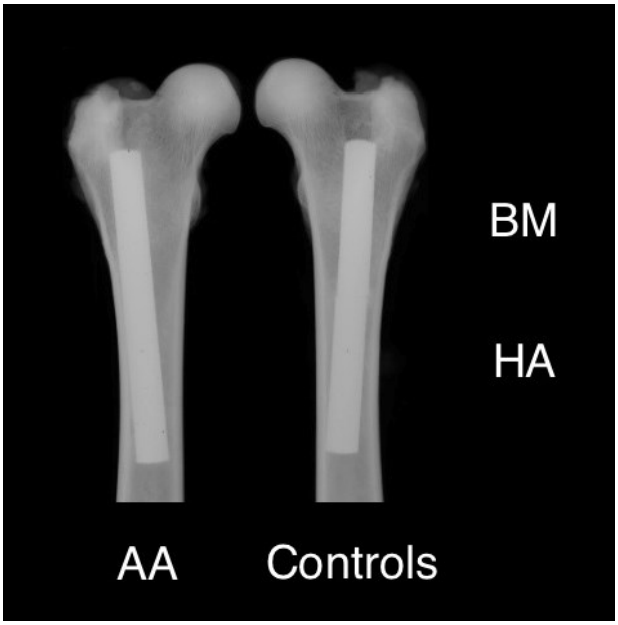

Figure 4.9 Contact radiograph of bilateral femora after sacrifice, demonstrating the placement of the femoral implants. The 90 mm long AA implant is on the left and the two stacked 45 mm control implants are on the right - there is no gap between the BM and HA control implants.

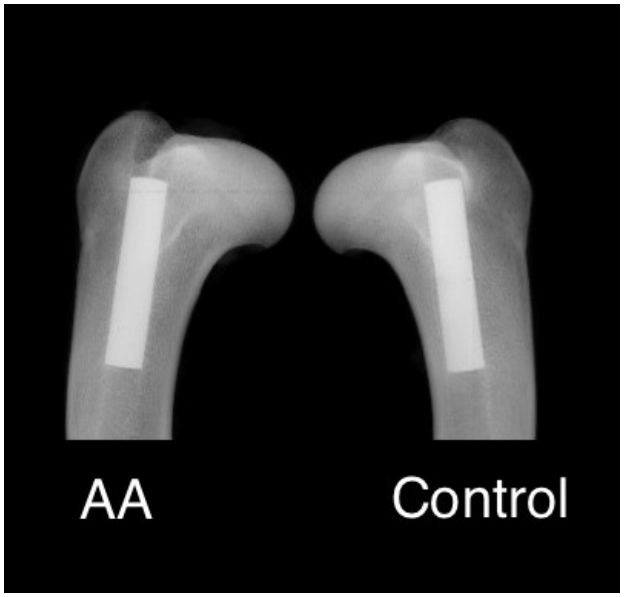

Figure 4.10 Contact radiograph of bilateral humeri after sacrifice, demonstrating the placement of the implants within the proximal metaphysis.

4.3 Undecalcified Thin Section Histology Procedure

All harvested bones underwent a dehydration process by being immersed in 75% ethanol (EtOH) for two days. Two mm drill holes were made at various points along the specimens to facilitate sufficient infiltration of the embedding solutions. Each specimen was kept in their own container and placed in 95% EtOH for another 2 days. A 1:1 ratio mixture of ether and acetone (E/A) was used for the defatting step for 2 days with one full day on a magnetic stirrer to agitate the solution. The specimens were placed in a 100% EtOH solution for the final dehydration step for another 2 days. This ensured the removal of both residual water and E/A. A 5% polymethylmethacrylate (PMMA) solution was prepared by mixing 4.5 g benzoyl peroxide (the catalyst) to 900 mL methylmethacrylate monomer. The samples began the infiltration process with the prepared 5% PMMA for four days where the mixture was kept at 4°C to ensure minimal polymerization. Individual specimens were transferred to their corresponding handmade aluminum boat for the process of the PMMA vacuum infiltration (Figure 4.11). Each specimen was subsequently vacuum infiltrated with a more polymerized and viscous 5% PMMA. After multiple days of repeated vacuum-on and vacuum-off cycles, samples were left at room temperature to cure and harden into clear acrylic blocks for approximately 6 weeks (Figure 4.12).

With a diamond-bladed cut-off machine (Buehler, Lake Bluff, Illinois), all hardened femoral and humeral acrylic blocks were then transversely cut at a low-speed to create 2-3 mm serial sections for undecalcified thin section histology (Figure 4.13).

Figure 4.11 Photograph of a canine femur in an aluminum bone boat with dimensions made according to size of the individual bone sample.

Figure 4.12 Photograph illustrating vacuum infiltration of a pair of femora contained in handmade aluminum boats filled with 5% PMMA.

Figure 4.13 Left: Photograph of the fully polymerized PMMA acrylic bone block with aluminum casing being removed; Right: Photograph of the PMMA acrylic block being cut transversely by a diamond blade precision saw into 2-3 mm thick sections.

4.4 Transverse Radiography Procedure

After completely sectioning each pair of femora and humeri, high-resolution contact radiographs of the thin transverse histological sections were made to allow for visual comparison between the control and AA coated implants (Hewlett Packard Faxitron, Oregon, USA) (Figure 4.14). Paired sections for analysis were matched according to their cortical bone anatomy, and chosen without any artificial drill holes that were made to assist in vacuum infiltration. The radiographs ensured that the sections to be imaged were without any artificial drill holes or large air pockets due to the embedding process. Three locations, the most proximal, middle, and most distal pairs were chosen for subsequent backscattered electron microscopy (BSEM) analysis. The 3 humeral pairs for each dog compared the AA-dosed implant and bare-metal control. There were 6 femoral pairs analyzed for each dog. The 90 mm AA-dosed implant was divided in half so that the proximal, middle and distal transverse sections of the proximal and distal halves were compared to its matched proximal 45 mm BM control and the distal 45 mm HA-coated control on the contralateral side (Figure 4.15).

4.5 Backscattered Scanning Electron Microscopy Procedure

The selected thin, transverse histological sections were polished by hand on a Buehler Polimet 1 Polisher (Markham, ON) beginning with the 120 grit silicon carbide abrasive disc and progressively ending at a 1200 grit size (Figure 4.16). The samples were then sputter-coated with gold-palladium under a vacuum for 3 minutes (Hummer VI sputtering system, Anatech LTD, Union City, USA). Digital BSEM images were produced at 25 kV, 100 μA, and with a magnification of 15-20X, on a Hitachi S-3000 VP-SEM, High Technologies America, Inc. (USA) (Figure 4.17). Due to the limitations of the machine, multiple images, ranging from 15-40, were taken to capture the entire sample; The BSEM images were manually stitched together using Adobe Photoshop CC to create the entire image for analysis.

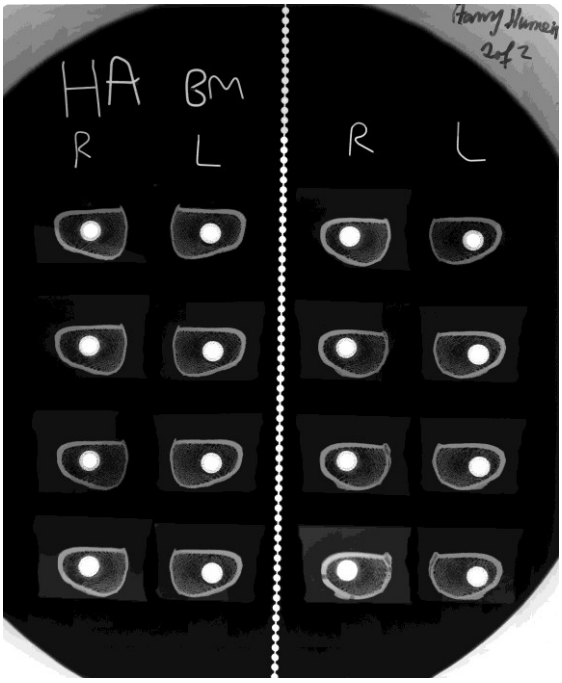

Figure 4.14 A contact radiograph of anatomically paired humeral histological transverse sections. The AA dosed implants are in the right humerus and the BM control is in the left.

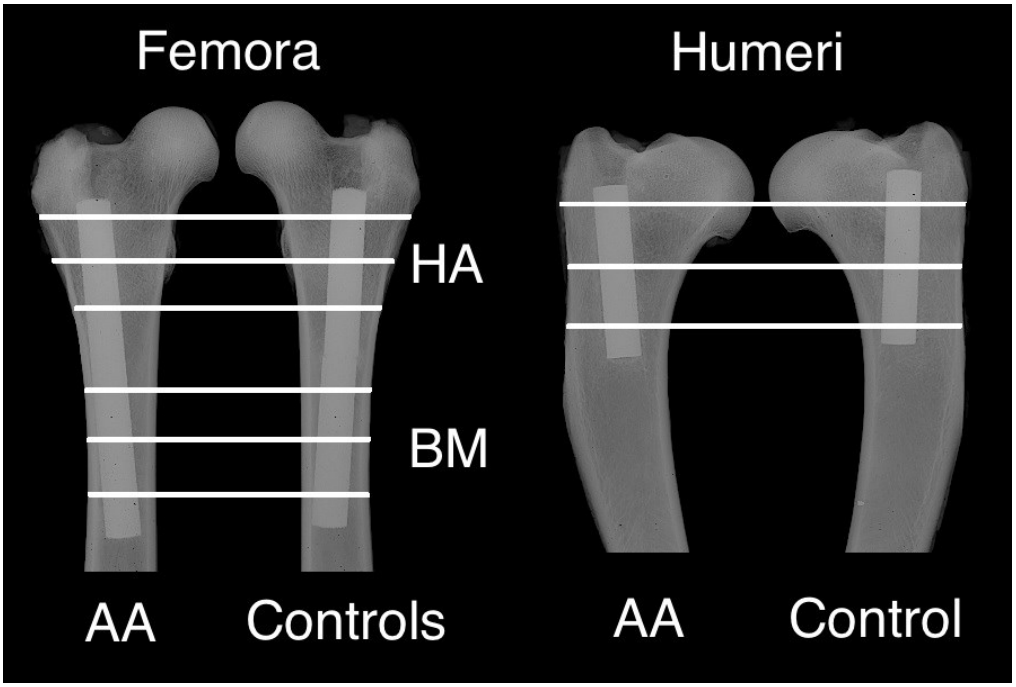

Figure 4.15 A Contact radiograph with labelled locations of the 6 pairs of femoral sections and 3 pairs of humeral sections selected for BSEM. The horizontal lines on the contact radiograph illustrate the regions selected for analysis.

Figure 4.16 Photograph illustrating the preparation for BSEM by polishing selected sections on a silicon carbide abrasive disc.

Figure 4.17 Photograph of the Hitachi S-3000 VP-SEM used for BSEM.

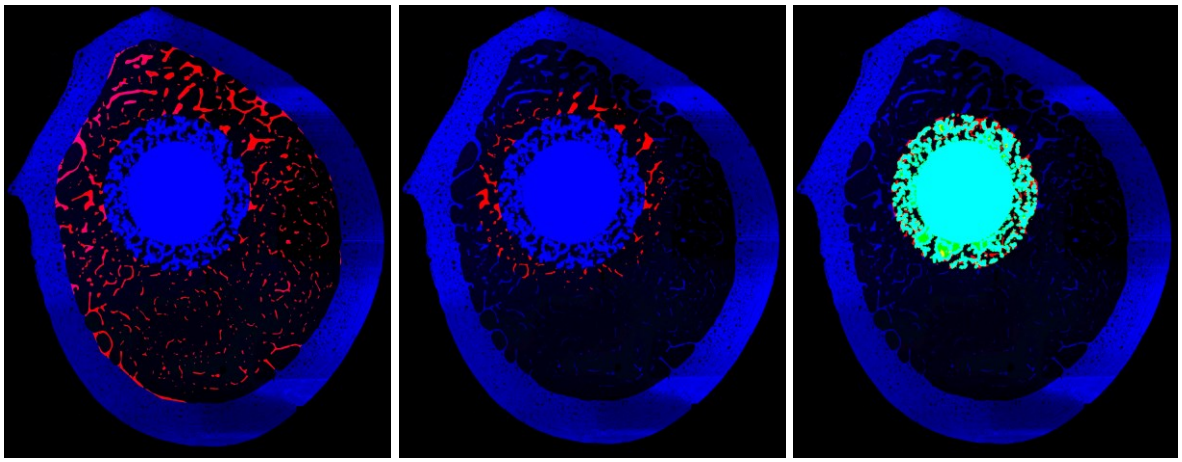

Figure 4.18 ImageJ images representing the analysis using (left) the total bone within the intramedullary space in red, (middle) the peri-implant area with the bone in red, (right) and the bone, in red, within the porous coating of the implant.

4.6 ImageJ Procedure

The grayscale-computerized images obtained from BSEM underwent analysis with the program ImageJ software version 1.47 (National Institutes of Health, Bethesda, MD) to detect and quantify bone ingrowth, bone apposition and peri-implant bone in association with each implant. ImageJ generates data through the differentiation of the grayscale image (Figure 4.18). It does so by assigning the shades to represent particular elements such as black to indicate void space, white to represent the implant, and gray to specify bone. A macro, written by Dr. Adam Hacking, PhD (a former student at JMORL), was used to best differentiate bone and the implant. Each section was run in triplicate to account for user variability and a mean value was generated for the 3 parameters.

Bone apposition was defined as the percentage of the implant perimeter that was in direct contact with bone (Figure 4.18). This is calculated by quantifying the total length of each bone segment that is completely at the interface of the implant then dividing that value by the circumference of the implant.

Bone ingrowth was defined as the percentage to which the bone has occupied the accessible space within the porous coating of the implant (Figure 4.19). The defined region of interest (ROI) was identified as the total area that the implant (seen as white) covered. The implant's area was subtracted from the total ROI to generate the remaining area as void space. Within this available space, the percentage of grey color was identified as bone. This value resulted in the percent bone ingrowth based on the total area minus the implant.

Peri-implant bone was defined as the area surrounding the implant (Figure 4.20). A radius of 2.5 mm from the implant was specified based on prior studies that showed that bone formation that resulted from local bisphosphonate elution was very localized to the peri-implant region [75]. Peri-implant bone was calculated by taking the percentage of bone found within the area of the 2.5 mm radius and dividing this by the total area defined by this medullary space, not including the area of the implant. To account for implants in contact with cortical bone or within the designated peri-implant space, the area occupied by the cortical bone was excluded.

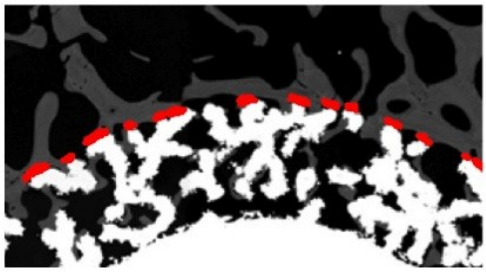

Figure 4.19 BSEM grayscale image with the implant seen as white, bone as gray, and void space as black. Bone apposition is defined as the percentage of the entire implant perimeter that was in direct contact with bone (seen in red).

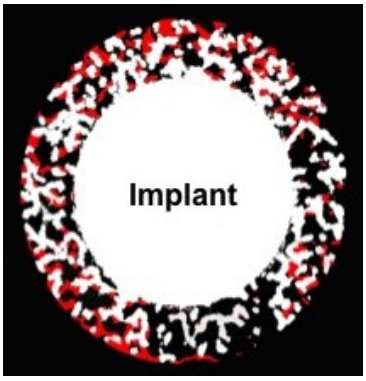

Figure 4.20 BSEM grayscale image with the implant seen as white, bone as gray, and void space as black. The bone ingrowth parameter, seen in red, is quantified by the percentage of bone found within the void space of the random porous coating.

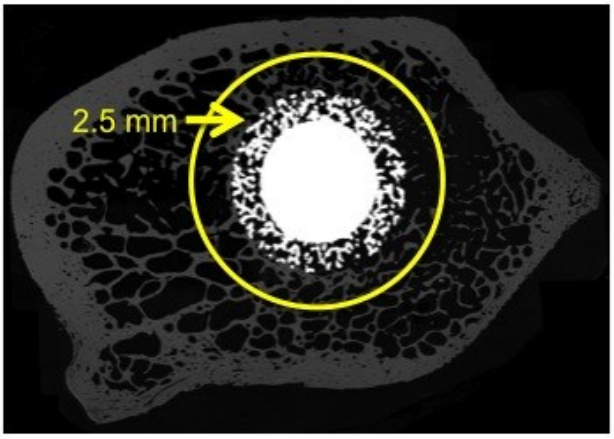

Figure 4.21 BSEM grayscale image with the implant seen as white, bone as gray, and void space as black. The peri-implant space of 2.5 mm, encircled in yellow, designates the area to be quantified.

4.7 Statistical Analysis

Means were taken from the data generated for bone apposition, bone ingrowth, and peri-implant bone for each humeral and femoral cohort in the 0.02 mg/cm^2, 0.06 mg/cm^2, and 0.18 mg/cm^2 AA dose according to their BM or HA-coated controls. Relative differences in the means for the AA-dosed implants with their corresponding controls were used to determine level of significance ($p \leq 0.05$). Each cohort was analyzed using paired Student's t tests.

CHAPTER 5. RESULTS

5.1 Post-Operative Follow-Up

It was observed on post-mortem radiography that the alendronate-coated implant of one dog in the 12-week 0.06mg/cm^2 AA cohort was surgically malpositioned and perforated the femoral intramedullary canal. Since this removed the possibility of paired data comparison, this dog was excluded from the data analysis. This resulted in the 4-week and 12-week humeral and femoral data for five dogs in the 0.02 mg/cm^2 AA and 0.18mg/cm^2 AA cohorts. In the 0.06mg/cm^2 AA cohort, there was 4-week humeral data for five dogs and 12-week femoral data for four dogs**.**

5.2 Post-Operative Radiography

The anteroposterior and lateral radiographs of both the humeri and the femora demonstrated no changes in the bone adjacent to any of the AA-dosed or control implants (Figure 5.1-5.3). There was no evidence of cancellous condensation (spot welds) or trabecular reorientation in any of the radiographs. All implants appeared stable with no evidence of migration, radiolucencies or pedestal formation. There were no cases of osteolysis. There was no noticeable difference in the amount of peri-implant bone for any of the doses based on plain radiograph inspection.

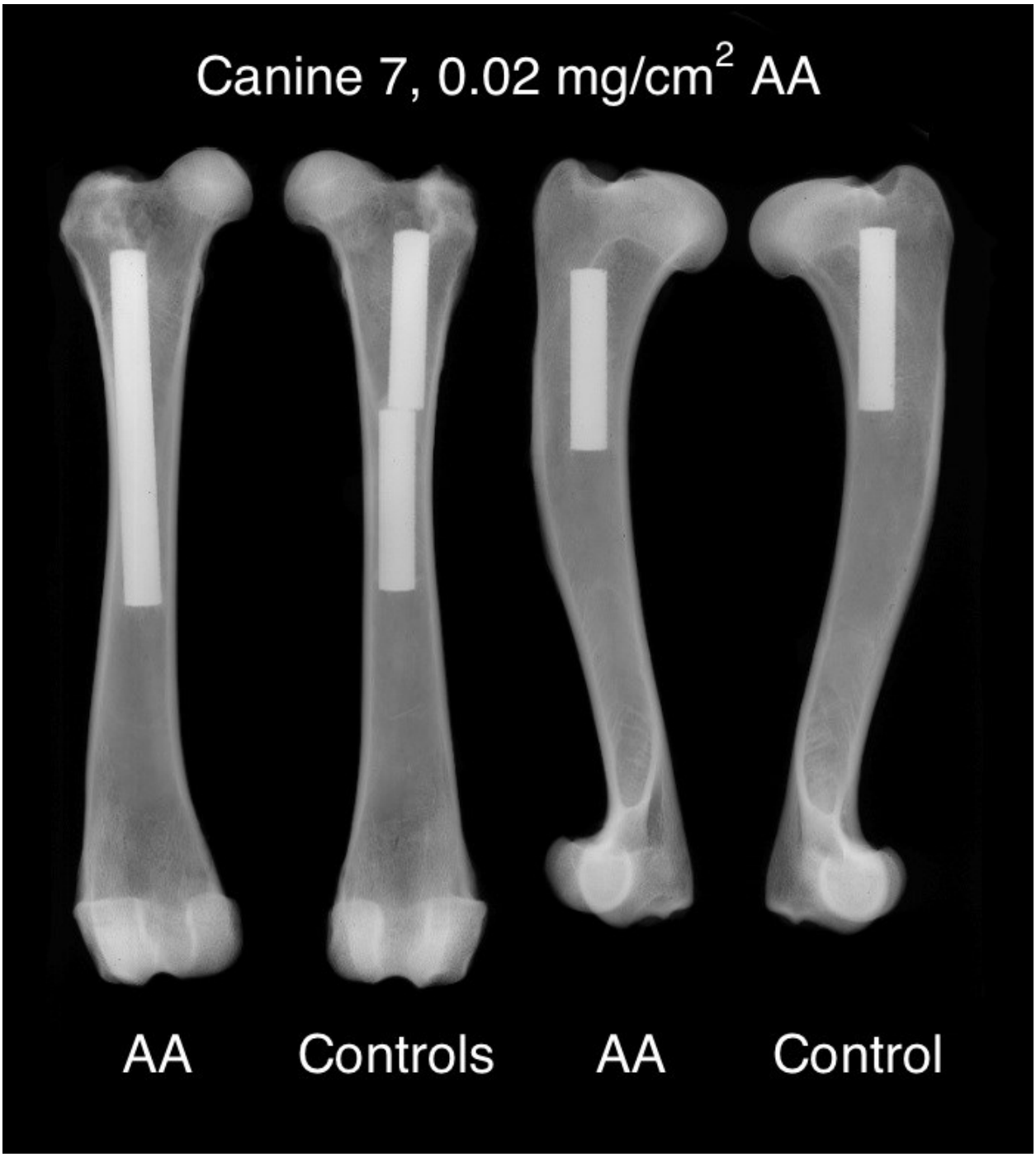

Figure 5.1 High-resolution contact anteroposterior radiograph of the femora (left) and humeri (right) in a 0.02 mg/cm^2 AA dose dog. The two femoral controls stacked upon each other are apparent. Note the absence of any reaction around the AA and control implants.

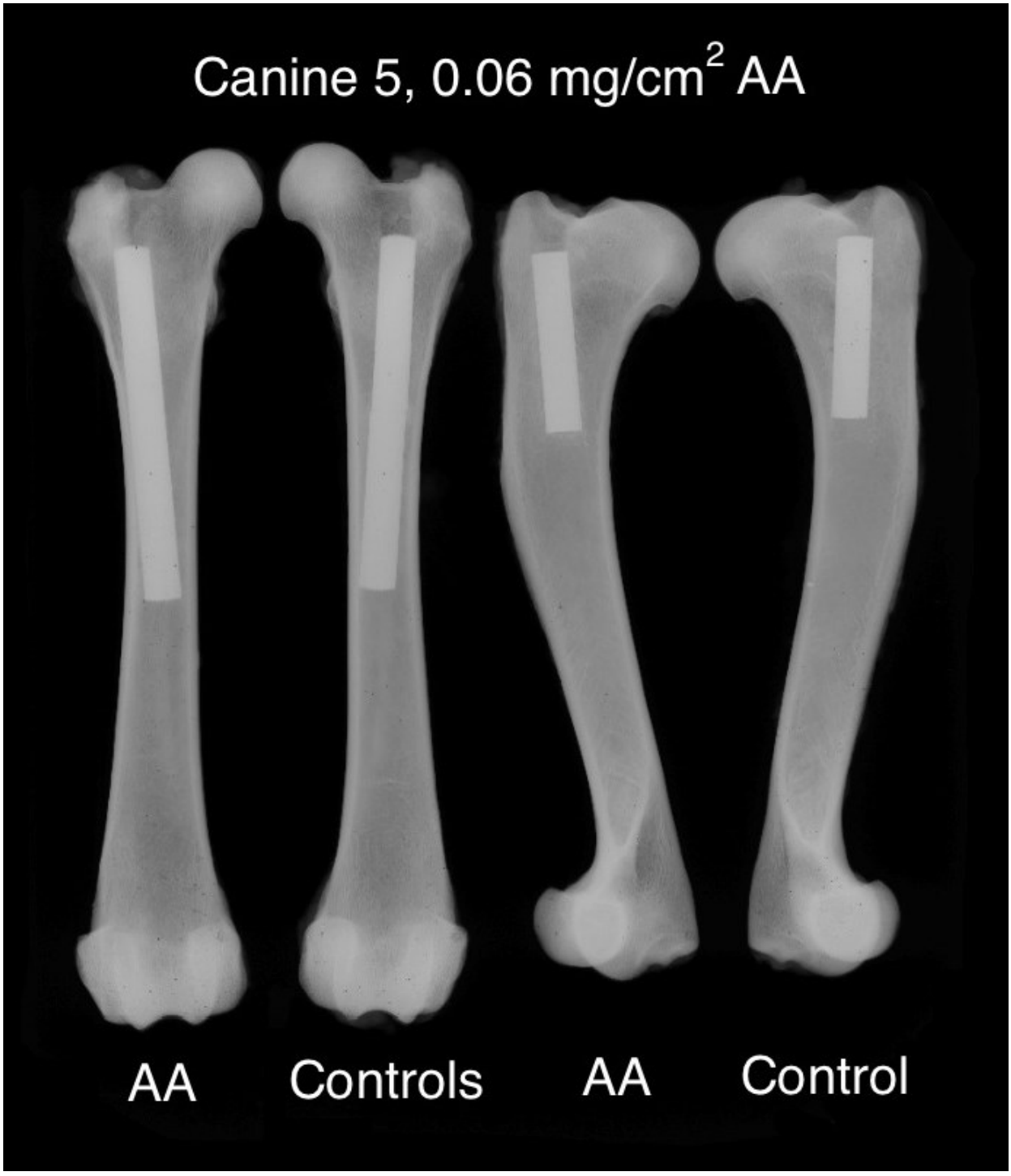

Figure 5.2 High-resolution contact anteroposterior radiograph of the femora (left) and humeri (right) in a 0.06 mg/cm^2 AA dose dog. The two femoral controls stacked upon each other are apparent. Note the absence of any reaction around the AA and control implants.

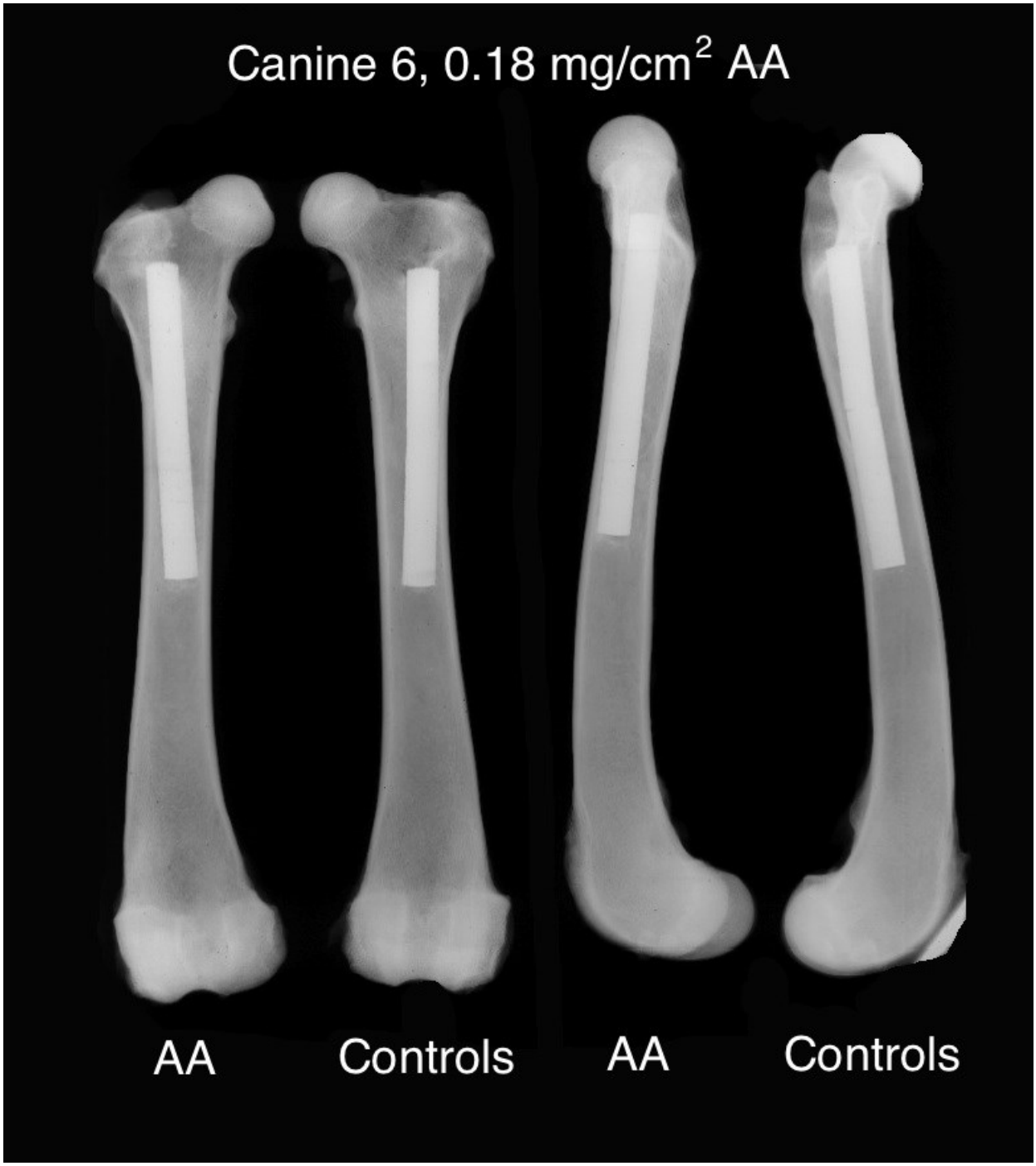

Figure 5.3 High-resolution contact anteroposterior (left pair) and lateromedial (right pair) radiograph of the femora in a 0.18 mg/cm^2 AA dose dog (left pair). The two femoral controls stacked upon each other are apparent. Note the absence of any reaction around the AA and control implants.

5.3 Undecalcified Thin Section Histology

Alendronate and control implants were surrounded by normal appearing bone with no evidence of radiographic loosening. The contact radiographs of all the control implants at 4- and 12-weeks demonstrated direct apposition of bone to the implant and varying degrees of bone formation and condensation of the peri-implant bone (Figures 5.4-5.8). A similar radiographic appearance was noted in the 0.02 mg/cm^2 AA dose cohort at 4- and 12-weeks. There was no apparent difference between the AA implants and the contralateral control implants at this dose (Figure 5.4). The 0.06 mg/cm^2 AA dose implants demonstrated direct apposition of bone to the implants with varying, but slightly increased, amounts of peri-implant bone formation and condensation as compared to the contralateral controls. The increased bone was seen within a few millimetres of the implant (Figure 5.6). Visual comparison of paired high-resolution radiographs of the thin transverse histologic sections from the 0.18 mg/cm^2 AA cohort demonstrated an obvious increase in peri- implant bone on the Alendronate side of the femur and humerus compared with controls (Figure 5.8). However, the femora in the 0.18 mg/cm^2 AA cohort consistently showed regions of gaps adjacent to the implant. The size and location of these gaps varied from implant to implant.

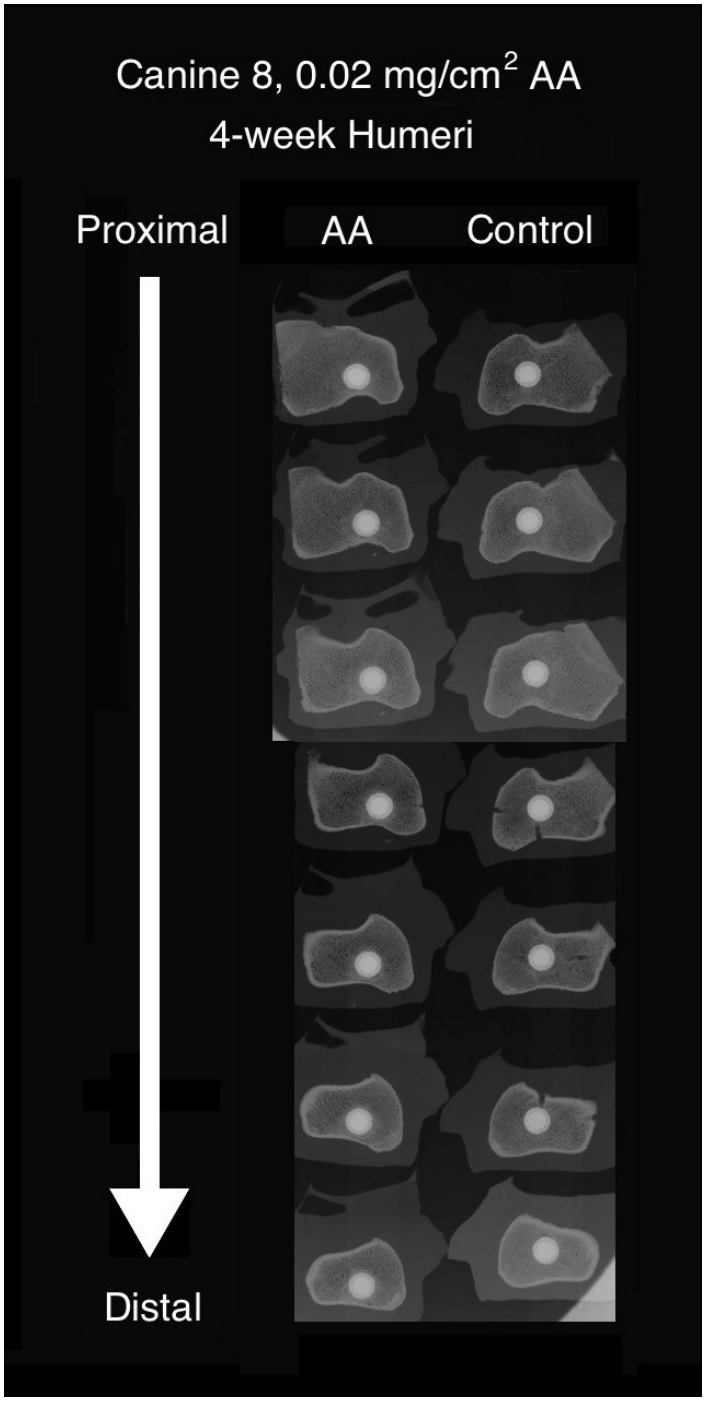

Figure 5.4 High-resolution contact anatomically paired transverse radiograph of the humeri in the 0.02 mg/cm^2 AA dose cohort. The sections are arranged from proximal to distal. Note the bone directly apposed to the implant. There is increased condensation of peri-implant bone in the AA implants. There is no evidence radiographic loosening.

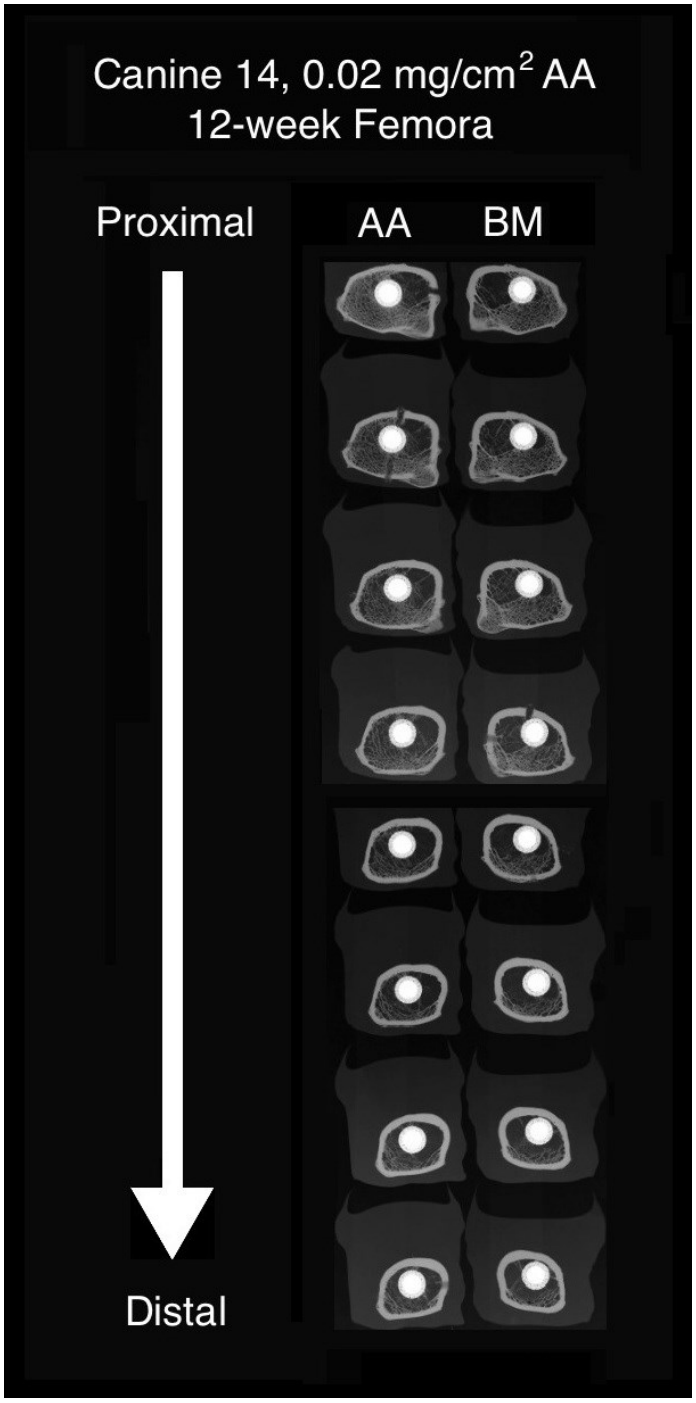

Figure 5.5 High-resolution contact anatomically paired transverse radiograph of the femora in the 0.02 mg/cm^2 AA dose cohort. The sections are arranged from proximal to distal. Note the bone directly apposed to the implant. There is increased condensation of peri-implant bone in the AA implants. There is no evidence radiographic loosening.

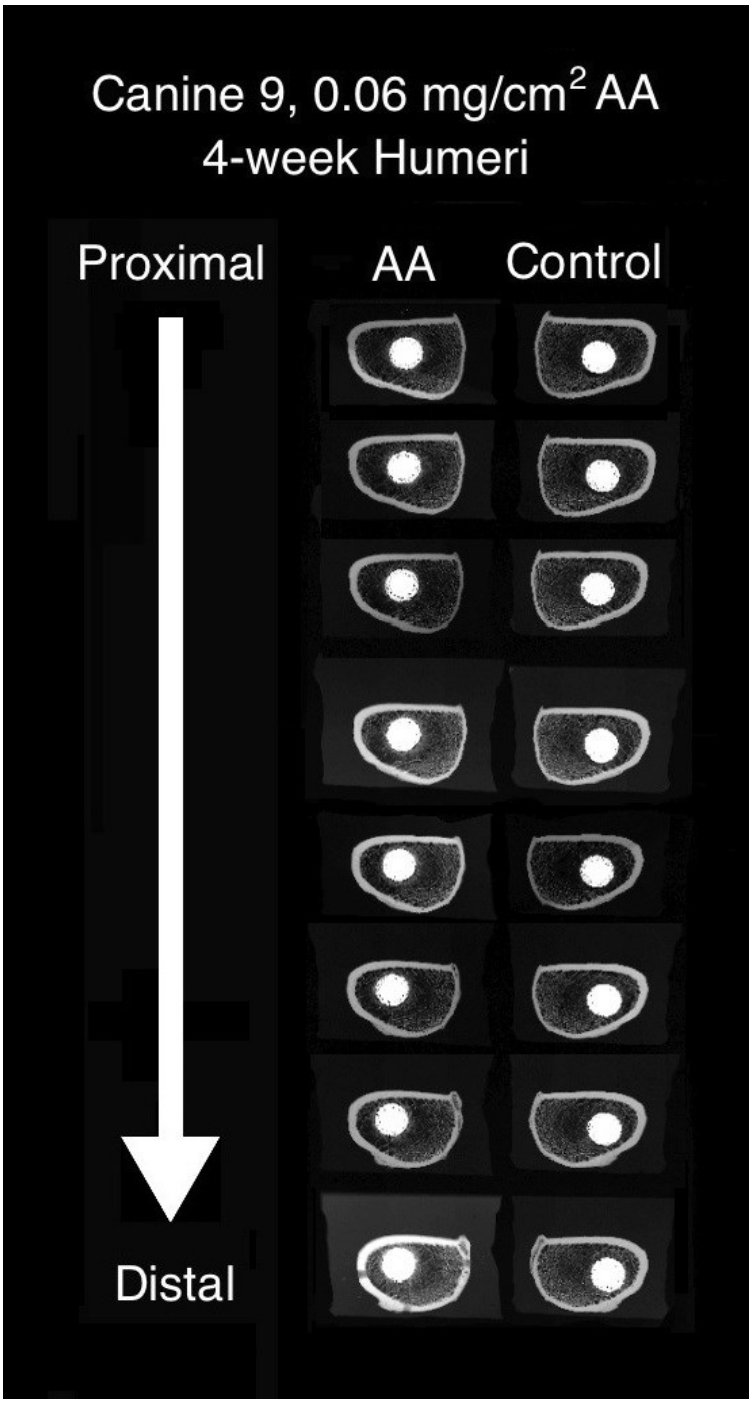

Figure 5.6 High-resolution contact anatomically paired transverse radiograph of the humeri in the 0.06 mg/cm^2 AA dose cohort. The sections are arranged from proximal to distal. Note the bone directly apposed to the implant. There is increased condensation of peri-implant bone in the AA implants. There is no evidence radiographic loosening.

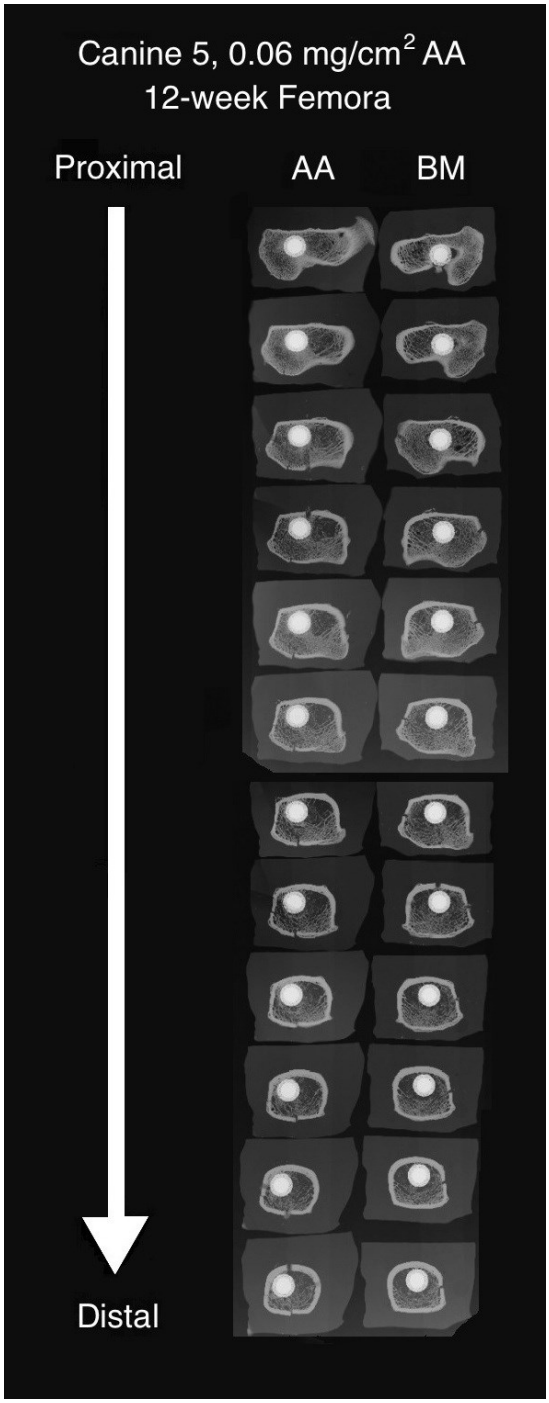

Figure 5.7 High-resolution contact anatomically paired transverse radiograph of the femora in the 0.06 mg/cm^2 AA dose cohort. The sections are arranged from proximal to distal. Note the bone directly apposed to the implant. There is increased condensation of peri-implant bone in the AA implants. There is no evidence radiographic loosening.

Figure 5.8 High-resolution contact anatomically paired transverse radiograph of the femora in the 0.18 mg/cm^2 AA dose cohort. The sections are arranged from proximal to distal. Note the bone directly apposed to the implant. There is increased condensation of peri-implant bone in the AA implants. Emphasized by the arrows are the areas of radiolucencies.

5.4 Backscattered Scanning Electron Microscopy

The BSEM images further corroborated and better defined the visual observations of the paired high-resolution radiographs of the thin transverse histologic sections. The Alendronate cohort showed demonstrated additional peri-implant bone compared with controls in both the humeri and femora. This difference was noticeably more pronounced with increasing Alendronate dose in the femora and for the two lower doses in the humeri.

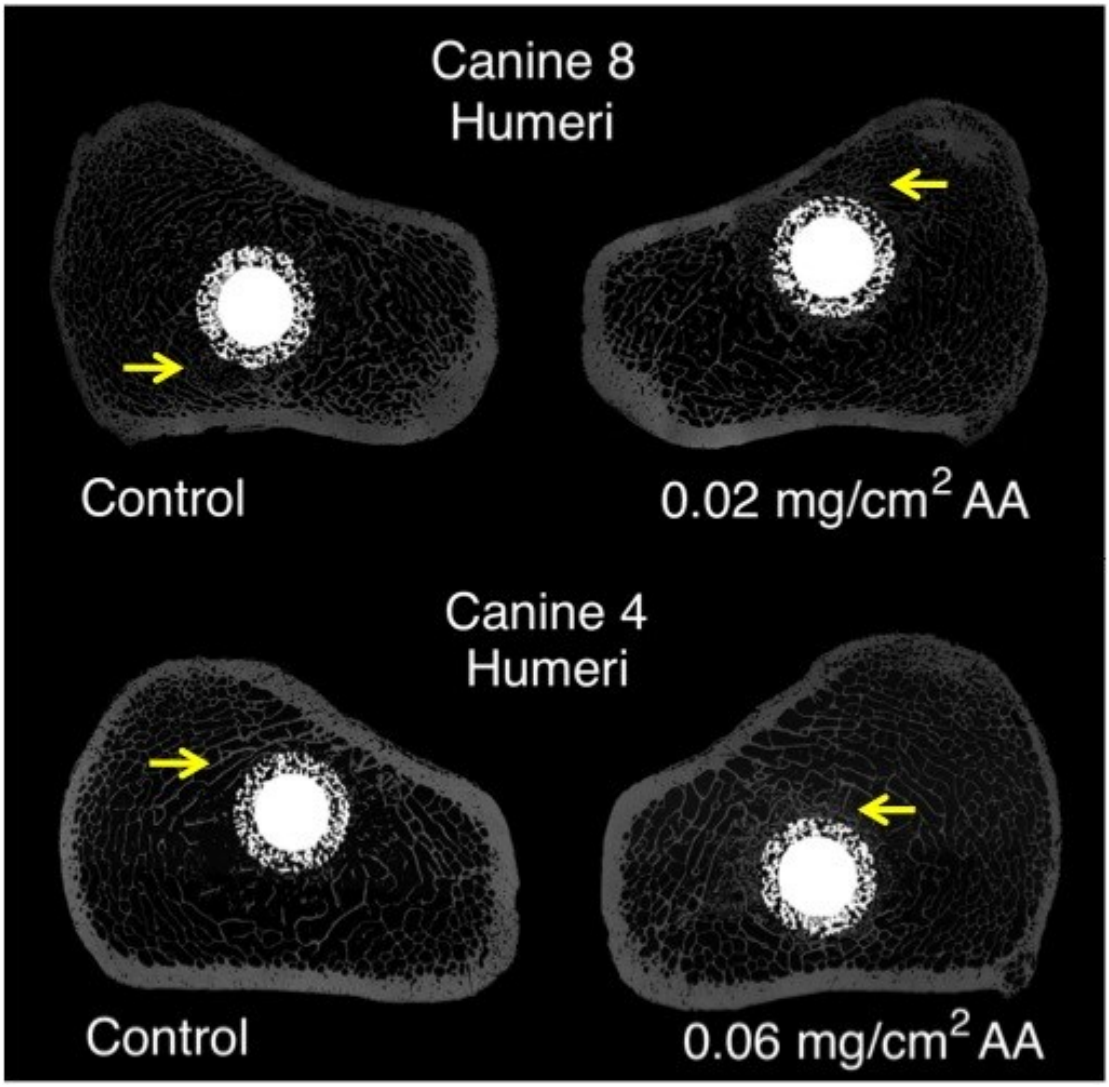

Figure 5.9 BSEM paired 4-week humeral images the 0.02 mg/cm^2 AA (top pair), and 0.06 mg/cm^2 AA (bottom pair) dose cohort. The sections are through the proximal metaphyseal region. Note the marked, localized, condensation and new bone formation adjacent to the AA implants.

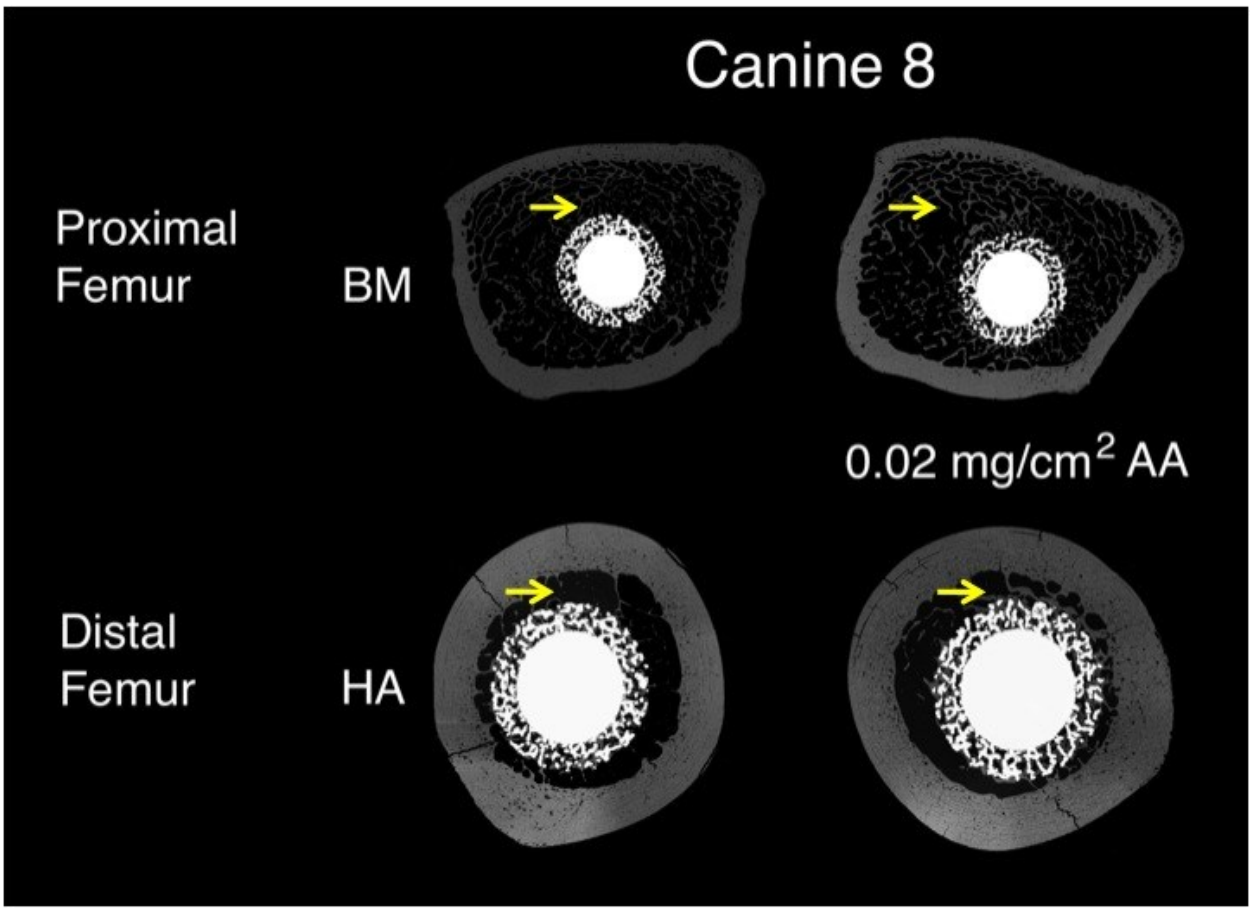

Figure 5.10 BSEM paired 12-week femoral images of the 0.02 mg/cm^2 AA dose cohort with both BM and HA controls. Note the increased peri-implant bone formation around the AA dosed implants as compared to the contralateral controls. The bone response is increased with increasing dose of AA.

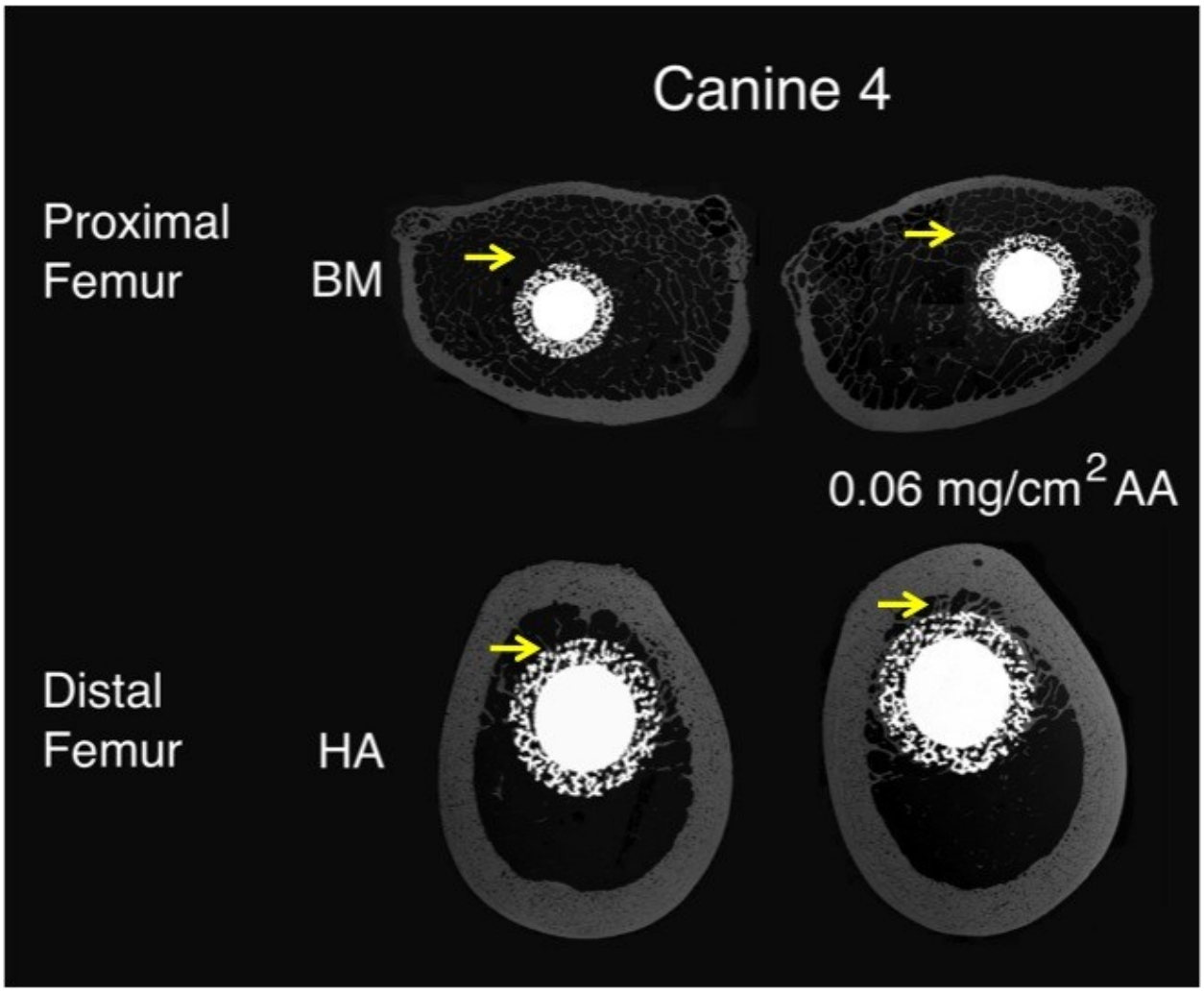

Figure 5.11 BSEM paired 12-week femoral images of the 0.06 mg/cm^2 AA dose cohort with both BM and HA controls. Note the increased peri-implant bone formation around the AA dosed implants as compared to the contralateral controls. The bone response is increased with increasing dose of AA.

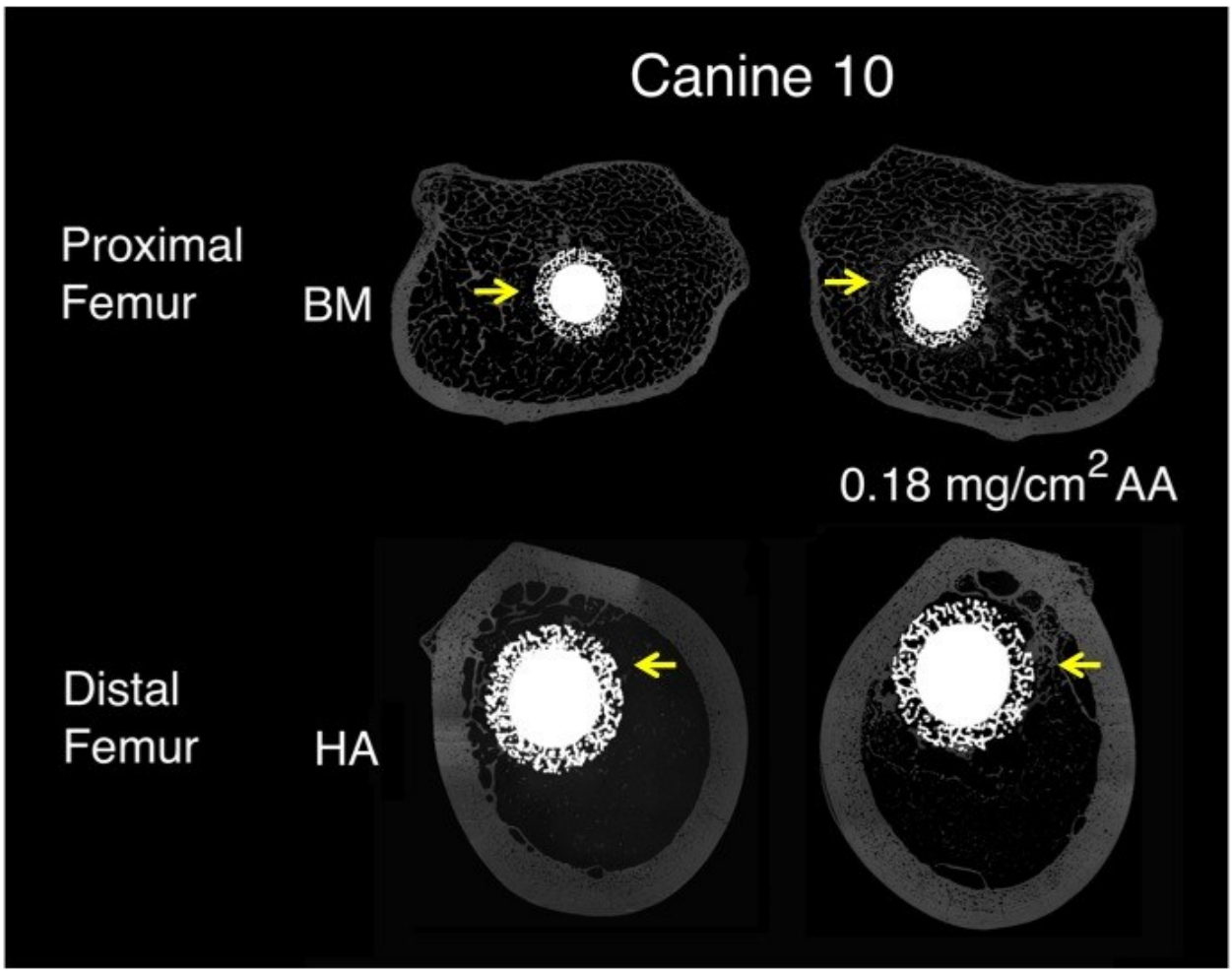

Figure 5.12 BSEM paired 12-week femoral images of the 0.18 mg/cm^2 AA dose cohort with both BM and HA controls. Note the increased peri-implant bone formation around the AA dosed implants as compared to the contralateral controls. There is an increase in peri-implant bone formation around the AA-dosed implant identified by the arrow with the presence of a gap in the proximal femur AA-dosed implant.

5.5 ImageJ Quantification

In Tables 5.1-5.5, the three parameters are shown as a summary for the mean values of all the canines within their respective doses and time points.

The bone ingrowth, bone apposition, peri-implant bone for the 0.02 mg/cm^2 AA dose at four weeks had an average of 24.5%, 33.9%, and 27.3% compared to their controls which were 19.9%, 25.5%, and 18.9%, respectively (Table 5.1). At the 0.06 mg/cm^2 AA dose, the parameters had averages of 13.1%, 24.4%, and 32.8% compared to the controls with 14.3%, 20.0%, and 14.1%, respectively (Table 5.1).

The 12-week femora at the 0.02 mg/cm^2 AA dose had a mean measurement of 25.0%, 24.3%, and 14.2% for bone ingrowth, bone apposition, peri-implant bone, respectively. The BM control values for the parameters in the same order were 21.9%, 17.9%, and 11.5% (Table 5.2). In the 0.06 mg/cm^2 AA dose for the femora, averages obtained for bone ingrowth, bone apposition, peri-implant bones were 22.2%, 24.3%, and 14.2%, respectively. The corresponding BM controls were 22.1%, 16.3%, and 9.1%, respectively (Table 5.2). For the upper dose of 0.18 mg/cm^2 AA compared to the BM control, the acquired averages were 9.4% versus 16.2%, 20.8% versus 17.3%, and 22.7% versus 10.6%, respectively (Table 5.2).

For the femora, bone ingrowth, bone apposition, and peri-implant bone was 26.9%, 26.8%, and 6.4%, for the 0.02 mg/cm^2 AA cohort respectively and 27.1%, 19.1%, and 7.9%, respectively for the HA controls (Table 5.3). The femora in the 0.06 mg/cm^2 AA cohort were found to have 21.6%, 22.2%, and 9.0% bone ingrowth, bone apposition, and peri-implant bone, respectively. The corresponding HA controls averaged 25.5%, 13.9%, and 4.5%, respectively. Finally, the mean bone ingrowth, mean bone apposition, and mean peri-implant bone for 0.18 mg/cm^2 AA implants compared to the HA control were 15.1% versus 22.1%, 24.3% versus 19.6%, and 14.1% versus 8.5%, respectively (Table 5.3).

For the 4-week humeri, the relative differences of bone ingrowth, bone apposition, and peri-implant bone between the 0.02 mg/cm^2 AA cohort and the contralateral controls was +34%, +42%, and +60%, respectively (Table 5.4). In the 0.06 mg/cm^2 AA dose cohort, the relative differences in these parameters were -4%, +20%, and +135%, respectively (Table 5.4).

Relative differences for the 12-week femora in the 0.02 mg/cm^2 AA cohort compared its BM control were +7%, +44%, and +46%, with respect to bone ingrowth, bone apposition, and peri-implant bone (Figure 5.5). In the 0.06 mg/cm^2 AA dose cohort, a relative difference of +37%, +82%, and +92%, were obtained for the three parameters when compared to the contralateral controls (Figure 5.5). Finally, the 0.18 mg/cm^2 AA cohort had 35% less bone ingrowth, 17% more bone apposition, and 114% peri-implant bone compared to the contralateral controls (Figure 5.5).

The relative differences for the 12-week femora in the 0.02 mg/cm^2 AA cohort compared its HA control were -6%, +45%, and +4%, with respect to bone ingrowth, bone apposition, and peri-implant bone (Figure 5.5). In the 0.06 mg/cm^2 AA dose cohort, a relative difference of -3%, +85%, and +108%, were obtained for the three parameters when compared to the contralateral controls (Figure 5.5). Finally, the 0.18 mg/cm^2 AA cohort had 7% less bone ingrowth, 5% more bone apposition, and 6% peri-implant bone compared to the contralateral controls (Figure 5.5).

4-Weeks	**Bone Ingrowth**		**Bone Apposition**		**Peri-Implant Bone**	
AA Dose	**BM**	**AA**	**BM**	**AA**	**BM**	**AA**
0.02 mg/cm^2	19.9 ± 11.8	24.5 ±10.8	25.5 ± 13.6	33.9 ± 17.3	18.9 ± 12.0	27.3 ± 13.5
0.06 mg/cm^2	14.3 ± 5.3	13.1 ± 7.1	20.0 ± 2.0	24.4 ± 8.6	14.1 ± 1.1	32.8 ± 8.8

Table 5.1 Mean values of bone ingrowth, bone apposition, and peri-implant bone for the 4-week humeral at 0.02 mg/cm^2 AA, and 0.06 mg/cm^2 AA with BM controls.

12-Weeks	Bone Ingrowth		Bone Apposition		Peri-Implant Bone	
AA Dose	BM	AA	BM	AA	BM	AA
0.02 mg/cm^2	20.8 ± 7.6	22.2 ± 8.0	17.1 ± 6.5	23.3 ± 8.8	10.9 ± 6.7	14.1 ± 7.7
0.06 mg/cm^2	20.6 ± 13.2	26.1 ± 12.1	14.3 ± 4.0	25.4 ± 7.1	8.1 ± 2.7	13.8 ± 1.6
0.18 mg/cm^2	16.5 ± 5.0	10.6 ± 5.7	18.4 ± 3.2	22.2 ± 9.4	11.2 ± 3.5	23.6 ± 6.5

Table 5.2 Mean values of bone ingrowth, bone apposition, and peri-implant bone for the 12-week femora at 0.02 mg/cm^2 AA, 0.06 mg/cm^2, and 0.18 mg/cm^2 with BM controls.

12-Weeks	Bone Ingrowth		Bone Apposition		Peri-Implant Bone	
AA Dose	HA	AA	HA	AA	HA	AA
0.02 mg/cm^2	27.1 ± 6.9	26.9 ± 14.4	19.1 ± 7.2	26.8 ± 10.6	7.9 ± 4.3	6.4 ± 2.9
0.06 mg/cm^2	25.5 ± 11.3	21.6 ± 13.4	13.9 ± 5.6	22.2 ± 8.0	4.5 ± 1.4	9.0 ± 2.2
0.18 mg/cm^2	22.1 ± 6.5	15.1 ± 18.7	19.6 ± 4.3	24.3 ± 25.3	8.5 ± 2.0	14.1 ± 8.6

Table 5.3 Mean values of bone ingrowth, bone apposition, and peri-implant bone for the 12-week femora at 0.02 mg/cm^2 AA, 0.06 mg/cm^2, and 0.18 mg/cm^2 with HA controls.

4-Week Humeri	Bone Ingrowth	Bone Apposition	Peri-Implant Bone
0.02 mg/cm^2 AA	+34%	+42%	+60%
0.06 mg/cm^2 AA	-4%	+20%	+135%

Table 5.4 Relative differences of bone ingrowth, bone apposition, and peri-implant bone for corresponding doses of 0.02 mg/cm^2 AA, 0.06 mg/cm^2 AA, and 0.18 mg/cm^2 AA with their controls, BM and HA.

	Bone Ingrowth		Bone Apposition		Peri-Implant Bone	
12-Week Femora	**BM**	**HA**	**BM**	**HA**	**BM**	**HA**
0.02 mg/cm^2 AA	+7%	-6%	+44%	+45%	+46%	+4%
0.06 mg/cm^2 AA	+37%	-3%	+82%	+85%	+92%	+108%
0.18 mg/cm^2 AA	-35%	-7%	+17%	+5%	+114%	+6%

Table 5.5 Relative differences of bone ingrowth, bone apposition, and peri-implant bone for corresponding doses of 0.02 mg/cm^2 AA, 0.06 mg/cm^2 AA, and 0.18 mg/cm^2 AA with their controls, BM and HA.

5.6 Statistical Analysis

Statistical analysis comparing the mean bone ingrowth, mean bone apposition and mean peri-implant bone for the 0.02 mg/cm^2 AA, 0.06 mg/cm^2 AA, and 0.18 mg/cm^2 AA dosed implants compared to mean of their contralateral controls are displayed in tables and bar graphs.

5.6.1 Humeri with Bare Metal Controls

Bone Ingrowth	BM Control	0.02 mg/cm^2 AA	BM Control	0.06 mg/cm^2 AA
Mean	19.9	24.5	14.3	13.1
Standard Deviation	11.8	10.8	5.3	7.1
Standard Error	5.3	4.9	2.4	3.2
P-Value	0.07		0.33	

Table 5.6 Statistical overview of the 4-week humeri for bone ingrowth between the 0.02 mg/cm^2 AA and 0.06 mg/cm^2 AA compared to their bare metal control (BM).

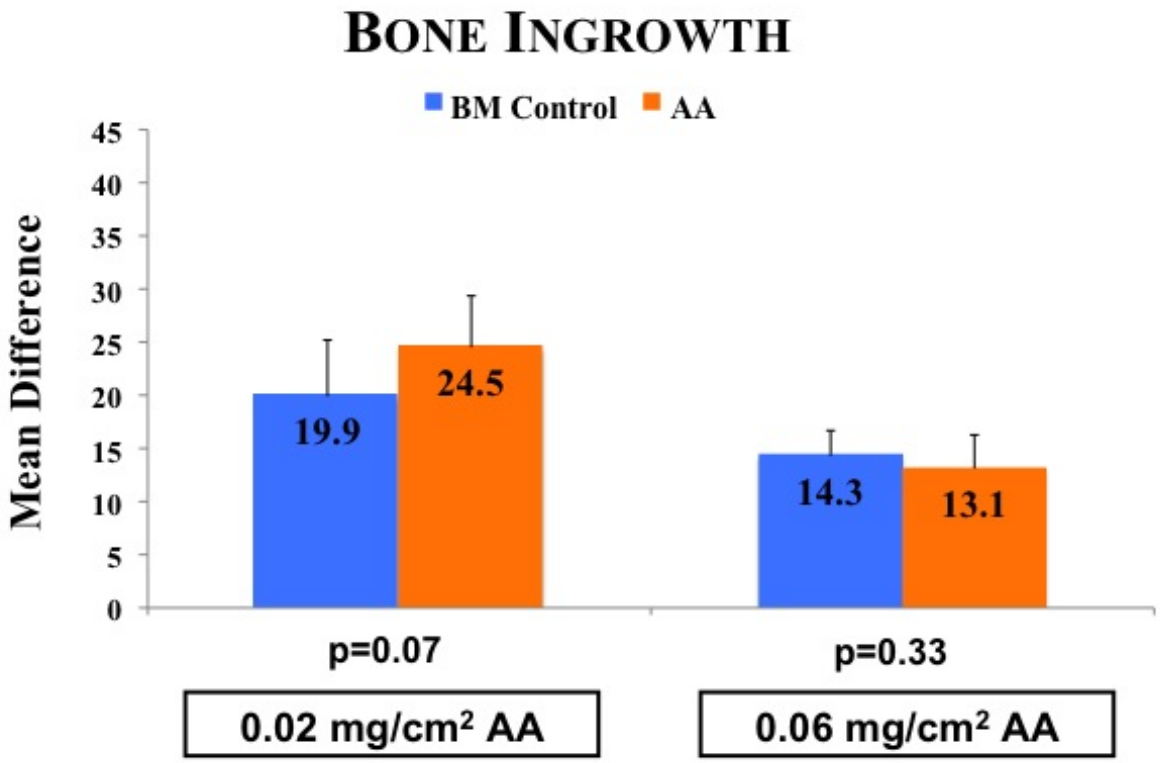

Figure 5.13 Graphical representation of the statistical overview of the 4-week humeri for bone ingrowth between the 0.02 mg/cm^2 AA and 0.06 mg/cm^2 AA compared to their BM control.

Bone Apposition	Control	0.02 mg/cm^2 AA	Control	0.06 mg/cm^2 AA
Mean	24.5	33.9	20.0	24.4
Standard Deviation	13.6	17.3	2.0	8.6
Standard Error	6.1	7.7	0.9	3.8
P-Value	0.01*		0.13	

Table 5.7 Statistical overview of the 4-week humeri for bone apposition between the 0.02 mg/cm^2 AA and 0.06 mg/cm^2 AA compared to their BM control. Significance, $p<0.05$ is represented by an asterisk (*).

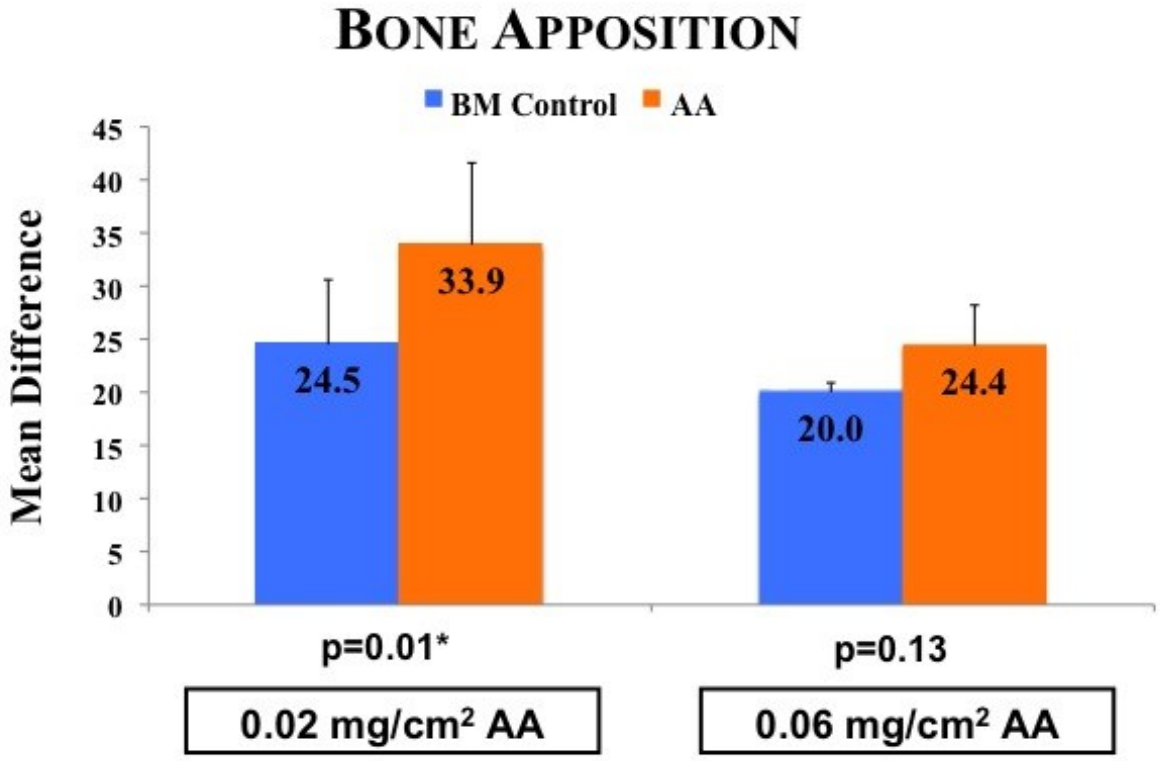

Figure 5.14 Graphical representation of the statistical overview of the 4-week humeri for bone apposition between the 0.02 mg/cm^2 AA and 0.06 mg/cm^2 AA compared to their BM control. Significance, $p<0.05$ is represented by an asterisk (*).

Peri-Implant Bone	Control	0.02 mg/cm^2 AA	Control	0.06 mg/cm^2 AA
Mean	18.9	27.3	14.1	32.8
Standard Deviation	12.0	13.5	1.1	8.8
Standard Error	5.4	6.0	0.5	3.9
P-Value	0.01*		0.01*	

Table 5.8 Statistical overview of the 4-week humeri for peri-implant bone between the 0.02 mg/cm^2 AA, and 0.06 mg/cm^2 AA compared to their BM control. Significance, $p<0.05$ is represented by an asterisk (*).

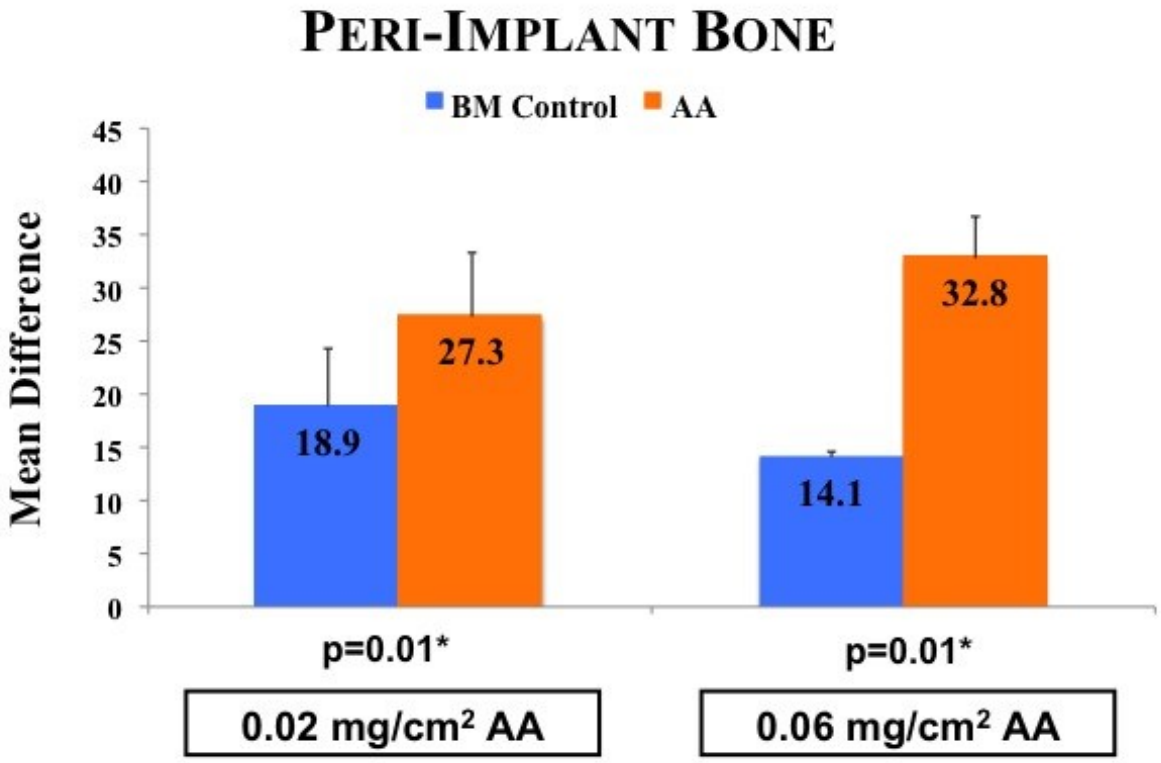

Figure 5.15 Graphical representation of the statistical overview of the 4-week humeri for peri-implant bone between the 0.02 mg/cm^2 AA and 0.06 mg/cm^2 AA compared to their BM control.

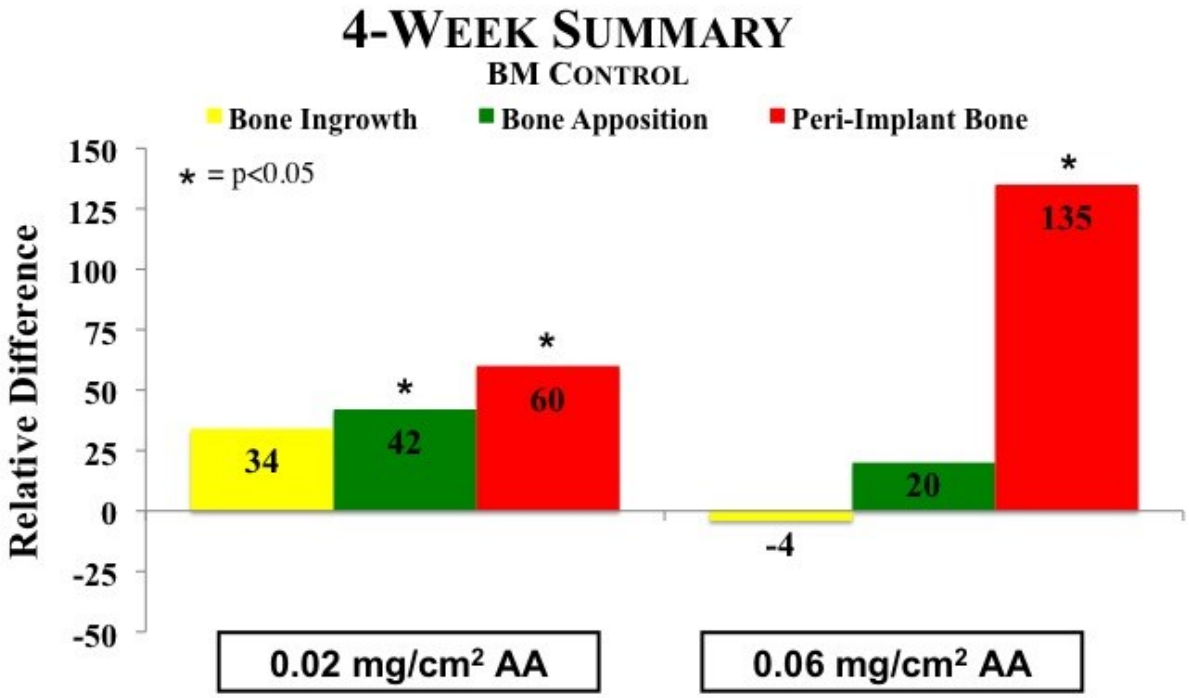

Figure 5.16 Summary of the 4-week humeral relative differences with the 0.02 mg/cm^2 AA, and 0.06 mg/cm^2 AA dose compared to their BM control. Asterisks (*) show a significance of p<0.05.

5.6.2 Femora with Bare Metal Controls

Bone Ingrowth	0.02 mg/cm^2 AA		0.06 mg/cm^2 AA		0.18 mg/cm^2 AA	
	BM	AA	BM	AA	BM	AA
Mean	21.9	25.0	22.1	22.2	16.2	9.4
Standard Deviation	8.0	10.4	16.0	4.6	4.6	4.1
Standard Error	3.6	4.6	8.0	2.3	2.1	1.8
P-Value	0.17		0.49		0.02*	

Table 5.9 Statistical overview of the 12-week femora for bone ingrowth between the 0.02 mg/cm^2 AA, 0.06 mg/cm^2 AA and 0.18 mg/cm^2 AA compared to their BM control. Significance, p<0.05 is represented by an asterisk (*).

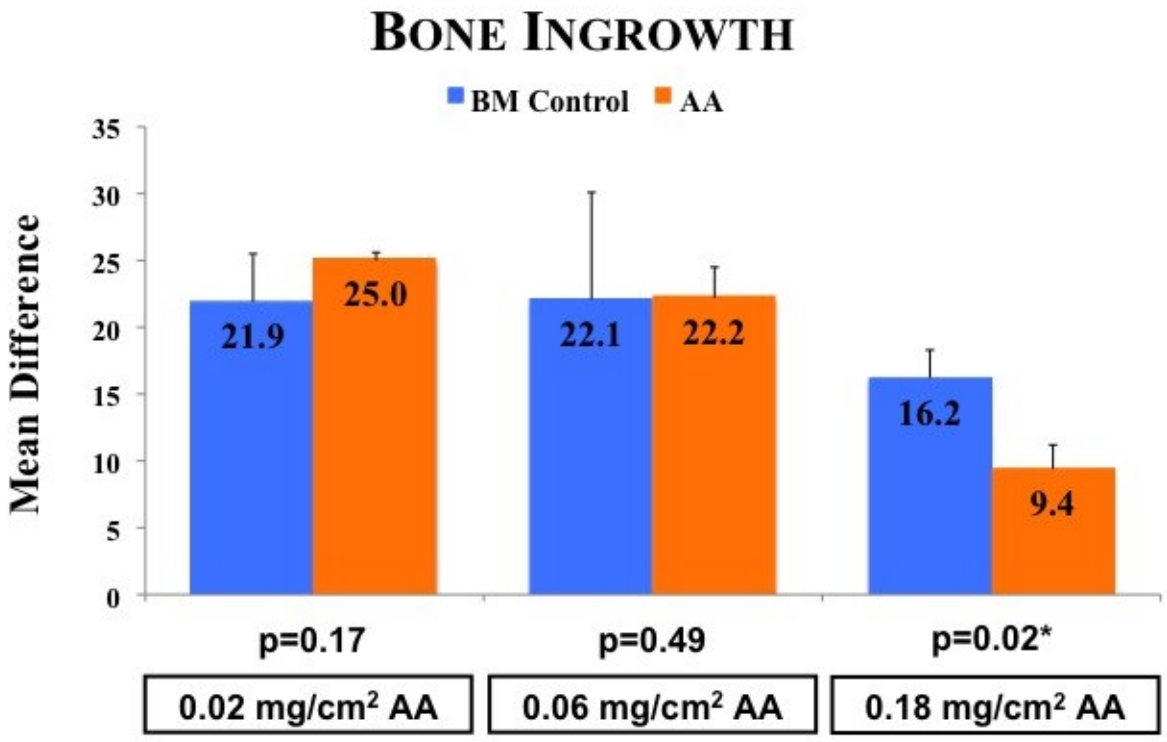

Figure 5.17 Graphical representation of the statistical overview of the 12-week femora for bone ingrowth between the 0.02 mg/cm^2 AA, 0.06 mg/cm^2 AA and 0.18 mg/cm^2 AA dose compared to their BM control.

Bone Apposition	0.02 mg/cm^2 AA		0.06 mg/cm^2 AA		0.18 mg/cm^2 AA	
	BM	AA	BM	AA	BM	AA
Mean	17.9	24.3	16.3	24.9	17.3	20.8
Standard Deviation	5.6	7.3	3.9	6.6	2.1	7.7
Standard Error	2.5	3.3	1.9	3.3	0.9	3.4
P-Value	0.07		0.02*		0.14	

Table 5.10 Statistical overview of the 12-week femora for bone apposition between the 0.02 mg/cm^2 AA, 0.06 mg/cm^2 AA and 0.18 mg/cm^2 AA compared to their BM control. Significance, p<0.05 is represented by an asterisk (*).

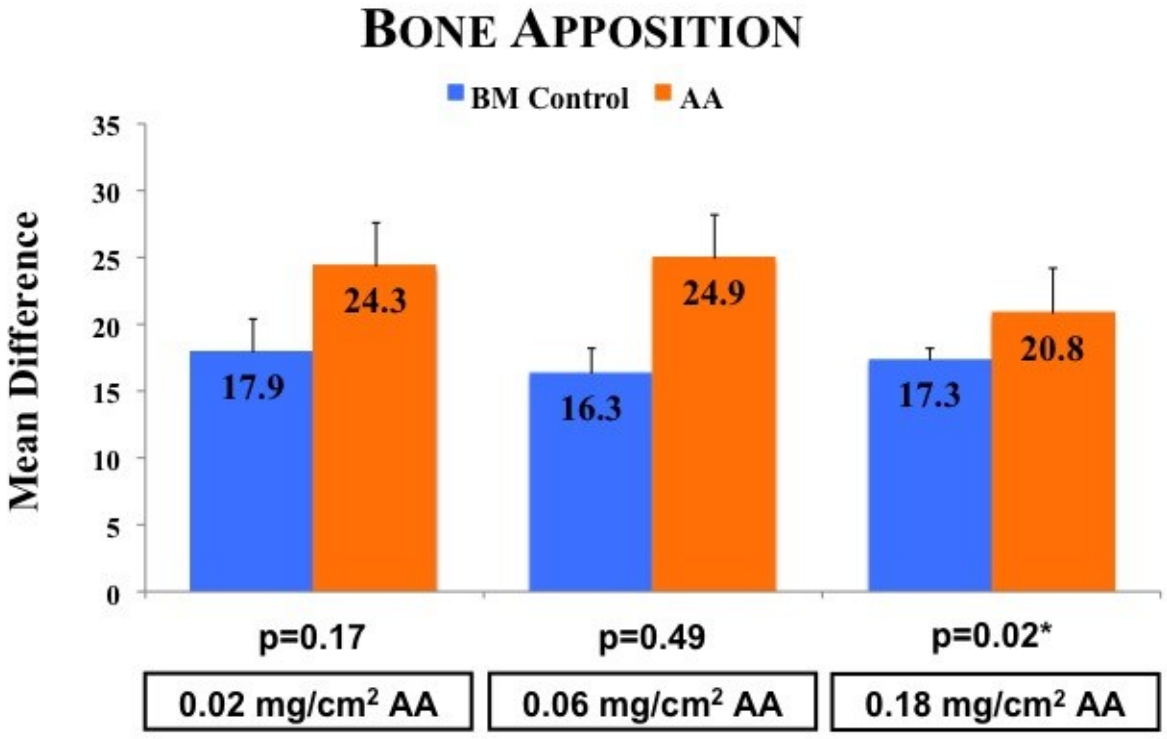

Figure 5.18 Graphical representation of the statistical overview of the 12-week femora for bone apposition between the 0.02 mg/cm^2 AA, 0.06 mg/cm^2 AA and 0.18 mg/cm^2 AA dose compared to their BM control.

Peri-Implant Bone	0.02 mg/cm^2 AA		0.06 mg/cm^2 AA		0.18 mg/cm^2 AA	
	BM	AA	BM	AA	BM	AA
Mean	11.5	14.2	9.1	14.2	10.6	22.7
Standard Deviation	7.2	6.8	1.3	3.4	2.6	6.2
Standard Error	3.2	3.1	0.6	1.7	1.2	2.8
P-Value	0.11		0.05*		0.001*	

Table 5.11 Statistical overview of the 12-week femora for peri-implant bone between the 0.02 mg/cm^2 AA, 0.06 mg/cm^2 AA and 0.18 mg/cm^2 AA dose compared to their BM control. Significance, p<0.05 is represented by an asterisk (*).

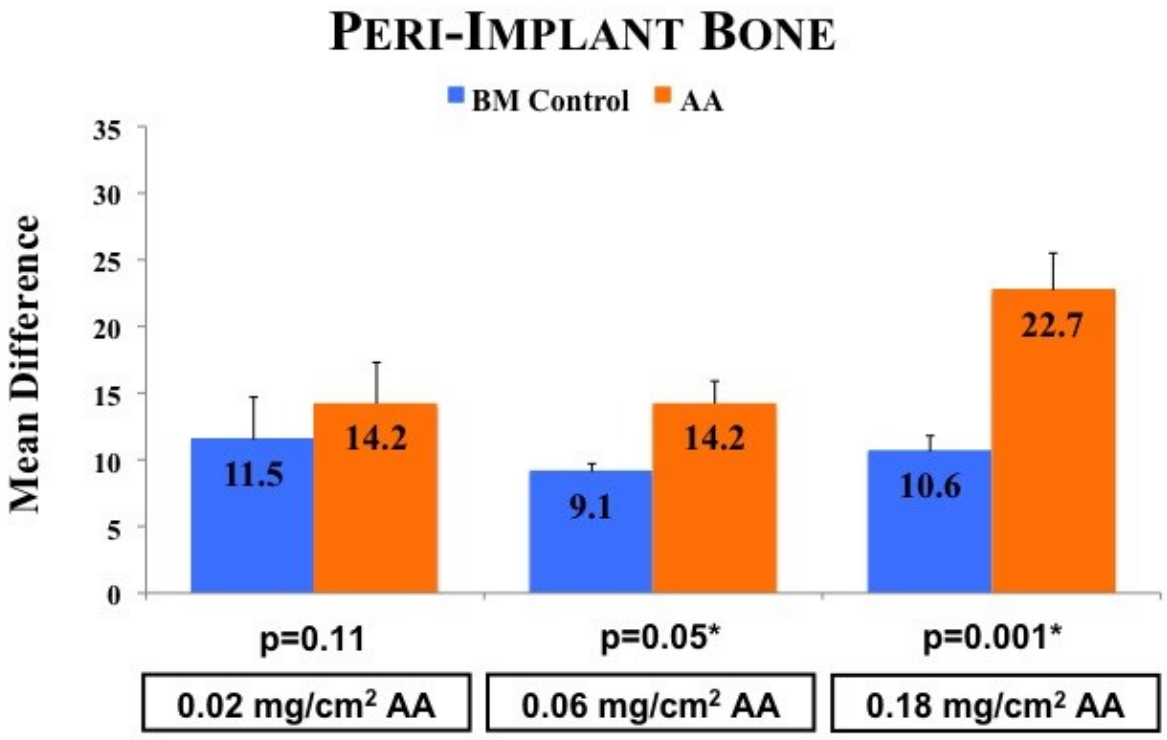

Figure 5.19 Graphical representation of the statistical overview of the 12-week femora for peri-implant bone between the 0.02 mg/cm^2 AA, 0.06 mg/cm^2 AA and 0.18 mg/cm^2 AA dose compared to their BM control.

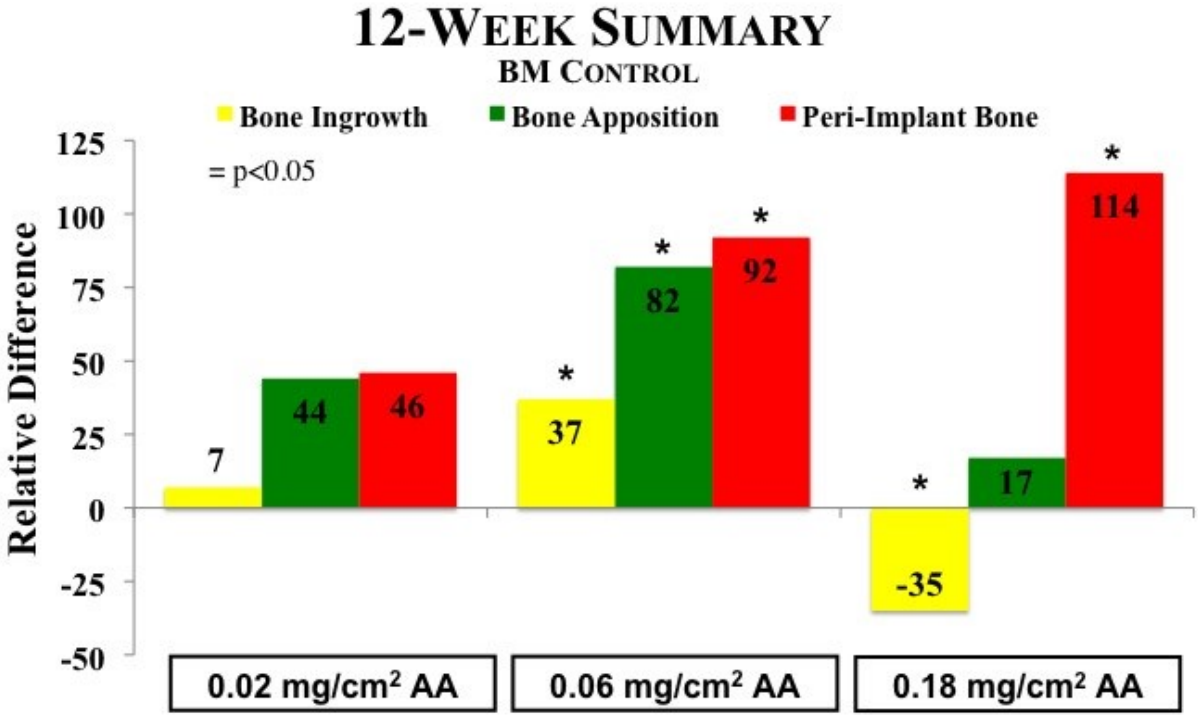

Figure 5.20 Summary of the 12-week femoral relative differences with the 0.02 mg/cm^2 AA, 0.06 mg/cm^2 AA and 0.18 mg/cm^2 AA dose compared to their BM control. Asterisks (*) show a significance of p<0.05.

5.6.3 Femora with Hydroxyapatite Coated Controls

Bone Ingrowth	0.02 mg/cm^2 AA		0.06 mg/cm^2 AA		0.18 mg/cm^2 AA	
	HA	AA	HA	AA	HA	AA
Mean	27.1	26.9	25.5	21.6	22.1	15.1
Standard Deviation	6.9	14.4	11.3	13.4	6.5	18.7
Standard Error	3.1	6.4	5.6	6.7	2.9	8.4
P-Value	0.48		0.29		0.20	

Table 5.12 Statistical overview of the 12-week femora for bone ingrowth between the 0.02 mg/cm^2 AA, 0.06 mg/cm^2 AA and 0.18 mg/cm^2 AA compared to their HA control. Significance, p<0.05 is represented by an asterisk (*).

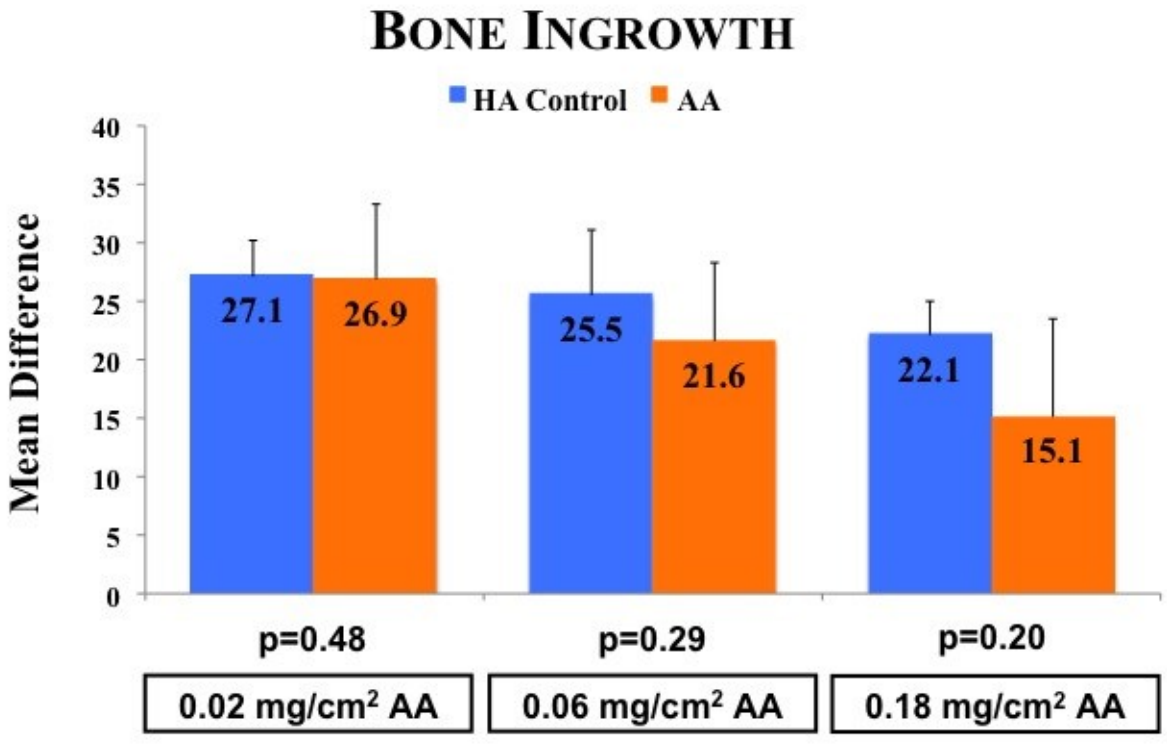

Figure 5.21 Graphical representation of the statistical overview of the 12-week femora for bone ingrowth between the 0.02 mg/cm^2 AA, 0.06 mg/cm^2 AA and 0.18 mg/cm^2 AA dose compared to their HA control.

Bone Apposition	0.02 mg/cm^2 AA		0.06 mg/cm^2 AA		0.18 mg/cm^2 AA	
	HA	AA	HA	AA	HA	AA
Mean	19.1	26.8	13.9	22.2	19.5	24.3
Standard Deviation	7.2	10.8	5.6	8.0	4.3	25.3
Standard Error	3.2	4.7	2.8	4.0	1.9	11.3
P-Value	0.07		0.11		0.34	

Table 5.13 Statistical overview of the 12-week femora for bone apposition between the 0.02 mg/cm^2 AA, 0.06 mg/cm^2 AA and 0.18 mg/cm^2 AA compared to their HA control. Significance, p<0.05 is represented by an asterisk (*).

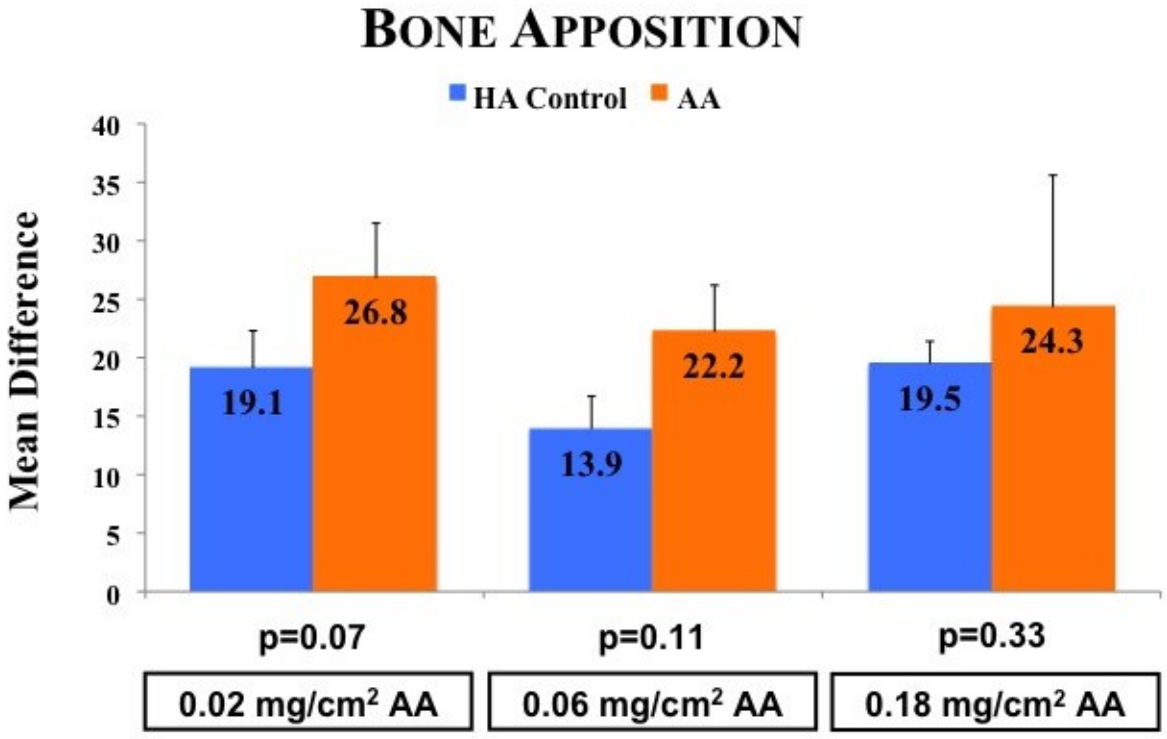

Figure 5.22 Graphical representation of the statistical overview of the 12-week femora for bone apposition between the 0.02 mg/cm^2 AA, 0.06 mg/cm^2 AA and 0.18 mg/cm^2 AA dose compared to their HA control.

Peri-Implant Bone	0.02 mg/cm^2 AA		0.06 mg/cm^2 AA		0.18 mg/cm^2 AA	
	HA	AA	HA	AA	HA	AA
Mean	7.9	6.4	4.5	9.0	8.5	14.1
Standard Deviation	4.3	2.9	1.4	2.3	2.0	8.6
Standard Error	1.9	1.3	0.7	1.1	0.9	3.9
P-Value	0.30		0.01*		0.13	

Table 5.14 Statistical overview of the 12-week femora for peri-implant bone between the 0.02 mg/cm^2 AA, 0.06 mg/cm^2 AA and 0.18 mg/cm^2 AA compared to their HA control. Significance, p<0.05 is represented by an asterisk (*).

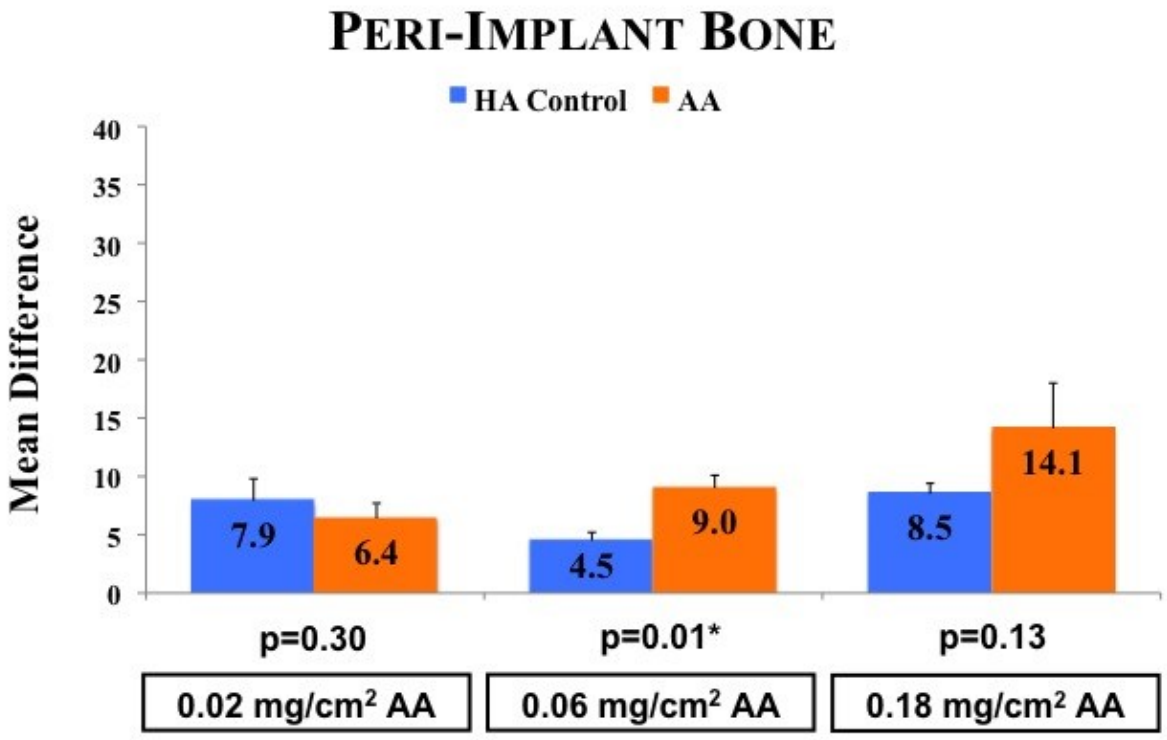

Figure 5.23 Graphical representation of the statistical overview of the 12-week femora for peri-implant bone between the 0.02 mg/cm^2 AA, 0.06 mg/cm^2 AA and 0.18 mg/cm^2 AA dose compared to their HA control.

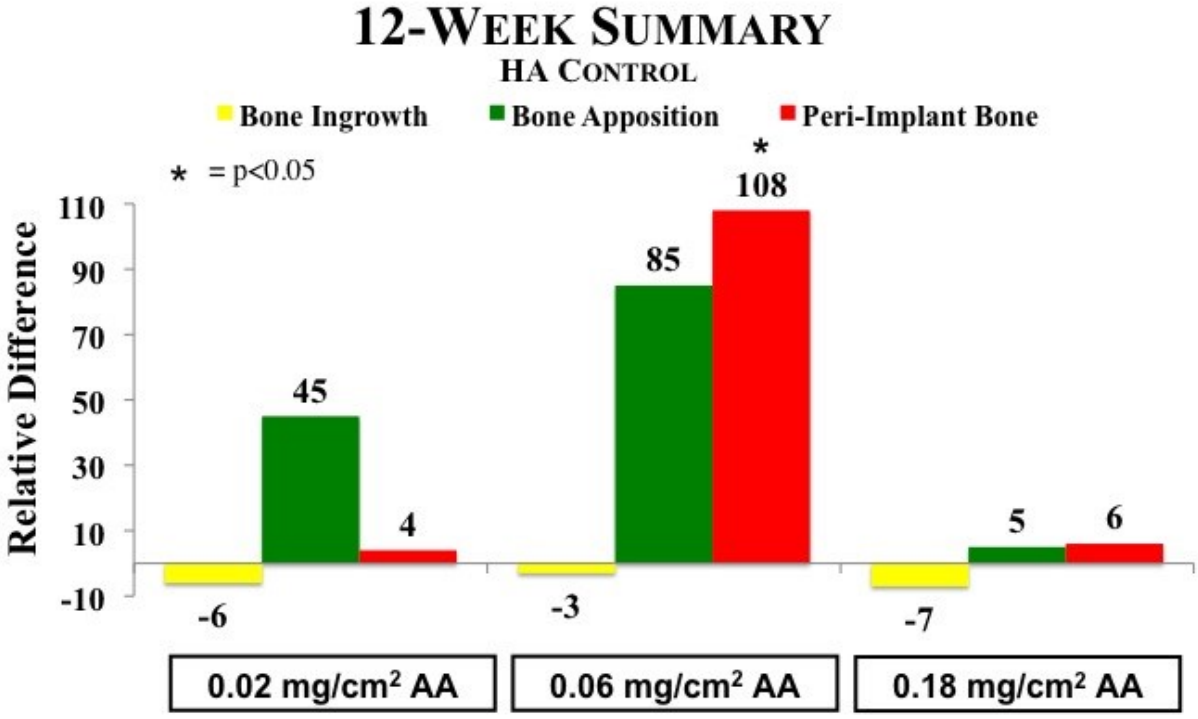

Figure 5.24 Summary of the 12-week femoral relative differences with the 0.02 mg/cm^2 AA, 0.06 mg/cm^2 AA and 0.18 mg/cm^2 AA dose compared to their HA control. Asterisks (*) show a significance of p<0.05.

Table 1. 12-week Dose Response Data According to Alendronate Dose.

CHAPTER 6. DISCUSSION

This study highlights the ability of the bisphosphonate, alendronate (AA), to modulate bone remodelling as an adjunct therapy in total joint replacement surgery. In circumstances when a patient's bone stock or healing potential is compromised, implant fixation is less reliably achieved with orthopaedic joint replacement implants. Currently, AA has been clinically effective for increasing bone mass and density in the treatment of osteoporosis. In order to eliminate systemic side effects and minimize the amount of drug required to be efficacious, AA was chemically attached to the implant thereby allowing the drug to directly elute to the surrounding bone. Using a porous implant to deliver the bisphosphonate, AA, to surrounding bone has been shown in animal studies to enhance local bone formation, but the optimum dose remains uncertain [78, 81]. This study specifically addressed the optimum dose of AA required on HA coated porous implants to enhance peri-implant bone and implant osseointegration. The dose range of 0.02 mg/cm^2 AA, 0.06 mg/cm^2 AA, and 0.18 mg/cm^2 AA was chosen based on a previous two dose study done by Bobyn et al [79]**.** This study confirmed that localized delivery of AA directly can influence the bone remodelling process yielding a net bone formation around the porous implants and that this response is dose dependent. At 4 and 12 weeks, the 0.02 mg/cm^2, and 0.06 mg/cm^2 alendronate dose implants showed that AA was able to positively modulate the bone response compared to the bare metal control implants. Peri-implant bone was significantly increased in all AA dosed implants compared to the bare metal control at both 4 and 12 weeks. The hydroxyapatite-coated control implants showed little to no change in bone response at 12 weeks for the 0.02 mg/cm^2 AA, and 0.18 mg/cm^2 AA doses. However, at 0.06 mg/cm^2 AA, there was a significant increase in peri-implant bone. Overall, an Alendronate dose of 0.06 mg/cm^2, showed the best overall bone response, resulting in significantly greater peri-implant bone compared to controls. As well, the peri-implant bone that formed around the alendronate-coated implants was reliably and reproducibly detectable.

The reason to have two different controls was based on the potential commercialization of the concept. At present time, there are no HA coated orthopaedic implants made by direct metal laser sintering technique that are FDA approved. All direct metal laser sintered implants used today are bare metal. As such, one control was the BM control, which was felt to be comparable

to present day implants. The other control evaluated was an HA coated implant without the drug. This control is scientifically the best control since it is exactly like the AA loaded implant, without the drug. Although *in vivo* studies have demonstrated HA can improve bone ingrowth and allow gap healing, its effectiveness in clinical use has been conflicting [82-84]. Subsequently, the reason for the variability in results of implants with HA has been elucidated by Hacking et al [30]. They found that 80% of the effect of HA on bone ingrowth was related to its surface roughness or topology, and not its chemistry. As a result, implants with smooth porous coatings or surfaces will a have greater benefit from HA coatings than implants that are rough. In this study, the smooth direct metal laser sintered porous coating did benefit from the HA coating. When the AA loaded implants were compared to the HA controls, there was no difference in bone ingrowth and bone apposition at any of the doses. However, as demonstrated in the previous study by Bobyn et al. [79], the primary effect of AA on porous implants is a dose-dependent net increase in peri-implant bone formation. In this study, the 0.06 mg/cm^2 AA implants had twice the amount of peri-implant bone than the HA contralateral controls, which was significant. This degree of peri-implant bone formation is even more impressive than that seen in the proximal femur because the diaphyseal segment of the canine femur is primarily filled with fatty marrow, rather than bone forming cells. The effect of AA on the formation of peri-implant bone in the diaphysis was highly dose dependent and was not seen in the lower 0.02 mg/cm^2 dosed implants.

The effect of AA on the extent of bone ingrowth, bone apposition and peri-implant bone was dose dependent. The implants with the highest dose, 0.18 mg/cm^2 AA, had significantly less bone ingrowth at 12 weeks in the metaphyseal region of the femur and no improvement in bone apposition, thereby excluding it as an appropriate dose. Although the same effect was not seen in the femoral diaphysis, the negative effect on bone ingrowth suggests that this very high dose may in fact be negatively impacting the host's ability to heal the surgical insult and limit osseointegration.

Alendronate has been shown to enhance bone formation in other animal models [78, 79, 85-87]. Garbuz et al. showed an increase in gap filling, bone ingrowth, and total bone formation with AA-soaked implants in the distal diaphyseal region of a rabbit's femur at 4 weeks time [78]. In this study, a dose of 1.4 μg/cm^2 AA was bound to an electrolytic coating of calcium phosphate.

This coating was designed to bind AA to all the porous surfaces, thereby eliminating the biphasic release of AA. The actual dose of AA released is not clear since the elution profile of this experimental model was not disclosed. However, it would certainly be less than the dose of 1.4 $\mu g/cm^2$. Compared with the group treated with the calcium phosphate-coated implants, the group treated with the implants coated with calcium phosphate and alendronate had a relative increase of 84% in the volume of gap filling ($p < 0.001$), 140% ($p < 0.001$) in bone ingrowth, and 111% ($p < 0.001$) in total new bone formation. The difference in response to AA seen in the present study can be due to the differences in the animal model used and the difference in cancellous bone density in the canine's intramedullary femur. In a canine study using HA coated plasma sprayed implants placed within compacted cancellous bone treated with topically administered alendronate (2 mg AA/mL saline), Jakobsen et al. [85] reported an increase in the amount of peri-implant bone with the AA-dosed implant by 1.3-fold. Bobyn et al. further corroborated these findings with BSEM analysis [79]. They used a canine model with two different Ti implant structures comparing bare metal control implants with two doses of AA: 0.2 mg AA (7.5 $\mu g/cm^2$) and 1.0 mg AA (37 $\mu g/cm^2$). As compared to the paired controls, the peri-implant bone density obtained was 1.5 times greater with the lower AA dose ($p=0.04$) and 2.7 times greater with the high AA dose ($p=0.01$). This present study had approximately 2 times the amount of peri-implant bone in the 0.06 mg/cm^2 AA dose compared to the 0.02 mg/cm^2AA dose. In comparison between the upper dose in the study by Bobyn et al. and the middle dose from this study, these two values may give insight to a more narrow range of the optimum dose: 37 $\mu g/cm^2$ AA – 60 $\mu g/cm^2$ AA.

It is imperative that the bone formed in response to the local elution of AA be normal host bone. In a review of preclinical studies, Hayes et al. summarized the effects of alendronate on bone quality [88]. They showed that systemic AA preferentially localised at bone resorption sites and "normalised bone turnover, promoted normal mineralization, and increased bone mass and strength" [88]. In this study, the BSEM appearance of the new peri-implant bone was identical in trabecular pattern and grey level density as the surrounding host bone. The quality and histopathology of bone around locally delivered alendronate at the implant interface was evaluated Bobyn et al. [89]. Using the same canine proximal humeral model as in this study, the mechanical shear strength and histologic appearance of 0.06 mg/cm^2 AA dosed implants were compared to controls at 4- and 12-weeks. An independent bone pathologist reviewed the

surrounding bone after the push-out test and found that all control and Alendronate-dosed specimens revealed normal appearing bone trabeculae adjacent, and distant to the empty implant site [90]. The cellular morphology of the hematopoietic cells surrounding the empty implant site was not altered in both the control and the test samples. According to the injury scale provided, all specimens, control and test samples, showed no signs of irritation. The mean relative increase in shear strength of the interface was 81% at 4 weeks and 51% at 12 weeks. Enhanced implant fixation strength from the AA induced bone formation indirectly confirms the quality of the bone and has been demonstrated by other researchers. Push-out testing done by Jakobsen et al. found the maximum shear strength increased by 2.1-fold and the maximum shear stiffness increased by 2.7-fold in the AA-dosed implants compared to the contralateral control [85]. In a rat model, Tengvall et al. demonstrated that the pull out strength doubled at 8 weeks, when stainless steel screws were coated with AA.

This study has several limitations, none of which affected the outcome. First, the implant model itself was not clinically realistic because it did not represent a loaded joint replacement prosthesis. In this study, no physiological loads were applied to the bone-implant interface that could otherwise influence bone remodelling. However, it is crucial to eliminate as many confounding variables as possible so that the results can be properly interpreted. The static intramedullary implant used in this study eliminated the variable of loading and the potential complications that can occur after joint replacement surgery. These complications, such as loosening and dislocation, are known to effect net bone formation around porous implants. A second limitation was that no biological assessment of the newly formed bone was performed in this study. As a result, there was no confirmation, at the cellular level, that the state of the surrounding bone was consisted of normal cells and mature bone. Nonetheless, the bone in and around the implant in this study appeared to be normal on BSEM, and the results obtained from an analogous study by Bobyn et al. [90] are reassuring in that the histologic appearance of the new peri-implant bone was normal. Another limitation was that the 4 and 12 week data were obtained in different bones. This was done in order to minimize he number of animals needed to carry out the study. However, the density of cancellous bone differs between these 2 sites, being more abundant in the proximal humerus. This is why the data was paired and each anatomic site was not compared to the other. A similar limitation was despite a careful surgical technique, not all implants were in exactly the same alignment or location within the intramedullary canal. As

a result, the paired sections were matched anatomically to prevent any differences of bone around the implant's length in that location. Also, the use of mongrel dogs of variable age and gender is not ideal. It would have been best to use a single breed of dog of the same age and gender to minimize these effects on the response the bone healing in the presence of bisphosphonate. Finally, although we looked at various doses based on the literature and our previous studies, it is not a comprehensive study of all potential doses. However, it does clearly indicate the dose region that is most effective.

This study is the first to provide a comprehensive overview of the dose dependent response of locally delivered Alendronate's effect on peri-implant bone. In this study, the preferred dose of AA has become apparent. Initial studies were able to confirm AA's localized elution, virtually eliminating the concerns with systemic side effects [79]. An additional study showed an increase in mechanical strength positively correlating the use of AA on implant fixation at the 0.06 mg/cm^2 dose [89]. The validation by a pathologist of normal bone formation without any inflammatory or deleterious reaction shows that the remodelling process is occurring without any local adverse effects [90]. This study has demonstrated the time response of AA is quite rapid, with initial stability obtained with the alendronate dosed implants by 4 weeks. Future studies are required to evaluate the long-term survival of implant fixation and bone remodelling using an AA-coated femoral stem in a total hip arthroplasty *in vivo* model.

CHAPTER 7. CONCLUSION

This thesis illustrates the clinical potential of Alendronate to be locally delivered by an implant to enhance biologic fixation around orthopaedic joint implants. There were many important insights from this study: In a 4-week and 12-week canine humeral and femoral intramedullary rod model, the use of clinically relevant metal laser sintered porous coated implants with AA was capable of further enhancing bone at and around the immediate implant space. The dose of AA required was based on the surface area, and not the overall dose. Therefore, the larger the implant, the higher the dose required. Nonetheless, due to the localized delivery of AA by the implant, very little drug was needed to produce the effects previously seen with a high systemic dose. The backscattered scanning electron microscopy analysis showed that AA's optimal dose was 0.06 mg/cm^2. Of the 3 doses studied, this demonstrated the best overall bone response. This *in vivo* study validates the potential use of Alendronate as an adjunct therapy for challenging orthopaedic joint replacement surgeries.

CHAPTER 8. REFERENCES

1. CJRR Hip and Knee Replacements in Canada 2012-2013 Quick Stats (Dec. 2013) Canadian Institute for Health Information2013 [cited 2014 February 4]. Available from: http://www.cihi.ca/CIHI-ext-portal/internet/EN/TabbedContent/types+of+care/specialized+services/joint+replacements/cihi021359.

2. Gomez PF, Morcuende JA. Early attempts at hip arthroplasty--1700s to 1950s. *The Iowa orthopaedic journal*. 2005;25:25-9.

3. Bloch B. International standards for surgical implants. *Annals of the Royal College of Surgeons of England*. 1984;66(5):369-71.

4. Landis WJ. The strength of a calcified tissue depends in part on the molecular structure and organization of its constituent mineral crystals in their organic matrix. *Bone*. 1995;16(5):533-44.

5. Roberts CS. The Musculoskeletal System. In: Walker HK, Hall WD, Hurst JW, editors. Clinical Methods: The History, Physical, and Laboratory Examinations. 3rd ed. Boston1990.

6. Hill PA. Bone remodelling. *British journal of orthodontics*. 1998;25(2):101-7.

7. Sommerfeldt DW, Rubin CT. Biology of bone and how it orchestrates the form and function of the skeleton. *Eur Spine J*. 2001;10:S86-S95.

8. Greer RB, 3rd. Wolff's Law. *Orthopaedic review*. 1993;22(10):1087-8.

9. Jones HH, Priest JD, Hayes WC, Tichenor CC, Nagel DA. Humeral hypertrophy in response to exercise. *The Journal of bone and joint surgery American volume*. 1977;59(2):204-8.

10. Bragdon CR, Jasty M, Greene M, Rubash HE, Harris WH. Biologic fixation of total hip implants. Insights gained from a series of canine studies. *The Journal of bone and joint surgery American volume*. 2004;86-A Suppl 2:105-17.

11. Bobyn JD, Hacking SA, Chan SP, Toh KK, Krygier JJ, Tanzer M, editors. Characterization of a New Porous Tantalum Biomaterial for Reconstructive Orthopaedics. Proceedings of the American Academy of Orthopaedic Surgeons Annual Meeting; 1999; Anaheim, CA.

12. Chu PK, Liu X. Biomaterials fabrication and processing handbook. Boca Raton: CRC Press/Taylor & Francis; 2008. xv, 701 p. p.

13. Ritter MA, Vaughn BK, Frederick LD. Single-stage, bilateral, cementless total hip arthroplasty. *The Journal of arthroplasty*. 1995;10(2):151-6.

14. Rao RR, Sharkey PF, Hozack WJ, Eng K, Rothman RH. Immediate weightbearing after uncemented total hip arthroplasty. *Clinical orthopaedics and related research*. 1998(349):156-62.

15. Taunt CJ, Jr., Finn H, Baumann P. Immediate weight bearing after cementless total hip arthroplasty. *Orthopedics*. 2008;31(3):223.

16. Andersson L, Wesslau A, Boden H, Dalen N. Immediate or late weight bearing after uncemented total hip arthroplasty: a study of functional recovery. *The Journal of arthroplasty*. 2001;16(8):1063-5.

17. Bobyn JD, Pilliar RM, Cameron HU, Weatherly GC. Osteogenic phenomena across endosteal bone-implant spaces with porous surfaced intramedullary implants. *Acta orthopaedica Scandinavica*. 1981;52(2):145-53.

18. Kienapfel H, Sprey C, Wilke A, Griss P. Implant fixation by bone ingrowth. *The Journal of arthroplasty*. 1999;14(3):355-68.

19. Bobyn JD, Pilliar RM, Cameron HU, Weatherly GC, Kent GM. The effect of porous surface configuration on the tensile strength of fixation of implants by bone ingrowth. *Clinical orthopaedics and related research*. 1980(149):291-8.

20. Karrholm J, Malchau H, Snorrason F, Herberts P. Micromotion of femoral stems in total hip arthroplasty. A randomized study of cemented, hydroxyapatite-coated, and porous-coated stems with roentgen stereophotogrammetric analysis. *The Journal of bone and joint surgery American volume*. 1994;76(11):1692-705.

21. Kuzyk PRT, Schemitsch EH. The basic science of peri-implant bone healing. *Indian J Orthop*. 2011;45(2):108-15.

22. Hollister SJ, Kikuchi N, Goldstein SA. Do Bone Ingrowth Processes Produce a Globally Optimized Structure. *Journal of biomechanics*. 1993;26(4-5):391-407.

23. Hanzlik JA, Day JS, Acknowledged Contributors: Ingrowth Retrieval Study G. Bone ingrowth in well-fixed retrieved porous tantalum implants. *The Journal of arthroplasty*. 2013;28(6):922-7.

24. Soballe K. Hydroxyapatite ceramic coating for bone implant fixation. Mechanical and histological studies in dogs. *Acta orthopaedica Scandinavica Supplementum*. 1993;255:1-58.

25. Panegrossi G, Ceretti M, Papalia M, Casella F, Favetti F, Falez F. Bone loss management in total knee revision surgery. *International orthopaedics*. 2014;38(2):419-27.

26. Kucera T, Soukup T, Krs O, Urban K, Sponer P. [Bone healing capacity in patients undergoing total hip arthroplasty]. *Acta chirurgiae orthopaedicae et traumatologiae Cechoslovaca*. 2012;79(1):52-8.

27. Kobayashi S, Eftekhar NS, Terayama K. Predisposing factors in fixation failure of femoral prostheses following primary Charnley low friction arthroplasty. A 10- to 20-year followup study. *Clinical orthopaedics and related research*. 1994(306):73-83.

28. Cooper HJ, Jacob AP, Rodriguez JA. Distal fixation of proximally coated tapered stems may predispose to a failure of osteointegration. *The Journal of arthroplasty*. 2011;26(6 Suppl):78-83.

29. Klokkevold PR, Nishimura RD, Adachi M, Caputo A. Osseointegration enhanced by chemical etching of the titanium surface. A torque removal study in the rabbit. *Clinical oral implants research*. 1997;8(6):442-7.

30. Hacking SA, Boyraz P, Powers BM, Sen-Gupta E, Kucharski W, Brown CA, et al. Surface roughness enhances the osseointegration of titanium headposts in non-human primates. *Journal of neuroscience methods*. 2012;211(2):237-44.

31. Ryan G, Pandit A, Apatsidis DP. Fabrication methods of porous metals for use in orthopaedic applications. *Biomaterials*. 2006;27(13):2651-70.

32. Dimitriou R, Babis GC. Biomaterial osseointegration enhancement with biophysical stimulation. *Journal of musculoskeletal & neuronal interactions*. 2007;7(3):253-65.

33. Willie BM, Yang X, Kelly NH, Han J, Nair T, Wright TM, et al. Cancellous bone osseointegration is enhanced by in vivo loading. *Tissue engineering Part C, Methods*. 2010;16(6):1399-406.

34. Schutzer SF, Jasty M, Bragdon CR, Harrigan TP, Harris WH. A double-blind study on the effects of a capacitively coupled electrical field on bone ingrowth into porous-surfaced canine total hip prostheses. *Clinical orthopaedics and related research*. 1990(260):297-304.

35. Chin HC, Frassica FJ, Markel MD, Frassica DA, Sim FH, Chao EY. The effects of therapeutic doses of irradiation on experimental bone graft incorporation over a porous-coated segmental defect endoprosthesis. *Clinical orthopaedics and related research*. 1993(289):254-66.

36. Tanzer M, Harvey E, Kay A, Morton P, Bobyn JD. Effect of noninvasive low intensity ultrasound on bone growth into porous-coated implants. *Journal of orthopaedic research : official publication of the Orthopaedic Research Society*. 1996;14(6):901-6.

37. Mourino V, Boccaccini AR. Bone tissue engineering therapeutics: controlled drug delivery in three-dimensional scaffolds. *Journal of the Royal Society, Interface / the Royal Society*. 2010;7(43):209-27.

38. Lind M. Growth factor stimulation of bone healing. Effects on osteoblasts, osteomies, and implants fixation. *Acta orthopaedica Scandinavica Supplementum*. 1998;283:2-37.

39. Lind M, Schumacker B, Soballe K, Keller J, Melsen F, Bunger C. Transforming growth factor-beta enhances fracture healing in rabbit tibiae. *Acta orthopaedica Scandinavica*. 1993;64(5):553-6.

40. Hofmann AA, Bloebaum RD, Rubman MH, Bachus KN, Plaster RL. Microscopic analysis of autograft bone applied at the interface of porous-coated devices in human cancellous bone. *International orthopaedics*. 1992;16(4):349-58.

41. Peters C, Hines J, Bachus K, Craig M, Bloebaum R. Biological effects of calcium sulfate as a bone graft substitute in ovine metaphyseal defects. *J of Biomed Mater Res Part A*. 2006;76A(3):7.

42. Giger EV, Castagner B, Leroux JC. Biomedical applications of bisphosphonates. *Journal of controlled release : official journal of the Controlled Release Society*. 2013;167(2):175-88.

43. Russell RG, Rogers MJ. Bisphosphonates: from the laboratory to the clinic and back again. *Bone*. 1999;25(1):97-106.

44. Drake MT, Clarke BL, Khosla S. Bisphosphonates: mechanism of action and role in clinical practice. *Mayo Clinic proceedings Mayo Clinic*. 2008;83(9):1032-45.

45. Fleisch H. Bisphosphonates: pharmacology. *Seminars in arthritis and rheumatism*. 1994;23(4):261-2.

46. Fleisch H. Bisphosphonates: mechanisms of action. *Endocrine reviews*. 1998;19(1):80-100.

47. Green JR. Bisphosphonates: preclinical review. *The oncologist*. 2004;9 Suppl 4:3-13.

48. Papapoulos SE. Bisphosphonates: how do they work? *Best practice & research Clinical endocrinology & metabolism*. 2008;22(5):831-47.

49. Ebetino FH, Hogan AM, Sun S, Tsoumpra MK, Duan X, Triffitt JT, et al. The relationship between the chemistry and biological activity of the bisphosphonates. *Bone*. 2011;49(1):20-33.

50. Russell RG, Watts NB, Ebetino FH, Rogers MJ. Mechanisms of action of bisphosphonates: similarities and differences and their potential influence on clinical efficacy. *Osteoporosis international : a journal established as result of cooperation between the European Foundation for Osteoporosis and the National Osteoporosis Foundation of the USA*. 2008;19(6):733-59.

51. Russell RG. Bisphosphonates: the first 40 years. *Bone*. 2011;49(1):2-19.

52. Bellido T, Plotkin LI. Novel actions of bisphosphonates in bone: preservation of osteoblast and osteocyte viability. *Bone*. 2011;49(1):50-5.

53. Morris CD, Einhorn TA. Bisphosphonates in orthopaedic surgery. *The Journal of bone and joint surgery American volume*. 2005;87(7):1609-18.

54. Bobyn JD, Tanzer M, McKenzie K, Karabasz D, Krygier JJ, editors. Locally Delivered Bisphosphonate for Enhancement of Bone Formation and Implant Fixation. Proceedings of the American Academy of Orthopaedic Surgeons Annual Meeting; 2009; Las Vegas, NV.

55. Bobyn JD, Hacking SA, Krygier JJ, Harvey EJ, Little DG, Tanzer M. Zoledronic acid causes enhancement of bone growth into porous implants. *Journal of Bone & Joint Surgery, British Volume*. 2005;87-B(3):416-20.

56. Sugata Y, Sotome S, Yuasa M, Hirano M, Shinomiya K, Okawa A. Effects of the systemic administration of alendronate on bone formation in a porous hydroxyapatite/collagen composite and resorption by osteoclasts in a bone defect model in rabbits. *The Journal of bone and joint surgery British volume*. 2011;93(4):510-6.

57. Arabmotlagh M, Pilz M, Warzecha J, Rauschmann M. Changes of femoral periprosthetic bone mineral density 6 years after treatment with alendronate following total hip arthroplasty. *Journal of orthopaedic research : official publication of the Orthopaedic Research Society*. 2009;27(2):183-8.

58. Harding AK, Toksvig-Larsen S, Tägil M, W-Dahl A. A single dose zoledronic acid enhances pin fixation in high tibial osteotomy using the hemicallotasis technique. A double-blind placebo controlled randomized study in 46 patients. *Bone*. 2010;46(3):649-54.

59. Prieto-Alhambra D, Javaid MK, Judge A, Murray D, Carr A, Cooper C, et al. Association between bisphosphonate use and implant survival after primary total arthroplasty of the knee or hip: population based retrospective cohort study. *BMJ*. 2011;343:d7222.

60. Papapetrou PD. Bisphosphonate-associated adverse events. *Hormones*. 2009;8(2):96-110.

61. Lin JH. Bisphosphonates: a review of their pharmacokinetic properties. *Bone*. 1996;18(2):75-85.

62. Khan SA, Kanis JA, Vasikaran S, Kline WF, Matuszewski BK, McCloskey EV, et al. Elimination and biochemical responses to intravenous alendronate in postmenopausal osteoporosis. *Journal of bone and mineral research : the official journal of the American Society for Bone and Mineral Research*. 1997;12(10):1700-7.

63. Schneider JP, Hinshaw WB, Su C, Solow P. Atypical femur fractures: 81 individual personal histories. *The Journal of clinical endocrinology and metabolism*. 2012;97(12):4324-8.

64. Astrand J, Aspenberg P. Systemic alendronate prevents resorption of necrotic bone during revascularization. A bone chamber study in rats. *BMC musculoskeletal disorders*. 2002;3:19.

65. Astrand J, Aspenberg P. Topical, single dose bisphosphonate treatment reduced bone resorption in a rat model for prosthetic loosening. *Journal of orthopaedic research : official publication of the Orthopaedic Research Society*. 2004;22(2):244-9.

66. Kumar D, Kumar V, Little DG, Howman-Giles RB, Wong E, Ali SO. Evaluation of biodistribution by local versus systemic administration of 99mTc-labeled pamidronate. *Journal of orthopaedic science : official journal of the Japanese Orthopaedic Association*. 2006;11(5):512-20.

67. Roshan-Ghias A, Arnoldi J, Procter P, Pioletti DP. In vivo assessment of local effects after application of bone screws delivering bisphosphonates into a compromised cancellous bone site. *Clinical biomechanics*. 2011;26(10):1039-43.

68. Niu S, Cao X, Zhang Y, Zhu Q, Zhu J, Zhen P. Peri-implant and systemic effects of high-/low-affinity bisphosphonate-hydroxyapatite composite coatings in a rabbit model with peri-implant high bone turnover. *BMC musculoskeletal disorders*. 2012;13:97.

69. Yaffe A, Binderman I, Breuer E, Pinto T, Golomb G. Disposition of alendronate following local delivery in a rat jaw. *Journal of periodontology*. 1999;70(8):893-5.

70. Tanzer M, Karabasz D, Krygier JJ, Cohen R, Bobyn JD. The Otto Aufranc Award: bone augmentation around and within porous implants by local bisphosphonate elution. *Clinical orthopaedics and related research*. 2005;441:30-9.

71. Toksvig-Larsen S, Aspenberg P. Bisphosphonate-coated external fixation pins appear similar to hydroxyapatite-coated pins in the tibial metaphysis and to uncoated pins in the shaft. *Acta orthopaedica*. 2013;84(3):314-8.

72. Clark PA, Moioli EK, Sumner DR, Mao JJ. Porous implants as drug delivery vehicles to augment host tissue integration. *Faseb J*. 2008;22(6):1684-93.

73. Boanini E, Torricelli P, Gazzano M, Giardino R, Bigi A. Alendronate-hydroxyapatite nanocomposites and their interaction with osteoclasts and osteoblast-like cells. *Biomaterials*. 2008;29(7):790-6.

74. Bobyn JD, Hacking SA, Krygier JJ, Harvey EJ, Little DG, Tanzer M. Zoledronic acid causes enhancement of bone growth into porous implants. *The Journal of bone and joint surgery British volume*. 2005;87(3):416-20.

75. McKenzie K, Dennis Bobyn J, Roberts J, Karabasz D, Tanzer M. Bisphosphonate remains highly localized after elution from porous implants. *Clinical orthopaedics and related research*. 2011;469(2):514-22.

76. Li EC, Davis LE. Zoledronic acid: a new parenteral bisphosphonate. *Clinical therapeutics*. 2003;25(11):2669-708.

77. Acil Y, Moller B, Niehoff P, Rachko K, Gassling V, Wiltfang J, et al. The cytotoxic effects of three different bisphosphonates in-vitro on human gingival fibroblasts, osteoblasts and osteogenic sarcoma cells. *Journal of cranio-maxillo-facial surgery : official publication of the European Association for Cranio-Maxillo-Facial Surgery*. 2012;40(8):e229-35.

78. Garbuz DS, Hu Y, Kim WY, Duan K, Masri BA, Oxland TR, et al. Enhanced gap filling and osteoconduction associated with alendronate-calcium phosphate-coated porous tantalum. *The Journal of bone and joint surgery American volume*. 2008;90(5):1090-100.

79. Bobyn JD, Thompson R, Lim L, Pura JA, Bobyn K, Tanzer M. Local Alendronic Acid Elution Increases Net Periimplant Bone Formation: A Micro-CT Analysis. *Clinical orthopaedics and related research*. 2013.

80. Varenna M, Bertoldo F, Di Monaco M, Giusti A, Martini G, Rossini M. Safety profile of drugs used in the treatment of osteoporosis: a systematical review of the literature. *Reumatismo*. 2013;65(4):143-66.

81. Bobyn JD, McKenzie K, Karabasz D, Krygier JJ, Tanzer M. Locally delivered bisphosphonate for enhancement of bone formation and implant fixation. *The Journal of bone and joint surgery American volume*. 2009;91 Suppl 6:23-31.

82. Tanzer M, Kantor S, Rosenthall L, Bobyn JD. Femoral remodeling after porous-coated total hip arthroplasty with and without hydroxyapatite-tricalcium phosphate coating: a prospective randomized trial. *The Journal of arthroplasty*. 2001;16(5):552-8.

83. Capello WN, D'Antonio JA, Manley MT, Feinberg JR. Hydroxyapatite in total hip arthroplasty. Clinical results and critical issues. *Clinical orthopaedics and related research*. 1998(355):200-11.

84. Bloebaum RD, Dupont JA. Osteolysis from a press-fit hydroxyapatite-coated implant. A case study. *The Journal of arthroplasty*. 1993;8(2):195-202.

85. Jakobsen T, Baas J, Kold S, Bechtold JE, Elmengaard B, Soballe K. Local bisphosphonate treatment increases fixation of hydroxyapatite-coated implants inserted with bone compaction. *Journal of orthopaedic research : official publication of the Orthopaedic Research Society*. 2009;27(2):189-94.

86. Meraw SJ, Reeve CM. Qualitative analysis of peripheral peri-implant bone and influence of alendronate sodium on early bone regeneration. *Journal of periodontology*. 1999;70(10):1228-33.

87. Meraw SJ, Reeve CM, Wollan PC. Use of Alendronate in Peri-Implant Defect Regeneration. *Journal of periodontology*. 1999;70(2):151-8.

88. Hayes WC, Shea M, Rodan GA. Preclinical evidence of normal bone with alendronate. *International journal of clinical practice Supplement*. 1999;101:9-13.

89. Bobyn JD, Pura J, Tanzer M, editors. Local Alendronic Acid Elution Increases Implant-Bone Fixation Strength. Proceedings of the Orthopaedic Research Society; 2014; New Orleans, LA.

90. Pura J, Tanzer M, Bobyn JD, editors. Locally Delivered Alendronic Acid Increases Net Bone Formation Around Porous Titanium Implants. Proceedings of the Combined Meeting of The American Orthopaedic Association & The Canadian Orthopaedic Association; 2014; Montreal, QC.

APPENDIX A. LIST OF ABBREVIATIONS

The following table describes the significance of various abbreviations and acronyms used throughout this thesis. The stated page is where one can find the first mention or use of the abbreviation.

Abbreviation	Meaning	Page
AA	Alendronate	II
AFF	atypical femur fractures	14
Al	Aluminum	3
BAA	butorphanol, acepromazine, and atropine	27
BM	bare-metal	II
BP	bisphosphonate	10
BSEM	backscattered scanning electron microscopy	23
Ca	calcium	9
Co-Cr	cobalt chrome	3
D.A	direct application	15
ddH_2O	distilled deionized water	25
DMLS	direct metal laser sintering	23
E/A	ether/acetone	33
HA	hydroxyapatite	II
IV	intravenous	11
JMORL	Jo Miller Orthopaedic Research Laboratory	VI
OC	osteoclast	14
PAM	pamidronate	15
PDGF	platelet-derived growth factor	10
PMMA	polymethylmethacrylate	3
RIS	Risedronate	16
ROI	region of interest	38
SEM	Scanning electron microscope	VI
S.C	subcutaneous injection	15
SO_4	sulphate	9
Ta	tantalum	3
TGF	transforming growth factor	10
THA	total hip arthroplasty	1
Ti	titanium	3
TKA	total knee arthroplasty	2
V	vanadium	3
ZA	zoledronate	12